UNIVERSITA' DEGLI STUDI DI CAMERINO
School of Advanced Studies

Doctoral Course
in
SCIENCE AND TECHNOLOGY – COMPUTER SCIENCE
XXXII CYCLE

Cellulose Nanocrystals (NCC) from Cotton Waste
&
Mucilage and Fibers from *Opuntia Ficus Indica* (OFI)

Extraction and Application in

Paper and Thermoplastic Starch Films

Supervisor
Santulli Carlo

PhD Student
Scognamiglio Fabrizio

Co-supervisors
Mirabile Gattia Daniele
Roselli Graziella

ACADEMIC YEAR 2018/2019

The activities and the achievements of this PhD project, funded through the EUREKA program and organized with the participation of the company NEST S.r.l. of Fabriano, would not have been possible without the financial support of

Fondazione CARIFAC

Fondazione Cassa di Risparmio di Fabriano e Cupramontana

whose contribution is gratefully acknowledged.

To Mirko

& Maria

Index

Introduction

In recent decades, the global economic and financial crisis, and its effects in the social and environmental sectors, have dramatically highlighted the urgent need for a transition to a "green economy", environmentally responsible as well as more equitable and supportive of everyone (i.e. that neither damages future generations nor creates dangerous imbalances within current ones). Over time, this has been accompanied by a growing awareness that the eco-compatibility of a new economic paradigm does not inhibit wealth creation or depress employment opportunities. On the contrary, the large-scale deployment of 'green' sectors offers significant investment, growth and employment opportunities for the entire production system.

The environmental sustainability, the need to minimise human and industrial impact, and to optimize the use of available resources, have led all countries in the world, especially the industrialized ones, to take a number of decisions: the implementation of reforms and incentives for the protection of natural resources, the enhancement of environmentally-friendly infrastructures, the introduction of new market-based mechanisms for the diffusion of eco-technologies, the creation of investements for innovation and the elimination of environmentally harmful sibsidies.

All these choices are of enormous value especially if you think, for example, about the problem of the global use of synthetic plastics: of the total production, about 40% is used for packaging, a sector in which plastic products are used for short periods of time; the fact that they are usually not compostable and difficult to recycle determines the worsening of environmental problems, such as the increasing volume of waste and its disposal; in terms of pollution, therefore, plastics represent an inextinguishable waste.

With this mind, the utilization of renewable sources and the reuse of waste biomasses represent environmental imperatives, the foundations of new economic models recycling the by-products of various industries and protecting the environment from the long-term effects of pollution.

This PhD project, taking all these considerations into account, regarded the reuse of cellulose waste (Cellulosic Solid Residue – CSR) obtained from different sources, which guarantee a large and reasonably constant availability, namely cotton waste from worn out textiles and cladodes of *Opuntia ficus indica* (OFI, also referred to as Nopal) plants. The experimental procedures carried out aimed to recycle the CSR (zero waste strategy), whit the idea of operating as much as possible in conditions of circular economy, optimizing the low-cost production of valuable substances [Cellulose Nanocrystals (NCC) in the first case, Nopal (mucilage and fibers) in the second one] to be introduced

into different modern materials [Paper and Thermoplastic Starch (TPS) Films] in order to obtain their performance improvement (micro-morphological, mechanical and thermal properties were analyzed). The general objective of the entire work was to identify suitable applications for the specific waste materials mentioned above, of scarce or null economical value, suggesting the optimal processes for their treatment and final reuse, the whole in collaboration with important economic and cultural actors of Marche and Lazio regions (Italy).

Both NCC and Nopal are widely known in the international scientific panorama, as testified by the numerous research studies about their extraction, characterization and application (among all, for NCC: Börjesson and Westman, 2015; Moon et al., 2011; Klemm et al., 2011; Dufresne, 2013; Brinchi et al., 2013; for Nopal: Sepùlveda et al., 2007; Saenz et al., 2004; Del Valle et al., 2005; Gheribi et al., 2018). Regarding Nopal, in particular, it should be remembered that the Italian Research Agency ENEA in Rome (Italy) has been engaged for years in experimentations and projects concerning its use (Persia et al., 2016).
The project-choice of utilizing these materials in the field of papermaking (NCC and Nopal) and biocomposites (Nopal) was justified, for NCC, by the promising mechanical results (tensile strenght and bending number) of a previous work (Coccia et al., 2014) achieved introducing cellulose nanocrystals as reinforcing filler in a Paper sheet, and, for Nopal, by the willingness to investigate new innovative applications (in Paper and TPS) of this high potential material.

The research activies regardind NCC started with the extraction of Cellulose Nanocrystals from different sources (microcrystalline cellulose [Bondeson et al., 2006], bacterial cellulose [Roman and Winter, 2004] and cotton bush [Saraiva Morais et al., 2013]), carried out at the Department of Chemistry, Life Sciences and Environmental Sustainability of the University of Parma (Italy), and the morphological characterization via SEM of the obtained material, in order to validate the correctness of the process.
The second step was the extraction of NCC from cotton textile waste, resulting from discarded materials obtained from the development of pure cellulose paper products at a dedicated technical school (Istituto di Istruzione Superiore – I.I.S. “Merloni Miliani”) in Fabriano (Italy). Materials, methods and results of this study are reported in the here presented 1st Article.
The total NCC solutions obtained were introduced into modern Paper materials, subsequently characterized from a mechanical point of view (double fold test) in order to evaluate their performance improvement. These activities were carried out in collaboration with a specialized

technician of Cartiere Miliani Fabriano S.p.A. (Fabriano, Italy), and data regarding methods and results are available in the here presented Appendix to NCC.

For what it concerns Nopal, the first phase of the project regarded the extraction of mucilage from residues of *Opuntia Ficus Indica* (OFI) plants, namely from cladodes [Sepùlveda et al., 2007], carried out at the Department of Sustainability SSPT of the Italian Research Agency ENEA in Rome (Italy). Extraction processes and scientific analysis executed are described in the here presented 2nd Article. The Nopal solutions obtained were introduced into modern Paper materials, examining Zeta potential and folding resistance so as to check their performance improvement. These activities were carried out in collaboration with a specialized technician of Cartiere Miliani Fabriano S.p.A. (Fabriano, Italy), and data regarding methods and results are available in the here presented Appendix to Nopal.

As regards the application of Nopal (mucilage and fibers from OFI) as filler of Thermoplastic Starch (TPS) Films, all the research activities were carried out at the Department of Sustainability SSPT of the Italian Research Agency ENEA in Rome (Italy).
The first phase of the project involved the self-production of several starch-based composites [Mohammadi Nafchi et al., 2013; Rodriguez-Gonzalez et al., 2004], originating from three different commonly available starch types (potato, corn and rice) and with a variable content in glycerol, in order to select the most appropriate formulation and procedure.
The following step concerned the extraction of mucilage from Opuntia cladodes [Sepùlveda et al., 2007] and its introduction into TPS Films, whose micro-morphological, mechanical and thermal properties were analyzed. Materials, methods and results of this study are reported in the here presented 2nd Article.
With the idea of globally result into a full recycling of the OFI waste, a second study focused on the use of dry Nopal fibers to reinforce the TPS Films [Curvelo et al., 2001; Ma et al., 2005] and their thermal, mechanical, and morphological characterization. The outcomes of these scientific analysis are described in the here presented 3rd Article.
In order to complete the characterization of the obtained materials from the point of view of their biodegradability, it was decided to plan a series of suitable tests in collaboration with the company NOVAMONT S.p.A. of Novara (Italy), interested in patenting the products.

Since the results of these studies were considered of interest to use NCC and Nopal for the restoration of historical Paper artifacts, then it was decided to devote the last part of the research activities to the evaluation of this possibility.

A preliminary multidisciplinary study on handmade Paper manufacts (13^{th} – 15^{th} century) from Camerino-Fabriano area (Marche, Italy) was carried out, in collaboration with the Institute of Chemical Methodologies IMC of the National Research Council of Italy CNR in Rome (Italy), whose outcomes are reported in this thesis (4th Article). The principal aim of this work was the setup of a multi-analytical procedure to perform a diagnostic analysis of Paper samples, so as to proceed with comparative studies between extremely similar materials (before and after NCC and Nopal application) and to evaluate minimal differences or similarities among them.
At the moment, it is being set up an experimental procedure for the introduction of Cellulose Nanocrystals and OFI mucilage into ancient Paper materials, whose results will be available in future works.

Another potencial use of Nopal (mucilage and fibers from OFI) regards ancient Mortar.
The 2016-2017 Central Italy earthquake sequence severely damaged, and in some cases destroyed, several old historic towns in the Abruzzo, Lazio, Marche and Umbria regions, causing the loss of human lives and collapses of a very high number of buildings, churches and architectural monuments. Since the structural behaviour of masonry, particularly under seismic actions, is strongly influenced by masonry bond and mortar quality, then in the last phase of this PhD project it was decided to investigate the application of Nopal (mucilage and fibers from OFI) on ancient Mortar with restoration purpose. This research was widely justified by the numerous studies about the role of Nopal in Mortar performance (among all: Càrdenas et al., 1998; Ventolà et al., 2011; Ravi et al., 2016; Hernandez-Zaragoza et al., 2008).
The outcomes of a preliminary scientific (microstructural, chemical, mechanical and thermal) characterization of Mortar from sites damaged during the recent seismic sequence are reported in this thesis (5th and 6th Articles). The principal aim of these works was the setup of a multi-analytical procedure to perform a diagnostic analysis of Mortar samples, so as to proceed with comparative studies between extremely similar materials (before and after Nopal application) and to evaluate minimal differences or similarities among them.
At the moment, it is being realized the production of Mortars in laboratory, replicating the observed ancient compositions, and set up an experimental procedure for the introduction of Nopal into the obtained materials. The results of this project will be available in future works.

Finally, regarding the application of OFI materials in the field of Computer Science, at the moment it is being set up an experimental procedure for the modification of the TPS-Nopal composites in

view of their possible application in the field of 3D biomaterial printing. The results of this project will be available in future works.

Given the multisciplinary nature of the PhD project, and the multiplicity of methods, analytical techniques and results involved, then it was decided to structure this thesis into two chapters, every one regarding each valuable extracted material (NCC and Nopal) and comprehending all the articles, published or submitted during these years (all the commented papers are authors'final drafts for personal use, and therefore exempt from copyright), reporting the most of the procedures and achievements. The chapter about NCC contains the 1st Article and an appendix in which all the activities concerning the introduction of NCC into modern Paper materials are summarized. The second chapter regards Nopal: it contains the 2nd and 3rd Articles, describing the project about TPS-Nopal composites, and an appendix in which all the activities concerning the introduction of Nopal into modern Paper materials are summarized. Another chapter (4th, 5th and 6th Articles) deals with all the preliminary scientific characterizations carried out on ancient Paper and Mortar, in view of NCC and Nopal future application with restoration purposes. In the conclusions, the general results of the PhD project are discussed, while in the reference list are reported all the sources not mentioned in the articles.

Extraction of Cellulose Nanocrystals (NCC) from Cotton Waste and Morphology of NCC Obtained with Different Alkali Neutralization

Current Journal of Applied Science and Technology

Fabrizio Scognamiglio[1], Carlo Santulli[2*] and Graziella Roselli[1]
1 School of Science and Technology, Chemistry Division, University of Camerino, Via S. Agostino 1, 62032 Camerino, Italy
2 School of Architecture and Design, University of Camerino, Viale della Rimembranza 9, 63100 Ascoli Piceno, Italy
* Corresponding author. E-mail: carlo.santulli@unicam.it

Regarding the contribution of the PhD student Fabrizio Scognamiglio to the presented article, he managed the literature search and performed the statistical analysis.

Original Research Article

Abstract

The extraction of cellulose nanocrystals (NCC) from cotton textile waste, constituted by 70% long fibers and 30% cotton linter, was performed through the action of sulfuric acid followed by solution neutralization with two different alkalis, namely ammonia and sodium bicarbonate, which yielded microcellulose (MCC), then centrifuged to NCC. The action of the two alkalis was compared as for fiber repeatability and morphology, and the results obtained using ammonia were considered more suitable for possible introduction of NCC for the repair of historical paper artifacts. This evidence was obtained by applying optical/polarized light microscopy observation and dynamic light scattering (DLS) results.

Keywords: cotton waste; nanocellulose extraction; alkali neutralization; Dynamic Light Scattering (DLS)

1. Introduction

Extraction of cellulose nanocrystals (NCC) from cellulosic solid residue (CSR) represents an important way of upcycling it, therefore obtaining a material with some value, hopefully with a reasonable yield that would make the extraction worthwhile. Overtime the extraction of NCC has been performed from wastes obtained from the productive systems of different natural fibers, with the idea of operating as much as possible in conditions of circular economy, therefore using a zero waste strategy [1]. A common procedure for the purpose used involves the use of an acid solution, so to obtain hydrolysates of the waste stream: this is most frequently performed with sulfuric acid, and then neutralized using an alkaline solution [2]. Cellulosic waste stream from which NCC have been extracted includes, among others, materials from a large number of plants, in particular oil palm [3], pineapple leaves [4], Phormium tenax [5], hemp [6], okra bahmia [7], etc. In most cases the application of NCC, once extracted, has been their use as the reinforcement of polymer matrices, such as poly(vinylalcohol) (PVA) [8], etc. More recent studies have broadened even more the range of fibers, which can provide waste material for NCC extraction, with very variable yield, due to the different characteristics of plants, such as it is shown for example in [9-11].

In terms of practical use though, one of the main cellulosic products is represented by cotton, which is an abundant waste from textiles production and is basically almost pure cellulose, reaching up to 90% in weight. Cotton normally used in the textile industry is in the range that is indicated as medium length fibers, hence between 18 and 28 mm long. In contrast, shorter (cotton linter) and longer fibers are mostly considered as waste, therefore it can be deemed suitable for the extraction of nanocellulose.

In general terms, it proved effective for the purpose, whether colored or not, despite some differences in yield, in sulfonation efficiency and thermal stability [12]. More specifically, a study on the extraction of NCC from cotton linter originating from Brazil did demonstrate that controlling waste stream for extraction may result in a more uniform quality product: cotton linter is particularly adapted, in that it does not require pulping before extraction [13].

The particular aim of this study is to extract and characterize the morphology of cotton waste used, which results from discarded materials obtained from the development of pure cellulose paper products at a dedicated technical school in Fabriano, Italy. The idea is to possibly use the nanocellulose resulting as a material for restoration of precious ancient paper artifacts. However, the present work concentrates on the feasibility of the method and on the morphology of nanocellulose obtained using two different alkalis, namely sodium bicarbonate and ammonia.

2. Materials and Methods

2.1 Extraction

Crystalline nanocellulose (NCC) has been extracted starting from a raw mixed waste material consisting approximately of 100 mL of 70% long bleached fiber from cotton mass and 30% short fiber from cotton linter with bulk density of 0.6 g/mL; this yielded 2.9 g of cellulose through hydrolysis with 110 mL of H_2SO_4 96 wt%, T = 45°C ÷ 50°C, mechanical stirring, t = 3h 45 min) followed by the addition of 600 mL of icy distilled water to stop the hydrolysis. After this, decantation for one night was performed, followed by cycles of centrifugation (7000 rpm, t = 30 min) and washing with distilled water until a neutral pH is achieved. The final stage was composed by dialysis and sonication. The total NCC solution (approximately 150 mL) obtained was characterized by dynamic light scattering (DLS).

Two different alkalis, namely sodium bicarbonate and ammonia, were attempted to neutralize the solution, with attention to have the most repeatable and less dispersed fiber morphology. The neutralization was carried out with sodium bicarbonate according to the reaction:

$$2NaHCO_3 + H_2SO_4 \leftrightarrow Na_2SO_4 + 2H_2CO_3$$

and using ammonia according to the reaction:

$$2NH_3 + H_2SO_4 \leftrightarrow (NH_4)_2SO_4$$

2.2 Dynamic Light Scattering (DLS)

Different microscopy images have been acquired, at magnifications between x10 and x20, from a MT9200 Meiji Techno Co., Japan, polarized light optical microscope, equipped with a DeltaPix camera, subsequently Dynamic Light Scattering using a Malvern Zetasizer analyzer to obtain a size distribution of the fiber obtained.

Dynamic Light Scattering (DLS) is a non-invasive technique for the measurement of the dimension of molecules, nanoparticles or colloids, at dimensions under the micron and in this specific case it has been used to measuring the hydrodynamic diameter following from diffusion measurements, according to the Stokes-Einstein equation [14]. To obtain different evaluations of the cellulose fibers sizes, for a sounder reliability of the test, three DLS measurements were carried out on a 1 mL solution. The second and the third measurements were performed after 5 and 10 minutes from the first one, respectively.

Since the extraction yielded microcrystalline fibers, these underwent further to a centrifugation cycle at 7000 rpm, for 30 minutes, as reported above, in order to separate the dimensionally larger fraction from the supernatant, which constituted the nanometric fraction.

3. Results and Discussion

After the process of sulfonation and subsequent neutralization, microcellulose was obtained, whose characteristics are reported in Figs. 1-2 (ammonia neutralization) and Figs. 3-4 (sodium bicarbonate neutralization). In Figs. 1 and 3 fiber distribution in a drop of solution is shown under polarized light. In the case of ammonia neutralized microcellulose fibers, a considerable part of the material extracted has similar optical properties, yielding a more uniform color over fiber surface. This indicates both that their surface is even, and that they are also mechanically more regular. Also the limited presence of detached parts from the fiber suggests the possibility of a more frequent cylindrical geometry for fibers in Fig. 1 than in Fig. 3. Aspect ratios i.e., length/diameter of the fibers, appear to be the most various, although in general they are for both neutralization methods mostly above 10, therefore providing some prospective reinforcement effect for the introduction in a polymer matrix, such as e.g., poly(vinylalcohol) (PVA) [15]. In Figs. 2 and 4 some isolated fibers are depicted under normal light. In this case, striations were in particular observed in the micrographs, which are an indication that orientation of the filaments occurred, producing material with fibrillar morphology. This would lead as a result to a higher effect of tensile reinforcement for the microfiber, provided filaments not tend to be at an angle or detach from the bulk of the fiber, a case which is termed as “fibrillation” and

leads to more mechanical inconsistency [16]. Fibrillation appears more frequent with the sodium bicarbonate neutralized fibers in Fig. 4.

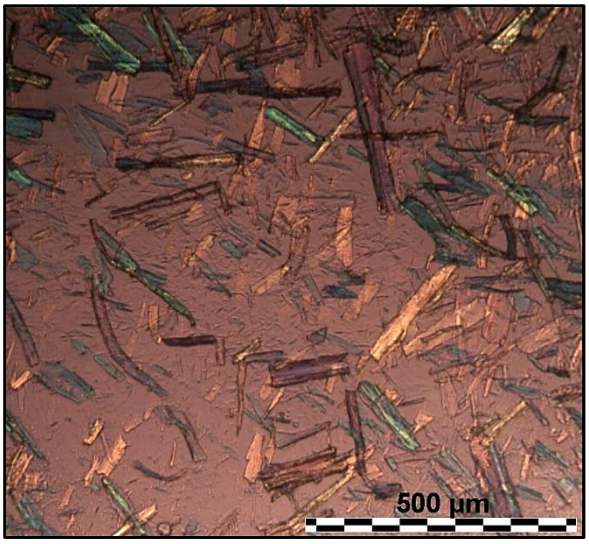

Fig. 1. Optical polarized light micrograph of cellulose extracted using NH_3 neutralization, before centrifugation

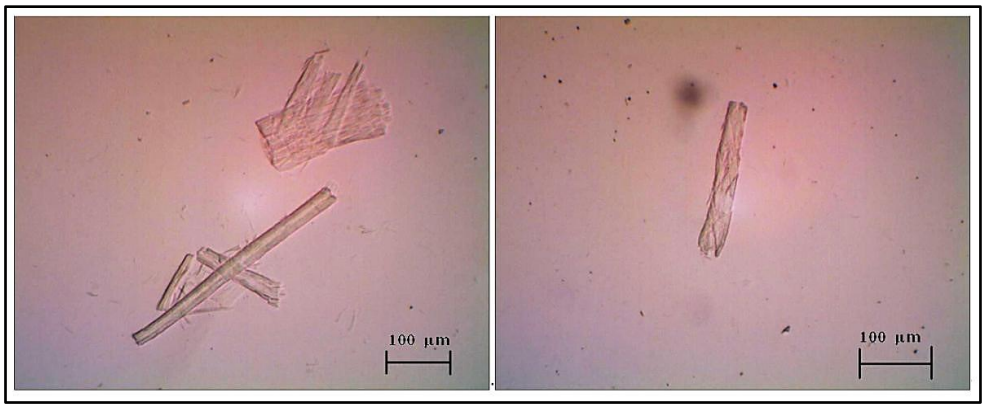

Fig. 2. Optical micrograph of cellulose extracted using NH_3 neutralization, before centrifugation

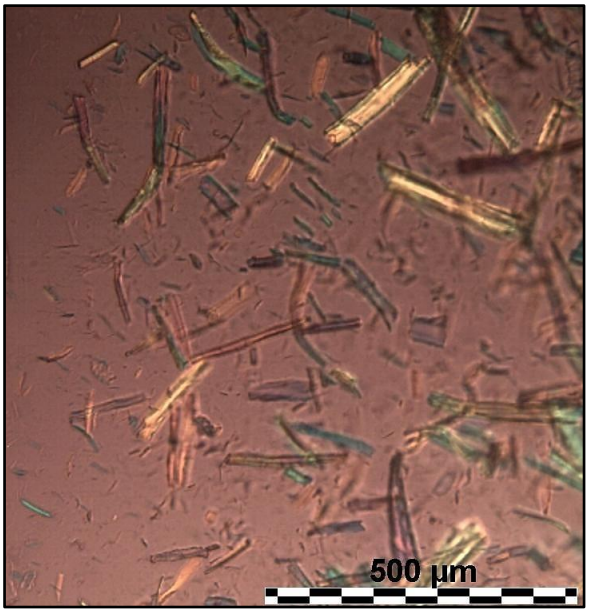

Fig. 3. Optical polarized light micrograph of cellulose extracted using $NaHCO_3$ neutralization, before centrifugation

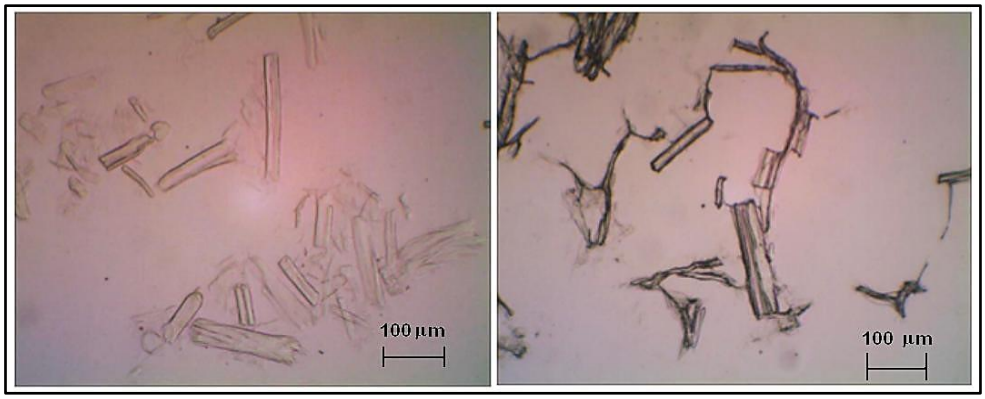

Fig. 4. Optical micrograph of cellulose extracted using $NaHCO_3$ neutralization, before centrifugation

The distribution of the fibers, as from DLS graph, did appear to present a number of peaks and also the three measurements on the same solution did not appear to be superposed, which suggests a scarce reliability of the measure, for neutralization with both alkalis (Fig. 5 for ammonia and 6 for sodium bicarbonate). This is considerably worsened in the case of neutralization with sodium bicarbonate, where the peaks revealed do not appear having any real correspondence in the three tests carried out.

As it is possible to notice in Fig. 7, referred to ammonia-extracted fibers, the fibers obtained after centrifugation are of nanometric dimension and therefore not apparent in the optical microscope image at 20x magnification.

After centrifugation, the evaluation carried out using DLS confirm the superiority of ammonia neutralization also in the case of NCC, since the dimensions appear more repeatable and less scattered with a statistical mode consistently in the region of 500 nm (Fig. 8). In contrast, in the case of sodium bicarbonate neutralization, it has been observed that the above statistical mode is only clearly indicated in one of the three measurements, in the other cases the values are still quite dispersed and confused (Fig. 9).

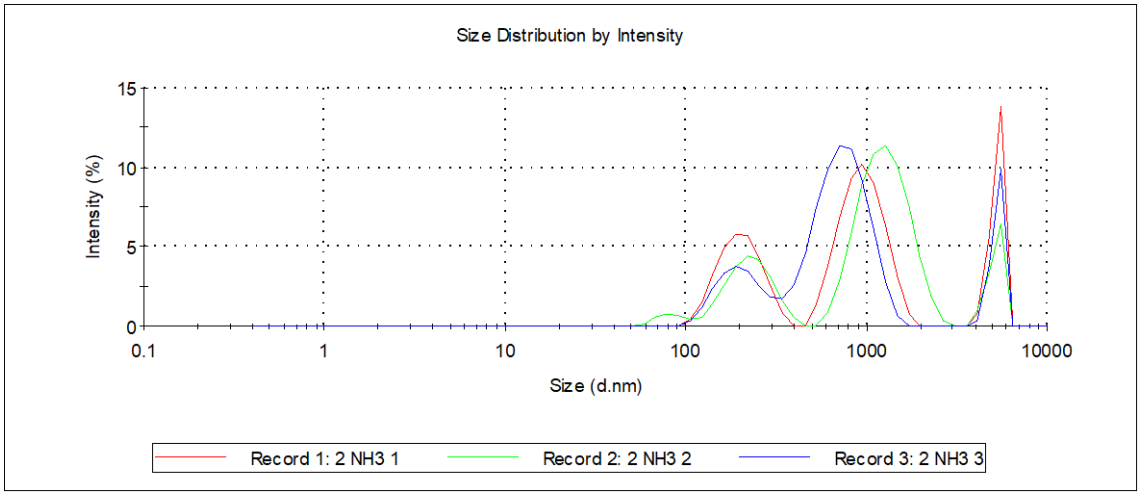

Fig. 5. DLS distribution of cellulose extracted using NH_3 neutralization, before centrifugation

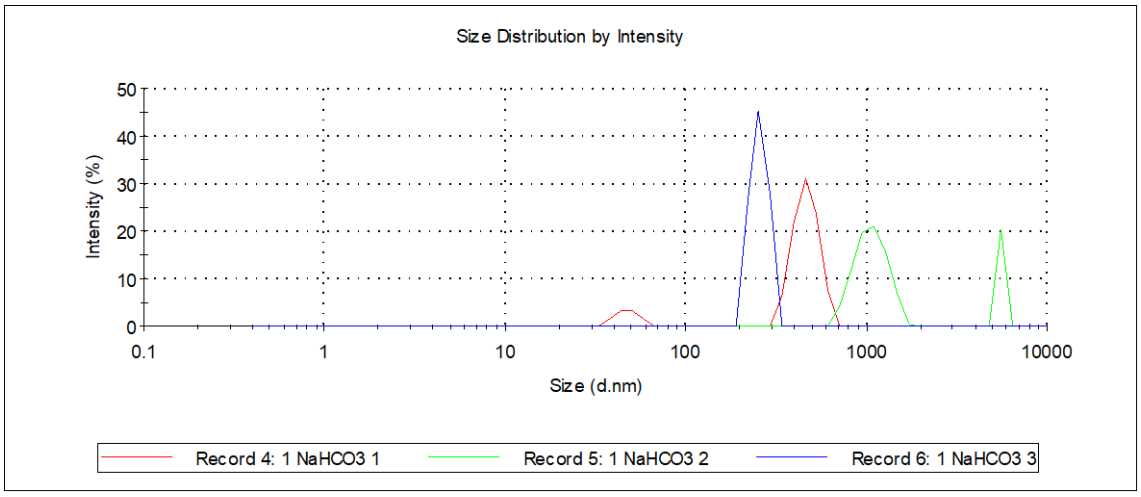

Fig. 6. DLS distribution of cellulose extracted using $NaHCO_3$ neutralization, before centrifugation

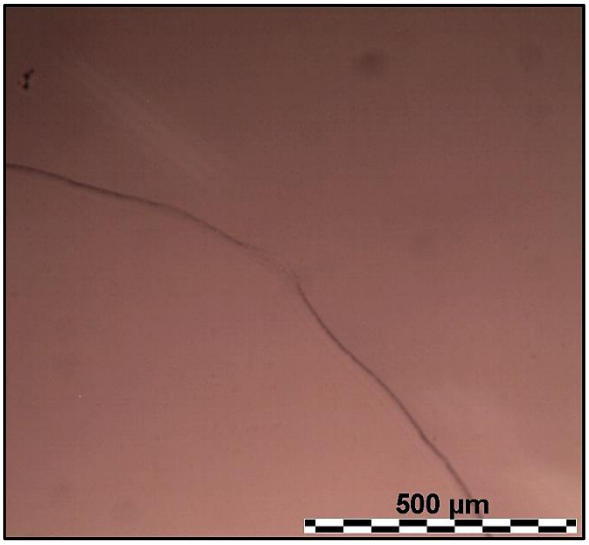

Fig. 7. Micrograph of cellulose extracted using NH_3 neutralization

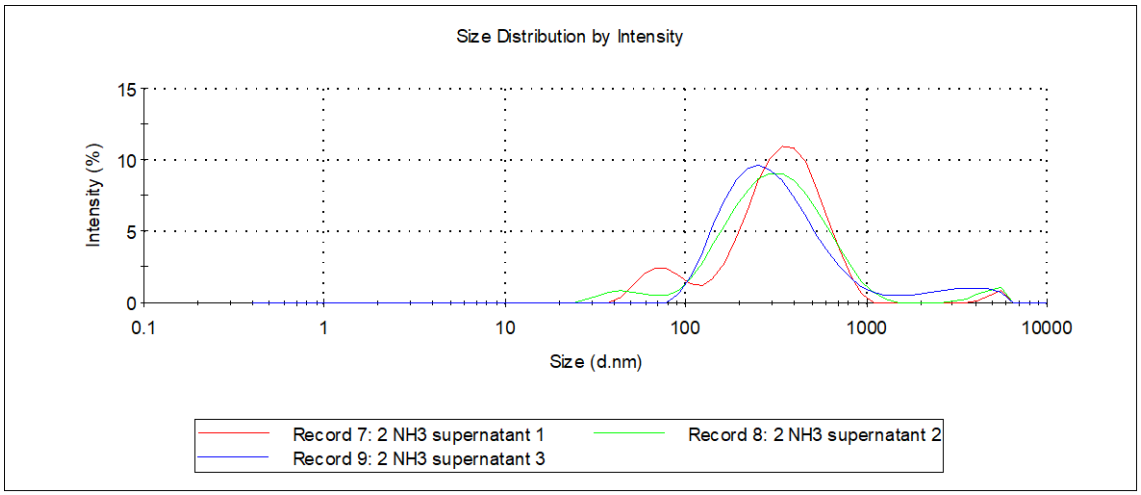

Fig. 8. DLS distribution of cellulose extracted using NH_3 neutralization, after centrifugation

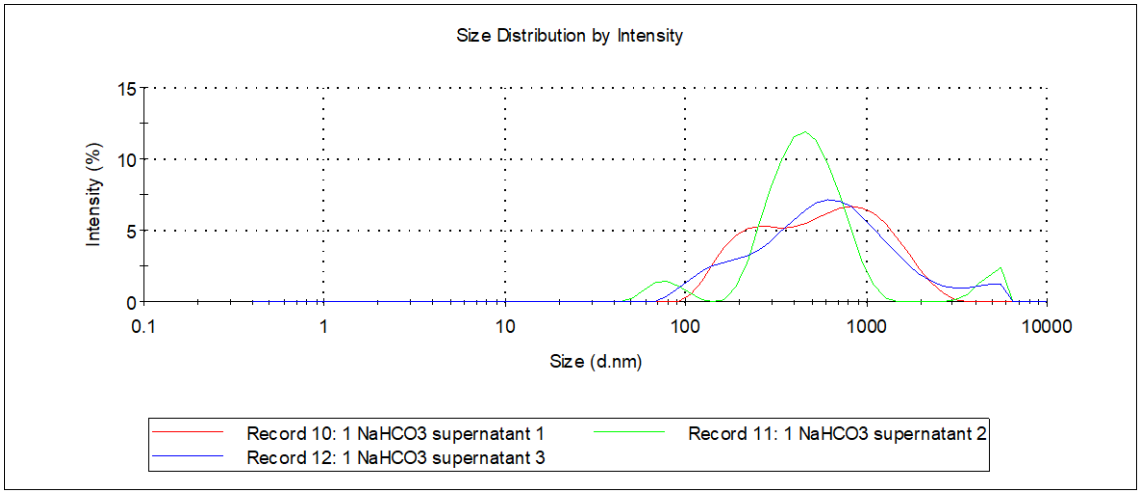

Fig. 9. DLS distribution of cellulose extracted using $NaHCO_3$ neutralization, after centrifugation

4. Conclusion

The extraction of cellulose nanocrystals (NCC) from cotton textile waste (70% long fibers and 30% cotton linter) through the action of sulfuric acid followed by solution neutralization with two different alkalis, namely ammonia and sodium bicarbonate proved effective in general terms. This yielded microcellulose (MCC) of good quality and uniformity, although in the latter case the fibers were thinner and of less regular shape than in the former one. A subsequent action of centrifugation led to obtaining NCC. Comparing the action of the two neutralizing alkalis, the materials obtained using ammonia can be considered superior. The evidence provided by optical/polarized light microscopy observation and dynamic light scattering (DLS) results suggested a higher geometrical regularity and fibrillar adhesion, together with a lower dimensional dispersion with respect to those yielded by applying sodium bicarbonate neutralization. The result of this study, hence the superiority of ammonia for the neutralization process, is considered of interest to prepare the procedure of extraction for the introduction of NCC for the repair of historical paper artifacts.

Competing Interests

Authors have declared that no competing interests exist.

Acknowledgements

For useful advice and availability of the testing labs, the authors wish to acknowledge the contribution of Dr. Serena Gabrielli, Dr. Cristina Cimarelli and Prof. Enrico Marcantoni, of the School of Science and Technology, University of Camerino, and for DLS distribution tests of Dr. Stefania Pucciarelli, of the School of Biosciences and Veterinary Medicine, University of Camerino.

References

1. Wang Q, Zhu JY, Considine JM. Strong and optically transparent films prepared using cellulosic solid residue recovered from cellulose nanocrystals production waste stream, ACS Appl Mater Interfaces. 2013;5(7):2527-2534.
2. Bondeson D, Mathew A, Oksman K. Optimization of the isolation of nanocrystals from microcrystalline cellulose by acid hydrolysis, Cellulose 2006; 13:171.
3. Lani NS, Ngadi N, Johari A, Jusoh M. Isolation, characterization and application of nanocellulose from oil palm empty fruit bunch fiber as nanocomposites. J Nanomater. 2014;13.
4. Cherian BM, Leão AL, Ferreira de Souza S, Thomas S, Pothan LA, Kottaisamy M. Isolation of nanocellulose from pineapple leaf fibres by steam explosion, Carbohydr Polym. 2010;81(3):720-725.
5. Fortunati E, Puglia D, Monti M, Santulli C, Kenny JM. Extraction of cellulose nanocrystals from Phormium tenax fibres, J Polym Envir. 2013;21(2):319-328.
6. Luzi F, Fortunati E, Puglia D, Lavorgna M, Santulli C, Kenny JM, Torre L, Optimized extraction of cellulose nanocrystals from pristine and carded hemp fibres, Ind Crops Prod. 2014;56:175–186.
7. Fortunati E, Puglia D, Monti M, Santulli C, Maniruzzaman M, Kenny JM. Cellulose nanocrystals extracted from okra fibres in PVA nanocomposites. J Appl Polym Sci 2013;128(5):3220–3230.
8. Coelho de Carvalho Benini KC, Cornelis Voorwald HJ, Hilário Cioffi MO, Milanese AC, Ornaghi Jr. HL, Characterization of a new lignocellulosic fiber from Brazil: Imperata brasiliensis (Brazilian Satintail) as an Alternative Source for Nanocellulose Extraction, J Natural Fib. 2017;14(1):112125.
9. Mariño M, Lopes da Silva L, Durán N, Tasic L, Enhanced Materials from Nature: Nanocellulose from citrus waste. Molecules. 2015;20(4):5908-5923.
10. Szlapak Franco T, Potulski DC, Viana LC, Forville E, de Andrade AS, Bolzónde Muniza GI, Nanocellulose obtained from residues of peach palm extraction (Bactris gasipaes), Carbohydr Polym. 2019;218:819.
11. Fortunati E, Luzi F, Puglia D, Terenzi A, Vercellino M, Visai L, Santulli C, Torre L, Kenny JM. Ternary PVA nanocomposites containing cellulose nanocrystals from different sources and silver particles: Part II, Carbohydr Polym. 2013;97(2):837–848.
12. De Morais Teixeira E, Corrêa AC, Manzoli A, de Lima Leite F, Ribeiro de Oliveira C, Capparelli Mattoso LH. Cellulose nanofibers from white and naturally colored cotton fibers, Cellulose. 2010;17(3):595–606.

13. Saraiva Morais JP, Morsyleide de Freitas R, Moreira de Souza Filho M, Dias Nascimento L, Magalhães do Nascimento D, Ribeiro Cassales A. Extraction and characterization of nanocellulose structures from raw cotton linter, Carbohydr Polym. 2013;91(1):229-35.
14. Pecora R. Dynamic light scattering measurement of nanometer particles in liquids. Journal of Nanoparticle Research. 2000;2(2):123–131.
15. Lee SY, Jagan Mohan D, Kang IA, Doh GH, Lee S, Ok Han S. Nanocellulose reinforced PVA composite films: Effects of acid treatment and filler loading. Fibr and Polym. 2009;10(1):77– 82.
16. Haapala A, Laitinen O, Karinkanta P, Liimatainen H, Niinimaki J, Optical characterisation of size, shape and fibrillarity from microfibrillar and microcrystalline cellulose and fine ground wood powder fractions, Appita Technology, Innovation, Manufacturing, Environment. 2013;66(4): 331-339.

Appendix to NCC

The NCC application in modern Paper materials, carried out at the Cartiere Miliani in Fabriano (Italy), was executed in several steps:

- Blue dyeing of the fibers, in order to visually detect their presence after the introduction into the hosting material.
- Surface treatment: each NCC solution (NH_3 and $NaHCO_3$ neutralization) was applied on both surfaces of a paper strip (width: 20 mm) previously impregnated with poly(vinylalcohol) (PVA, widely recognized as the strongest binder available in modern paper industry) (fig. 1).
- Preconditioning chamber, in which the samples were exposed to circulating air at 23 °C and 50% RH.
- Mechanical characterization, in order to evaluate the effects of NCC introduction. Double fold test (Table 1) was performed: it measures the resistance of paper to breaking repeated folding under standardized conditions; the sample is folded first backwards and then forwards about the same line, i.e. one complete oscillation (Baker, 2001).

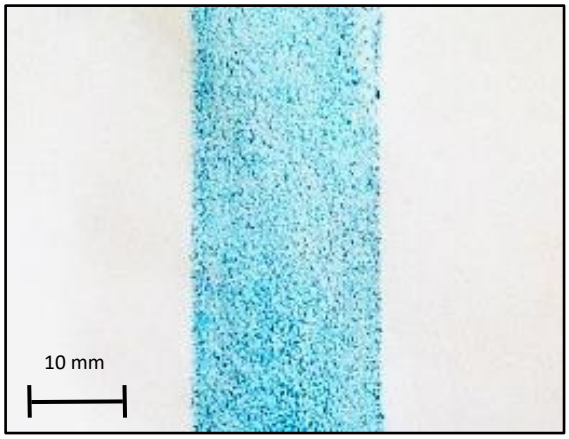

Fig. 1. Paper strip after the surface treatment with a blue dyed NCC solution

Table 1 – Number of double folds (*d*) for paper samples after NCC addition

Sample	***d***
Paper	50
Paper + PVA	299
Paper + PVA + NCC (NH_3 neutralization)	166
Paper + PVA + NCC ($NaHCO_3$ neutralization)	107

The analysis highlighted that the contribution of NCC to the mechanical resistance of modern Paper (Paper + PVA in Table 1) was negative. Nevertheless, the results obtained with the combined application of PVA+NCC, in particular that extracted using NH_3 neutralization, were quite appreciable if compared to that of raw material (Paper in Table 1). This outcome was considered of interest to evaluate the possible use of NCC for the restoration of ancient Paper: the principal aim of this research would be that of reducing the quantity of synthetic PVA utilized in this field, in favor of a natural product obtainable from a plurality of different renewable sources.

Thermoplastic starch (TPS) films added with mucilage from *Opuntia Ficus Indica*: mechanical, microstructural and thermal characterization

Materials

Fabrizio Scognamiglio[1], Daniele Mirabile Gattia[2], Graziella Roselli[3], Franca Persia[2], Ugo De Angelis[2] and Carlo Santulli[4*]

1 School of Science and Technology, Technologies and Diagnostics for Conservation and Restoration Laboratory, University of Camerino, Via Pacifici Mazzoni 2, 63100 Ascoli Piceno, Italy

2 Department of Sustainability SSPT – ENEA – Casaccia Research Center, Via Anguillarese 301, 00123 Rome, Italy

3 School of Science and Technology, Chemistry Division, University of Camerino, Via S. Agostino 1, 62032 Camerino, Italy

4 School of Science and Technology, Geology Division, University of Camerino, Via Gentile III da Varano, 62032 Camerino, Italy

* Corresponding author. E-mail: carlo.santulli@unicam.it

Regarding the contribution of the PhD student Fabrizio Scognamiglio to the presented article, he managed conceptualization, methodology, writing-original draft preparation, writing-review and editing.

Abstract

Opuntia cladodes are a typical vegetable waste, from which a mucilage in gel form can be extracted. This work proposes blending it with a self-produced thermoplastic starch (TPS), originating from potato starch with a high content in glycerol (ca. 30%). Three methods were compared for extraction, bare maceration (MA), mechanical blending (ME) and mechanical blending following maceration (MPM) to produce films with an approximate thickness of 150 microns. For the comparison, tensile testing, differential scanning calorimetry and scanning electron microscopy were used. The MPM process proved the most effective, not only for extraction yielding, but also to obtain a larger deformation of the samples with respect to the one allowed by the pure TPS films. However, the mechanical performance is still quite poor, and the expected effect of the calcium and magnesium salts contained in the mucilage to improve the rigidity of the TPS film was not really revealed. Prospected improvements would concern the fabrication process and the investigation of other possible loading modes and sample geometries.

Keywords: cactus mucilage; thermoplastic starch; bioplastics; extraction process

1. Introduction

Opuntia Ficus Indica, also referred to as "nopal", is a plant used in many countries e.g., around the Mediterranean Sea, but also in colder countries, both for ornamental value and for the production of Indian figs, which amount in Italy, according to data supplied from the National Institute of Statistics (ISTAT), to around 750,000-900,000 quintals per year. In most cases, be it for fruits production or for ornamental purposes, it is essential that Opuntia plants are pruned during the winter with the removal of cladodes i.e., flattened leaf-like stems, which include a mucilage rich also in inorganic components, such as calcium carbonate compounds, and therefore of wide industrial interest for their bioavailability [1]. A number of uses have been suggested for mucilage, a highly branched heteropolysaccharide, for example as an industrial hydrocolloid as a source of cellulosic fibers, which could have a dietary value when fresh [2]. Another possible use of the mucilage is an industrial hydrocolloid, in which case the extraction method followed presents some importance on its rheological properties [3]. In particular, as far as rheology is concerned the viscous response appears to be predominant at low frequencies, while the elastic ones dominates at high frequencies [4]. In recent years, the food packaging industry has become widely interested in cactus mucilage, proposing its application by developing films and coatings with it [5]. The advantage of using this mucilage, as close as possible to its natural state, only removing the spines and the most fibrous parts would be its perfect adaptability to contain food, up to the point that even edible films based upon it have been

proposed [6]. Plasticizers are normally applied for the purpose of film fabrication, the most diffuse of which is glycerol, normally affecting neither food preservation nor the edibility characteristics, though slightly reducing films' rigidity [7].

However, in practical terms, one of the most diffuse applications for cactus mucilage is its use in a blend with another biopolymer of industrial origin. In previous studies, one of the most suitable candidates appeared to be poly(vynilalcohol) (PVA), which was able to yield, in combination with corn starch and glycerol, nopal mucilage films stable up to above 150 °C [8]. Trying to optimize the respective contents of chitosan, PVA and mucilage in the films to improve their resistance, the introduction of more chitosan proved beneficial for the scope [9]. Despite these limitations, using the sole Opuntia mucilage with plasticizers to try to obtain a structural biopolymer film appears to be of an interest, in particular as regards the idea to use as much as possible waste material of biological origin, such as that from the cladode. Attempts have been performed of this way of proceeding, referred to as the production of "Do-It-Yourself (DIY) bioplastics", mainly based on the introduction of different types of waste. This proved adapted to some uses, such as packaging, biomedical or other structural applications, such as coating, despite the limitation of being hardly able to be used above the gelling temperature of starch e.g., around 80°C [10-12].

This work proceeds from an extensive study over Opuntia cladode waste, with the idea of globally result into a full use of the material obtained. In particular, the crystalline fraction of the cellulose content was disposed of by obtaining nanocellulose fibers [13], while a second study concerned the use of dry nopal fibers to reinforce a starch-glycerol thermoplastic polymer [14]. Here, the examination is completed by evaluating the mechanical and thermal characteristics of Opuntia mucilage extracted with different methods to be introduced again in a TPS matrix.

2. Materials and Methods

2.1 Mucilage extraction and preliminary measurements

The procedures adopted to extract the mucilage, from the raw material obtained from the cladode, shown in Figure 1, are three:

- Maceration (MA): isolation and cutting of parenchyma in approximately cubic pieces of around 1 cm side (Figure 2), and maceration in distilled water (1 g per ml of parenchymal material) for 24 hours in the dark, and separation of the macerated material by different filtration stages, from 2 mm to 250 microns mesh. The macerated material is depicted in Figure 3, after filtration.

- Mechanical (ME): the cubic pieces of isolated parenchyma are mechanically treated in an immersion blender for extraction.
- Mechanical post-maceration (MPM): extraction was performed using an immersion blender using the macerated material separated by filtration. This would allow using as much as possible the parenchymal material.

In all cases, the pH of the extracted mucilage was in the region of 4.7 ± 0.3, without significant changes. As expected, its behavior was that of a non-Newtonian fluid, and the viscosity of the solution was measured, yielding results in the region of 10 cps for MA extraction, 150 cps for MPM extraction and 220 cps for ME extraction.

Following extraction, the concentration of the mucilage has been carried out in an oven at 70-75 °C until the complete evaporation of water is achieved, which takes several hours, followed by cooling down at ambient temperature. In this way, different concentrations are obtained: in particular for MA extraction, the concentration is 8±0.5 g of dry mucilage/l, for MPM extraction is 21±1.5 g/l, and for ME extraction is 12±3 g/l. This suggests that in any of the three cases, the concentration of the mucilage led to the removal also of water linked into further components of mucilage, such as carbohydrates, because the amount of free water in the cladode is between 88 and 95% [15]. Despite this, the most conservative approach appears to be MPM extraction.

To summarize, in view of the production of the films, mechanical extraction gives more concentrated mucilage solutions, yet makes more difficult the processing in view of their higher viscosity.

Figure 1. Cladodes after cutting for mucilage isolation, before starting the different procedures

Figure 2. Pieces of isolated parenchyma in a distilled water solution for maceration

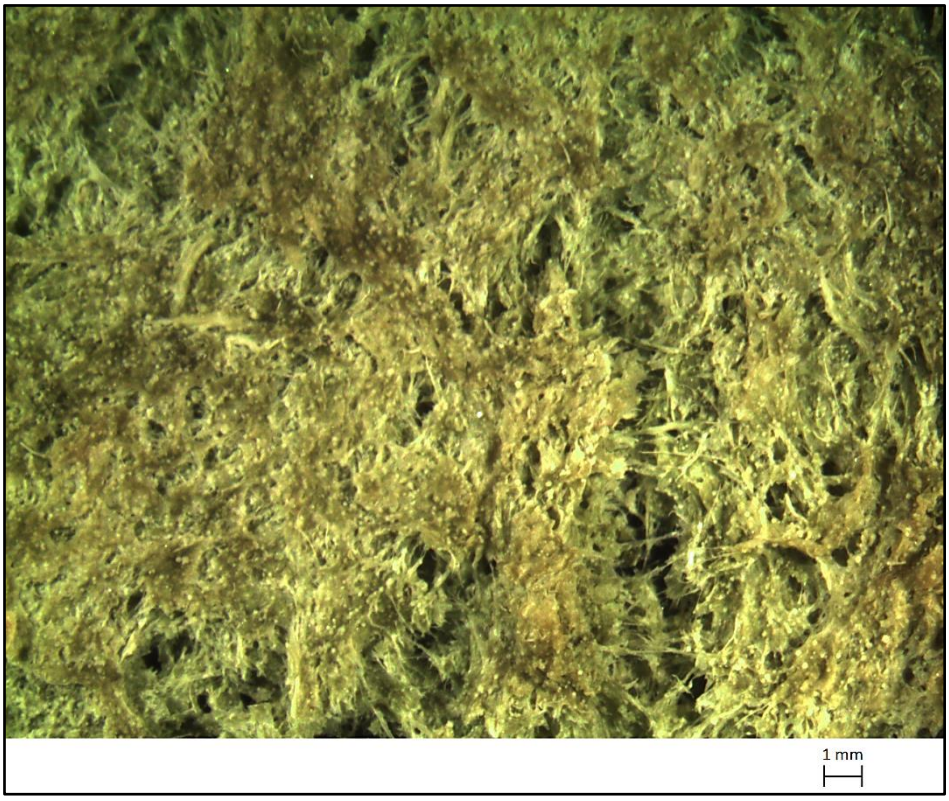

Figure 3. Material retained after 250 microns mesh filtering

2.2 Films' preparation

A number of films were prepared:

- A thermoplastic starch (TPS) film was prepared by using 10 g of sieved potato starch, filtered under a 250 microns mesh, as to remove moisture-generated lumps, containing 23 wt.% amylose, 25% dry matter and with an average granule dimension of 50 microns, and 4 ml of glycerol, reagent grade, in 400 ml of distilled water. The solution was stirred manually for approximately 10 minutes, until its appearance is uniform. It was then subsequently poured in an uncovered steel mold with the surface covered in Teflon, to ease demolding, and then kept there for an hour at 70 °C, and finally at 45 °C overnight.
- Nopal films with 10 g of sieved potato starch and 4 ml of glycerol, reagent grade, in 400 ml of nopal mucilage, which therefore replaces distilled water, using the same procedure for production, as before. Three different nopal films were produced using the different extraction procedures, therefore defined as *maceration (MA)*, *mechanical (ME)* and *mechanical post-maceration (MPM)* films, respectively.

Optical microscopy of the mucilage was carried out, after drying it completely at 75 °C in an oven.

2.2 Films' characterization

The measurements carried out involved, apart from basic morphological characterization, such as film thickness measurement, other sounder methods of analysis, which included in particular:

- Optical microscopy and scanning electron microscopy (SEM) of the films as received, to evaluate their morphology and after tensile tests, to study the fracture surfaces. The SEM apparatus used was a Zeiss EVO MA15. Using SEM, also a qualitative analysis of the elements present on the surface was carried out by EDS (energy dispersive X-ray spectrometry).
- Tensile tests were performed using the Testometric model MICRO 350 5 kN system, with a 50 N load cell. Tests were carried out in displacement control mode at a cross-head velocity equal to 2 mm/minute, using dog-bone specimens with a gauge length equal to 40 mm. Typical dimensions of the samples are shown in Figure 4.
- Differential scanning calorimetry (DSC) to evaluate the evolution of the films' behavior with temperature by heating at a rate of 10°C/minute, from 25 to 180°C, using the Mettler Toledo HPDSC system. Temperatures for the different transition moments (i.e., onset, peak and ending temperature) were determined using the first derivative of the heat capacity calculated from DSC.

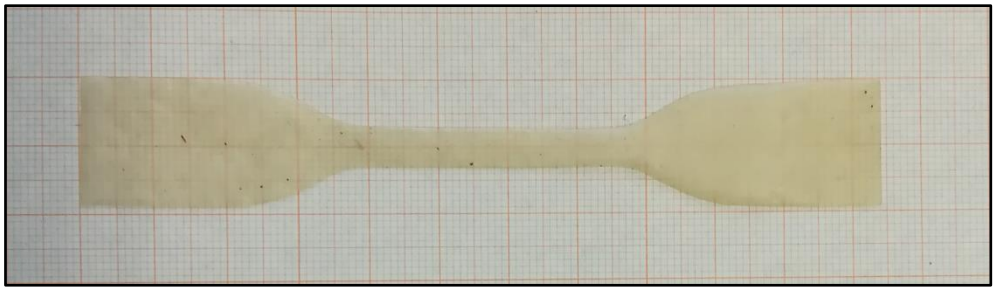

Figure 4. Typical dog bone dimensions (in the image a MA film sample is shown as an example)

3. Results

In general terms, the use of cladode material, which is worn out and therefore with a high level of maturity, would imply the presence into it of high levels of calcium salts, as suggested e.g., in [16]. In practice, the possible use of nopal mucilage dispersion to produce edible gels, which requires sufficient strength, despite its viscoelastic behavior, does depend on the combined presence of gel-promoting cations, such as Ca^{2+}, with sucrose, resulting in calcium-rich polysaccharides, generally defined as pectins [17]. This gives a strong gelling capacity, defined as the presence of "egg-box" junctions [18]. The optical micrographs of the dried mucilage samples did indicate the presence of very regular three-dimensional structures, of dendritic type, as revealed from Figure 5. Previous studies had been reported that the content of calcium not included in ashes in nopal mucilage is close to 10%, mainly represented by calcium oxalates [19].

The comparison between the three films obtained by blending TPS with the same amount of mucilage needs starting from the consideration that the MPM film offers in principle a better yield in terms of extraction of mucilage over the waste, as reported in Section 2.1. Thickness values are reported in Table 1. It is noteworthy that the MA films obtained, besides being in general terms slightly thicker, does also present very thinner ends, which were removed from the plates and excluded from thickness calculation, and in practice not used for tensile testing and other observations.

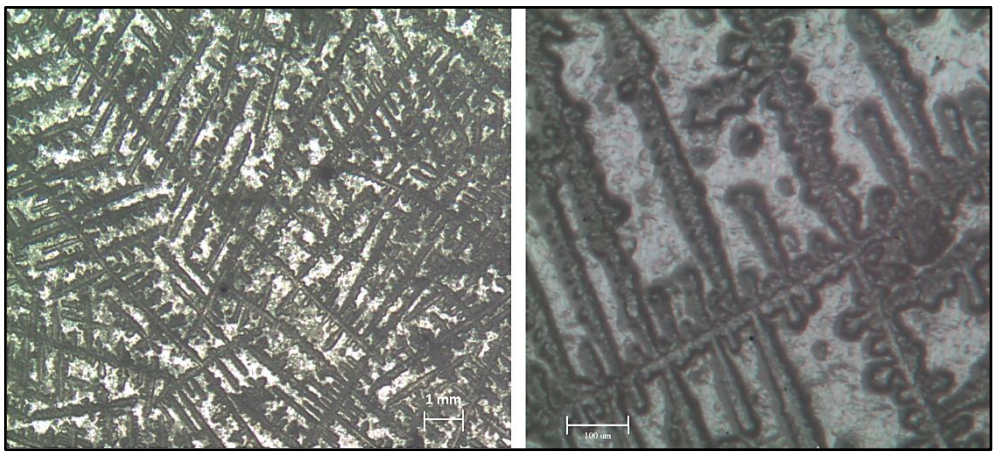

Figure 5. Optical micrographs of dry Opuntia mucilage at different magnifications: 7x (left) and 90x (right)

Table 1 – Thickness of TPS and TPS-nopal mucilage films

Material	Thickness (mm)
TPS	0.125 ± 0.015
MA FILM	0.150 ± 0.009
ME FILM	0.145 ± 0.01
MPM FILM	0.139 ±0.008

After obtaining the films, macrographs of surfaces of differently produced mucilage-TPS blend films have been taken. The respective colors would suggest that the one which achieved the least effective homogenizing was the MA film, which retained also more markedly the original color of the waste used, whereas the best one is the MPM one (Figure 6). Tensile data indicate a large variability between the samples, which could be attributed though to the use of TPS, since the latter does show it as well, as from Figure 7. On the other side, it is evident that the structure of the mucilage does allow obtaining a substantial increase of final elongation, when more thoroughly mixed, therefore for MA and MPM films (Table 2). Examining the morphology of tensile failure, as from Figure 8, it appears that TPS is evidently brittle, with a straight line of fracture, whereas in the cases of films with nopal mucilage the lines are always somehow curved, therefore it can be suggested that the filler has some toughening effect. The three different composite films including nopal mucilage were also compared by microscopically observing their edges after tensile fracture (Figure 9). This enabled to carry out the evaluation of the effectiveness of the different extraction procedures on the performance of the final composites. In particular, only the MPM film did not indicate any sign of fibrillation i.e, separation of fibrils around the boundaries of the elementary fibers, during fracture, typical of polysaccharide-based fibrous materials, such as vegetable fibers [20]. The most critical situation was then observed for the ME film, which appeared to be split over the section, during most probably to the presence of air introduced as the consequence of the mechanical extraction of the mucilage, performed starting directly after cutting the pieces of parenchyma into cubes.

Thermoplastic starches rich in glycerol, like the one used in this investigation, which has a starch/glycerol ratio of 2.5, have characteristically a glass transition temperature below ambient temperature, which means having a thermal transition temperature depending on melting of crystallites [21]. This was determined by DSC (curves are reported in Figure 10 and results are given explicitly with an accuracy of ± 0.5°C in Table 3). It appears that the insertion of nopal mucilage tends in the case of ME films to shift the thermal transition towards higher temperatures, which would in principle extend the usability of the material, though on the other side its mechanical performance does constitute another limitation. Less significant are the differences obtained in the cases of other blended films, MA and MPM.

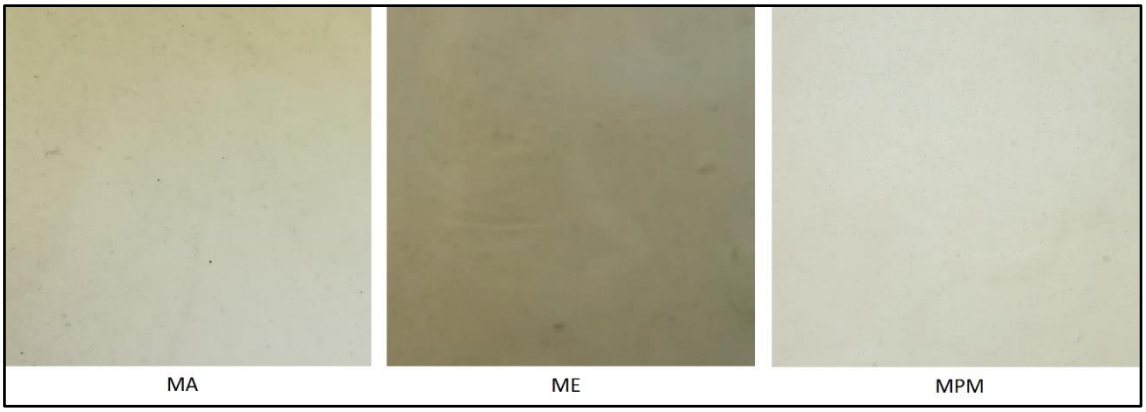

Figure 6. Surface appearance of the three TPS-mucilage films

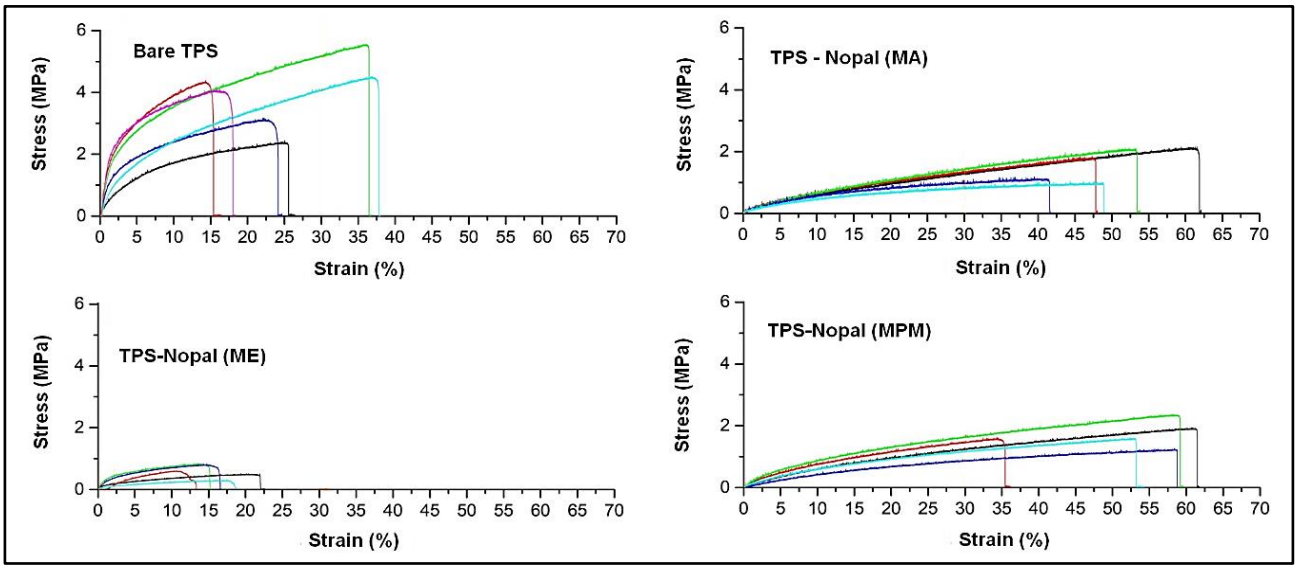

Figure 7. Tensile curves of thermoplastic starch (TPS) and its blended films with nopal mucilage (colors represent the curves for the different samples tested)

Table 2 – Tensile tests results for pure TPS and its blended films with nopal mucilage (type MA, MPM and ME)

Material	Max. stress (MPa)	Max. strain (%)
TPS	3.75 ± 1.16	23.4 ± 8.3
MA	1.45 ± 0.48	50.2 ± 7.8
ME	0.68 ± 0.22	17 ± 3.5
MPM	1.64 ± 0.36	53.7 ± 10.5

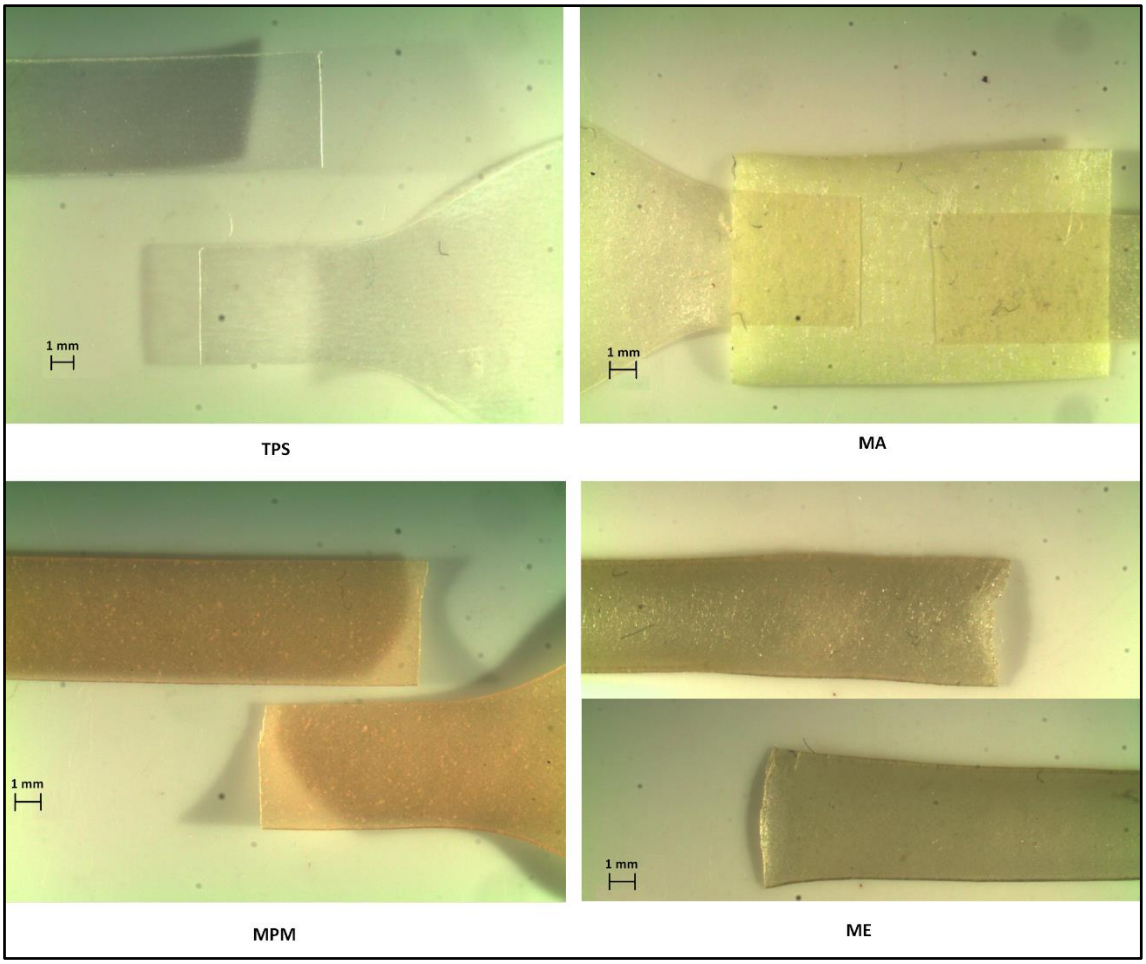

Figure 8. Tensile fractured samples of pure TPS and its blended films with nopal mucilage (type MA, MPM and ME)

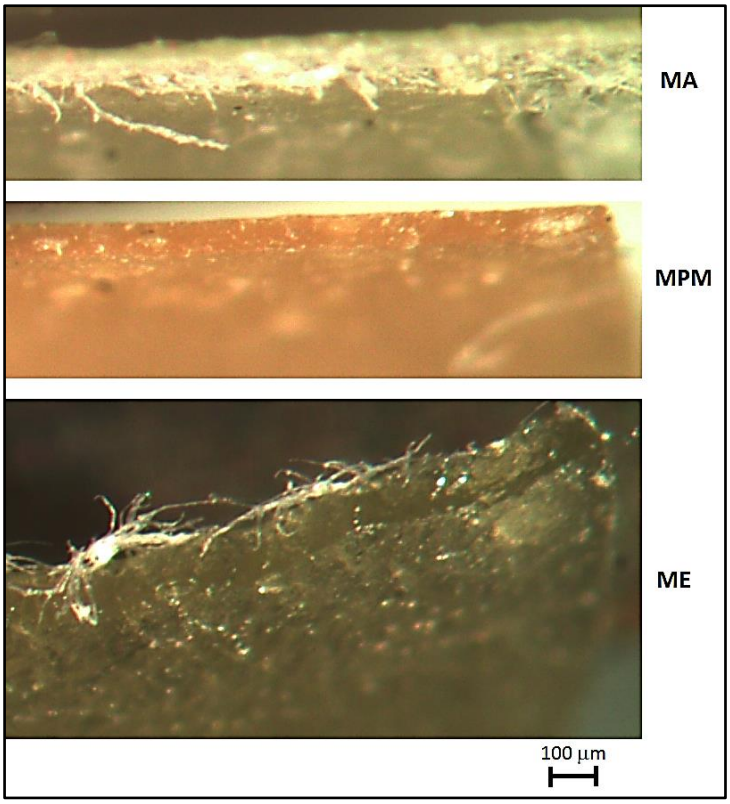

Figure 9. Micrographs of the edges of fractured MA, MPM and ME films after tensile tests

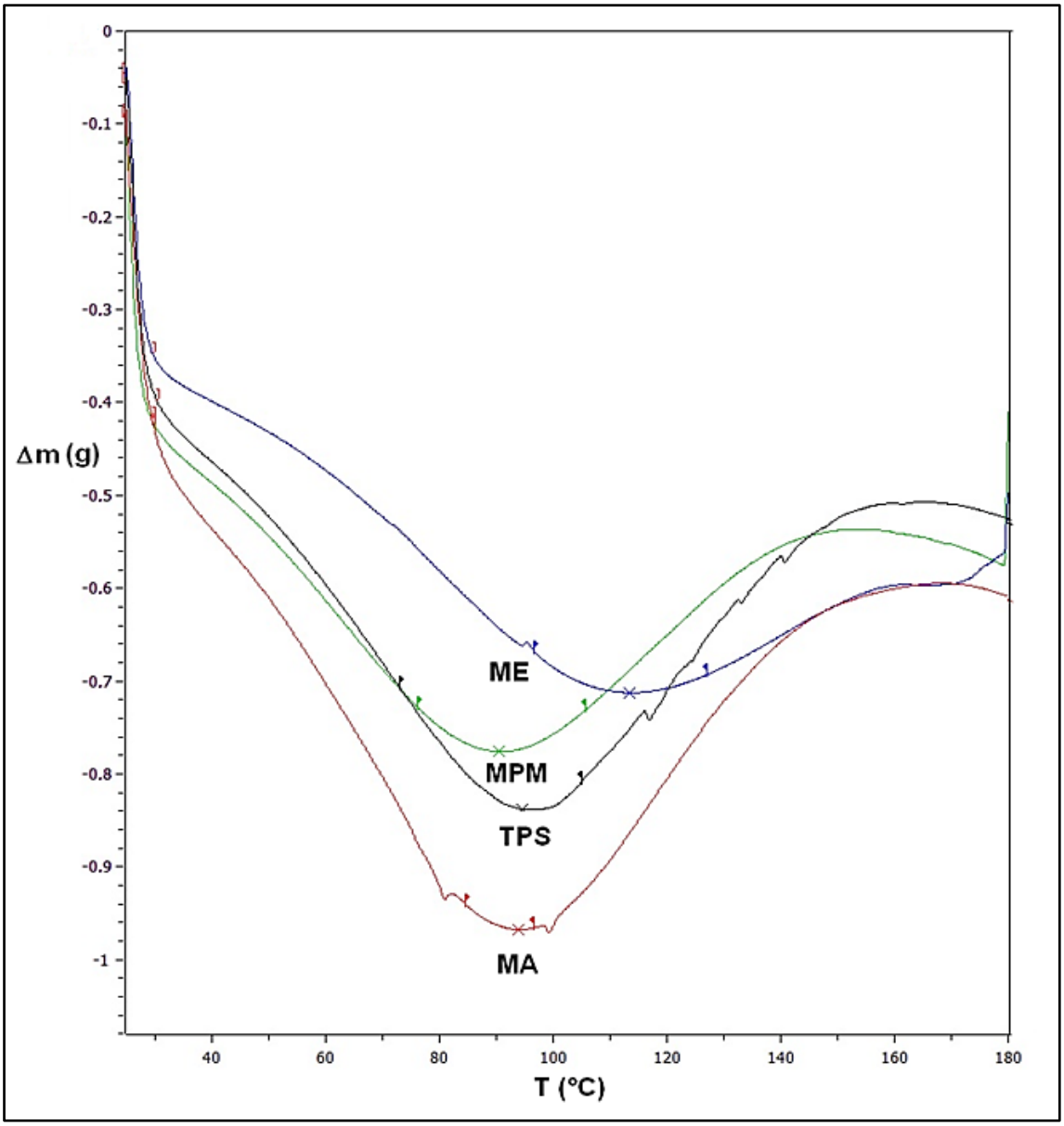

Figure 10. DSC curves for TPS and its films blended with nopal mucilage (type MA, MPM and ME)

Table 3 – Thermal transition temperatures of TPS and its films blended with nopal mucilage (type MA, MPM and ME)

Material	Onset temperature (°C)	Peak temperature (°C)	Ending temperature (°C)
TPS	72	95	106
MA	84	93	97
ME	96	112	126
MPM	77	91	108

SEM images of the film surfaces evidenced a lower brittleness of nopal added films with respect to the pure TPS ones, as visible in Figure 11. In contrast, as regards the ME films, the clear presence of air bubbles and the irregularity of the surface does suggest that the use of the blender without previous maceration results also in the large presence of defects, which can explain the poor mechanical performance of these films.

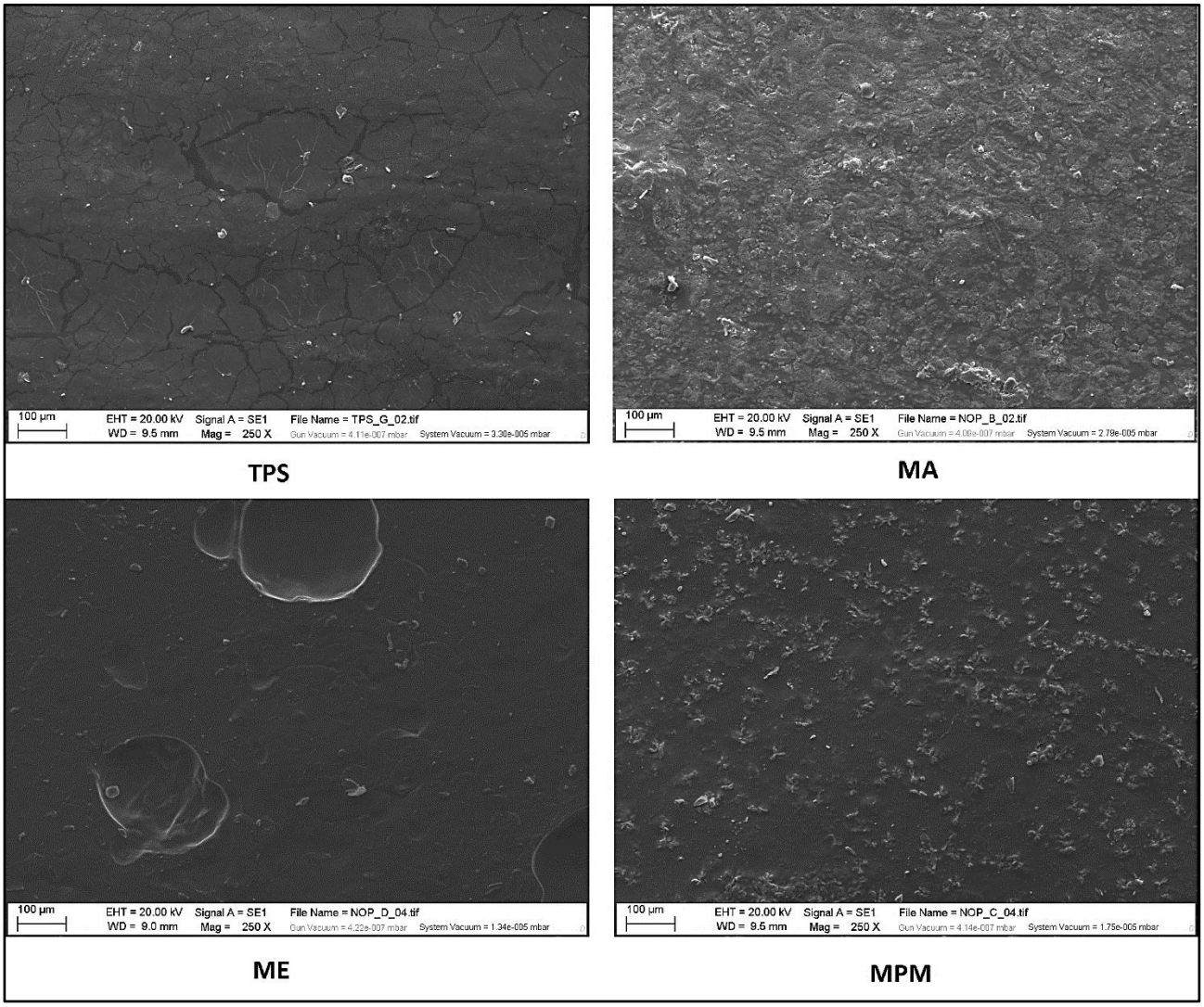

Figure 11. SEM images of thermoplastic starch (TPS) and its blended films with nopal mucilage (type MA, MPM and ME). Magnification: 250x

Despite the aforementioned brittleness, EDS analysis from SEM images highlighted the homogeneity of TPS in terms of retro-diffusion. On the other side, nopal insertion gave evidence of the variety of inorganic salts that are present in this vegetable material. In particular, MA films offered evidence in clear areas of the presence of potassium, sulfur, oxygen, magnesium, aluminum, calcium and chlorine, while in dark areas are present potassium, carbon, oxygen, chlorine, magnesium and traces of aluminum and silicon and sulfur is notably absent. The same elements are

present in MPM films, although morphologies appear more visible, in particular flowers, in the clear areas, as reported in Figure 12. Flower structures have been correlated to the presence of calcite in nopal mucilage [22]. In ME films, beyond the same elements as before, also phosphorus, silicon and sulfur are present in the clear areas, but without particularly recognizable morphologies.

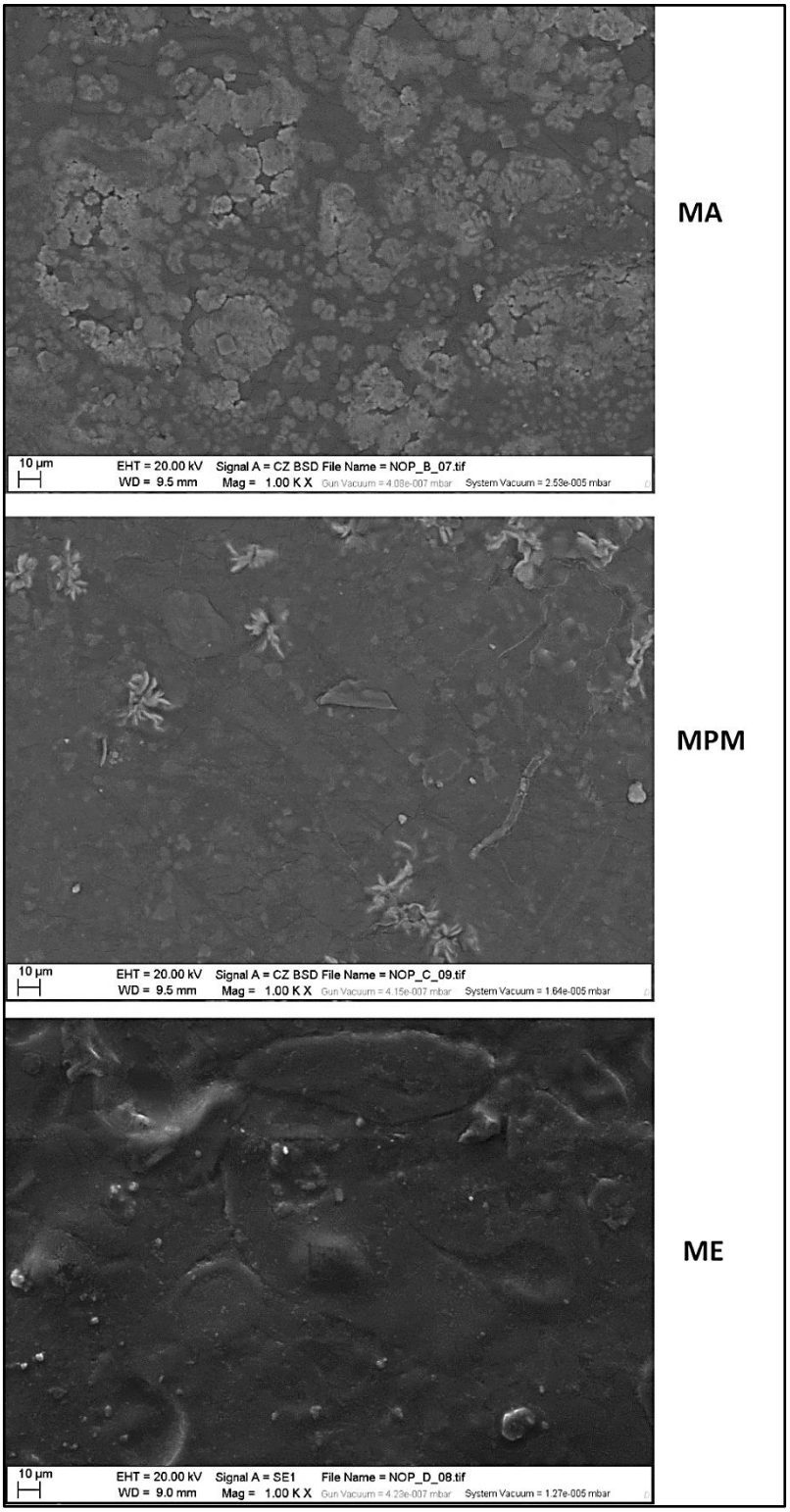

Figure 12. SEM images of blended films TPS-nopal mucilage (type MA, MPM and ME). Magnification 1000x

4. Conclusions

To overcome the limitations of self-produced thermoplastic starches (TPS), based in the specific case of potato starch and glycerol, the addition of nopal mucilage, obtained from Opuntia cladodes waste, has been attempted. Three different ways to extract the mucilage have been explored, maceration, mechanical blending only, and blending after maceration. The latter provided both the highest yielding in terms of mucilage extracted and offered an elongation considerably higher than it is the case for pure TPS. In contrast, pure mechanical extraction gave rise to the large presence of defects and air bubbles, leading to ineffective tensile loading. Limits observed are the fact that the production of film blends was not sufficient to improve neither the mechanical strength of TPS nor its variable performance. It might be suggested that the considerable presence of calcium carbonate and other calcium or magnesium salts would be suitable for the application of other types of loading, such as shear, which could be the objective of further investigation in the future.

Conflicts of Interest

The authors declare no conflict of interest.

Funding

The financial support of Fondazione CARIFAC (Fondazione Cassa di Risparmio di Fabriano e Cupramontana) is gratefully acknowledged, as regards in particular the PhD grant assigned to Mr. Fabrizio Scognamiglio.

References

1. Reyes-Agüero, A.J., Aguirre-Rivera, R.J., Hernández, H.M.: Systematic notes and a detailed description of Opuntia ficus-indica (L.) Mill. (Cactaceae). Agrociencia 2005, 39, 395–408.
2. Ayadi, M.A., Abdelmaksoud, W., Ennouri, M., Attia, H., Cladodes from Opuntia ficus indica as a source of dietary fiber: Effect on dough characteristics and cake making, Ind Crops Prod 2009, 30, 40-47.
3. Sáenz, C., Sepúlveda, E., Matsuhiro, B., Opuntia spp mucilage's: a functional component with industrial perspectives, J Arid Envir 2004, 57, 275-290.
4. Cárdenas, A., Higuera-Ciapara, I., Goycoolea F. M., Rheology and aggregation of cactus (Opuntia ficus-indica), J Professional Association for Cactus Development 1998, 2, 152-159.

5. Gheribi, R., Khwaldi, K., Cactus Mucilage for Food Packaging Applications, Coatings 2019, 9, 655-673.
6. Morais, M.A.; Fonseca, K.S.; Viégas, E.K.D.; Almeida, S.L.; Maia, R.K.M.; Silva, V.N.S.; Simoes, A.N., Mucilage of spineless cactus in the composition of an edible coating for minimally processed yam (Dioscorea spp.). J. Food Meas. Charact. 2019, 13, 2000–2008.
7. Allegra, A.; Inglese, P.; Sortino, G.; Settanni, L.; Todaro, A.; Liguori, G. The influence of Opuntia ficus-indica mucilage edible coating on the quality of 'Hayward' kiwifruit slices. Postharvest Biol. Technol. 2016, 120, 45–51.
8. Lopez-Garcia, F.; Jimenez-Martinez, C.; Guzman-Lucero, D.; Maciel-Cerda, A.; Delgado-Macuil, R.; Cabrero-Palomino, D.; Terres-Rojas, E.; Arzate-Vazquez, I. Physical and chemical characterization of a biopolymer film made with corn starch and nopal xoconostle (Opuntia joconsotle) Mucilage. Rev. Mex. Ing. Quim. 2017, 16, 147–158.
9. Dominguez-Martinez, B.M.; Martinez-Flores, H.E.; Berrios, J.J.; Otoni, C.G.; Wood, D.F.; Velazquez, G. Physical characterization of biodegradable films based on chitosan, polyvinyl alcohol and Opuntia Mucilage. J. Polym. Environ. 2017, 25, 683–691.
10. Troiano, M., Santulli, C., Roselli, G., Di Girolami, G., Cinaglia, P., Gkrilla, A., DIY bioplastics from peanut hulls waste in a starch-milk based matrix, FME Transactions 2018, 46, 503-512.
11. Caliendo, C., Langella, C., Santulli, C., Bove, A., Hand orthosis designed and produced in DIY biocomposites from agrowaste, Design for Health 2018, 2 (2), 211-235.
12. Battistelli D, Santulli C, Production and tensile characterization of thermoplastic starch films filled with iron scrap powder waste and molded on different support materials, J Mater Sci Res Rev 2019, 3 (4), 1-8.
13. Scognamiglio, F., Santulli, C., Roselli, G., Extraction of Cellulose Nanocrystals (NCC) from Cotton Waste and Morphology of NCC Obtained with Different Alkali Neutralization, Current J Appl Sci Technol 2019, 36 (5), 1-8.
14. Scognamiglio, F.; Mirabile Gattia, D.; Roselli, G.; Persia, F.; De Angelis, U.; Santulli, C. Thermoplastic Starch Films Added with Dry Nopal (Opuntia Ficus Indica) Fibers. Fibers 2019, 7, 99.
15. Stintzing, F.C., Carle, R., A review on their chemistry, technology, and uses, Mol. Nutr. Food Res. 2005, 49, 175 – 194, DOI 10.1002/mnfr.200400071.
16. Hernández-Urbiola, M.I., Contreras-Padilla, M., Pérez-Torrero, E., Hernández-Quevedo, G., Rojas-Molina, J.I., Cortes, M.E., Rodríguez García, M.E., Study of nutritional composition of nopal (Opuntia ficus-indica cv. redonda) at different maturity stages. Open Nutr J 2010, 4, 11–16.

17. Tabilo-Munizaga, G., Saenz-Hernandez, C., Herrera-Lavados, C., Influence of temperature, calcium and sucrose concentration on viscoelastic properties of Prosopis chilensis seed gum and nopal mucilage dispersions, Int J Food Sci Technol 2018, 53, 1781–1788.
18. Goycoolea, F.M., Cardenas, A., Pectins from Opuntia spp.: A short review, J Professional Assoc for Cactus Develop 2003, 17-29.
19. Simkovic I, Unexplored possibilities of all-polysaccharide composites, Carbohydr Polym 2013, 95, 697-715.
20. Sepùlveda, C., Sàenz, C., Aliaga. E., Aceituno, C. Extraction and characterization of mucilage in Opuntia spp., Journal of Arid Environments 2007, 68, 534-545.
21. Rodriguez-Gonzalez, F.J., Ramsay, B.A., Favis, B.D., Rheological and thermal properties of thermoplastic starch with high glycerol content, Carbohydr Polym 2004, 58, 139-147.
22. Contreras-Padilla, M.; Rivera-Muñoz, E.M.; Gutiérrez-Cortez, E.; Real del López, A.; Rodríguez-García, M.E. Characterization of crystalline structures in Opuntia ficus-indica. J Biol Phys 2015, 41, 99–112.

Thermoplastic Starch Films Added with Dry Nopal (*Opuntia Ficus Indica*) Fibers

Fibers

Fabrizio Scognamiglio[1], Daniele Mirabile Gattia[2], Graziella Roselli[3], Franca Persia[2], Ugo De Angelis[2] and Carlo Santulli[4*]

1 School of Science and Technology, Technologies and Diagnostics for Conservation and Restoration Laboratory, University of Camerino, Via Pacifici Mazzoni 2, 63100 Ascoli Piceno, Italy

2 Department of Sustainability SSPT – ENEA – Casaccia Research Center, Via Anguillarese 301, 00123 Rome, Italy

3 School of Science and Technology, Chemistry Division, University of Camerino, Via S. Agostino 1, 62032 Camerino, Italy

4 School of Architecture and Design, University of Camerino, Viale della Rimembranza 9, 63100 Ascoli Piceno, Italy

* Corresponding author. E-mail: carlo.santulli@unicam.it

Regarding the contribution of the PhD student Fabrizio Scognamiglio to the presented article, he managed conceptualization, methodology, writing-original draft preparation, writing-review and editing.

Abstract

Dry fibers coming from garden waste, originating from *Opuntia Ficus Indica*, were introduced in amounts of either 8 or 16 wt% into a self-produced thermoplastic starch (TPS) based on potato starch and glycerol. Thermal (differential scanning calorimetry, DSC), mechanical (tensile tests), and morphological characterization with scanning electron microscopy (SEM) and performing energy-dispersive X-ray spectrometry (microanalysis) were carried out. The results indicated that the uneven distribution and variable geometry of fibers introduced led to a reduction of tensile stress and strain with respect to pure TPS. However, the positive effects of prolonged mixing and increased thickness were highlighted, which suggest the fabrication of the composite could be improved in the future by controlling the manufacturing procedure.

Keywords: thermoplastic starch; Opuntia fibers; tensile tests; differential scanning calorimetry; SEM morphology

1. Introduction

Opuntia Ficus Indica, also referred to as“nopal”, is a plant that is used in Italy, as in many countries around the Mediterranean Sea, for its ornamental value and is therefore widely available, especially in the central and southern part of the country. Most Opuntia plants are used in Southern Italy for the production of Indian figs. According to data supplied from the Istituto Nazionale di Statistica (National Institute for Statistics) (ISTAT), 750,000–900,000 quintals per year of fruits are produced. In this case, plants need to be pruned during winter with the removal of cladodes (i.e., flattened leaf-like stems). In addition, the Opuntia is used as a garden plant in a much larger area in Italy to delimit allotments and prevent intrusion, thanks to its spines. The removal of worn-out cladodes from the plant does in any case generate some amount of waste. In particular, cladodes include mucilage, which is starting to receive some interest as an industrial hydrocolloid [1], and cellulosic fibers, which could have a dietary value when fresh [2], yet once dried are normally dumped or incinerated. It is possible, though, to use these fibers to reinforce a polymer matrix, especially aiming at improving its tensile properties. In particular, the use of a biopolymer, such as a starch–glycerol thermoplastic (TPS), could be suitable for this purpose. The use of cellulosic fibers for this purpose is widely documented in the literature; for example, those extracted from eucalyptus leaves bring a substantial increment of the tensile performance of the TPS [3]. Normally, this type of vegetable waste is introduced in the matrix in the form of short and randomly oriented fibers; therefore, it is important to ensure that a sufficient aspect ratio (length/diameter) of the fibers is obtained to have some reinforcement effect.

Passing to Opuntia cellulose content, a possibility that was investigated is to extract its crystalline fraction by obtaining nanocellulose fibers. This is of great interest, although it involves a quite intensive chemical treatment of the waste material, resulting in a limited yield of the process [4]. Aiming at the production of films, also, the extracted waste is acceptable in diameter to the orders of tens of microns, comparable with commonly used plant fibers and using the aforementioned waste as close as possible to the as-received state [5]. In general, it could be considered that due to the large presence of salts, such as calcium oxalates, forming real networks on the fibers, these could have a significant tensile strength, which is also at the origin of these being able to withstand the weight of the whole cladode, the leaf-reservoir typical of these plants [6, 7].

Discarding worn-out parts of the nopal plant in the normal situation of garden waste collection involves a quite long and hardly controllable time before pruning and during storage, with the result that the vegetable waste becomes naturally dry. Some studies on other vegetable waste, such as New Zealand's flax (*Phormium tenax*), used discarded fibers as filler in a biopolymer matrix, offering promising evidence of the suitability of this practice to fabricate biocomposites [8]. Of course, a possibility would be the acquisition and processing of a typical biopolymer, such as poly(lactic acid) (PLA); another way would be though the synthesis of TPS, with the added possibility of also using waste for it (e.g., expired corn starch). This has been defined in other works as the production of "Do-It-Yourself (DIY) bioplastics", mainly based on waste, and proved adapted to some uses, such as packaging or even biomedical applications, despite the limitation of hardly being able to be used above the gelling temperature of starch (e.g., around 80◦C) [9,10].

The present investigation concerns mechanical (tensile) and morphological investigation of TPS films reinforced with nopal dry fibers in view of their possible application in the field of plant fiber composites. These have seen a very large application in recent decades as replacement materials for some traditional composites, like fiberglass, for their inherent sustainability, especially when produced with a biopolymer matrix [11]. In particular, there is continuous search for other plant fibers for these applications, especially with local origin, so as to use them in a "zero-km" approach [12]. Some applications have already been performed on Opuntia fibers, either in an oil-based thermoset matrix, such as epoxy [13], or in a commercial biopolymer, such as in the case of poly(lactic acid) (PLA) [14]. The aim of this study is to analyze the self-production of the matrix in the form of thermoplastic starch and the direct processing of waste from Opuntia, to be used as filler, taking into account the inherent variability of its properties. The influence of two factors for production will be investigated (i.e., the amount of fibers and the stirring time of gelling solution obtained).

2. Materials and Methods

2.1 Fibers

The fibers used for the study were available after long storage at Agenzia nazionale per le nuove tecnologie, l'energia e lo sviluppo economico sostenibile (ENEA), in Anguillara, Italy, originating from some Opuntia plants, which were cut for garden area maintenance on the site. An example of the waste material as received is depicted in Figure 1. To obtain the fibers, the material obtained was first cleaned with compressed air and brush, after which they were washed and brushed, then cut in small pieces, in the order of 20 mm or so. After this, they were sonicated in distilled water for 30 min, then dried in an oven at 70 °C for 24 h and finally mashed in ball mill for 2 h. The final sizes of the fibers obtained were not higher than 1 mm in length, and with very variable aspect ratios, from close to 1, therefore in powder form, to others with up to 10–20.

Figure 1. Fibrous waste material as received

2.2 Films' preparation

A thermoplastic starch (TPS) film, aiming at a thickness of approximately 120 microns, was prepared using 10 g of sieved potato starch and 4 mL of glycerol, reagent grade, therefore with 99.5% purity, in 400 mL of distilled water. The solution was stirred manually for approximately 10 min, until its appearance was uniform. It was then subsequently poured in an uncovered steel mold with surface covered in Teflon, to ease demolding, and then kept there for an hour at 70 °C, and finally at 45 °C overnight. No pressure was purposely applied for production for simplicity and to observe which degree of consolidation was obtained in TPS and their composites in this way. A similar procedure was followed in [9].

After producing the TPS film for comparison, three types of films with added dry nopal fibers were produced, always following the above procedure, but proceeding to the addition of fibers, as follows:

- Composite A: contains an amount of fibers equal to 16 wt% of the total starch + glycerol content. In this case, the stirring lasted for 1 h.
- Composite B: contains an amount of fibers equal to 16 wt% of the total starch + glycerol content. In this case, the stirring lasted for 5 h to increase homogeneity.
- Composite C: produced as composite A, but with an amount of fibers equal to 8 wt% of the total starch + glycerol content.

The three different composites were produced to understand which effect appeared to be predominant on the properties of the composite between the one due to the amount of fibers introduced and the other due to the stirring time. For this reason, a significantly large variation in the amount of fibers introduced between A to B and C composites, and in the stirring time between A to C and B composites.

2.2 Films' characterization

The measurements carried out involve, apart from basic morphological characterization, such as film thickness measurement, other sounder methods of analysis, including, in particular:

- Optical microscopy and scanning electron microscopy (SEM) of the films as received, to evaluate their morphology and after tensile tests, to study the fracture surfaces. The SEM apparatus used is a Zeiss EVO MA15. Using SEM, qualitative analyses of the elements present on the surface were also carried out by EDS (energy-dispersive X-ray spectrometry).

- Tensile tests were performed using a Testometric model MICRO350 5 kN system, with a 50 N load cell. Tests were carried out in displacement control mode at a cross-head velocity equal to 2 mm/minute. The dimensions of the samples are shown in Figure 2.
- Differential scanning calorimetry (DSC) to evaluate the evolution of films and composites behavior with temperature by heating at a rate of 10 °C/min, from 25 to 180 °C, using a Mettler Toledo HPDSC system.

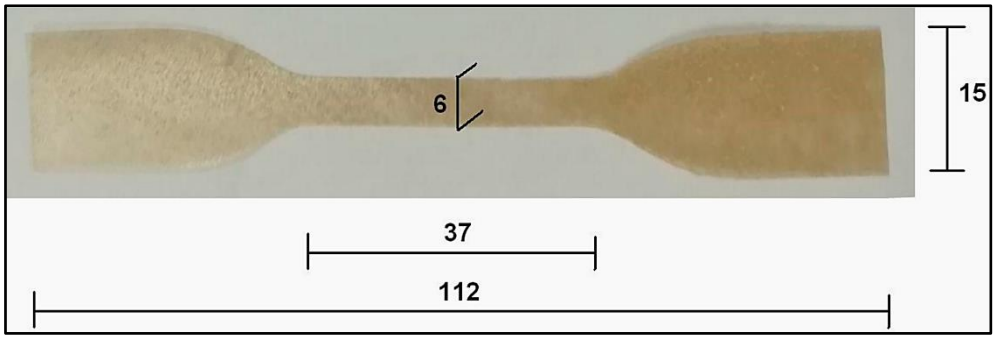

Figure 2. Example of a tensile dog-bone specimen (quotes in mm with tolerance ± 0.1 mm)

3. Results

To produce the composites, the use of nopal dry fibers to fill them was investigated; their aspect as received is represented in Figure 3a. The fibers were received as complex aggregates of fibrils only partly separated. This would affect the adhesion force of a polymer on it. It was therefore suggested that the fibers would be better ground to a much smaller maximum size in the order of a millimeter or less. It needs to be highlighted, nonetheless, that in this way, proceeding to size reduction via the use of a ball mill, some powder is also obtained, as reported above in Section 2.1. The fibrous material after grinding is depicted in Figure 3b, where its whitish aspect is contrasted against a dark background.

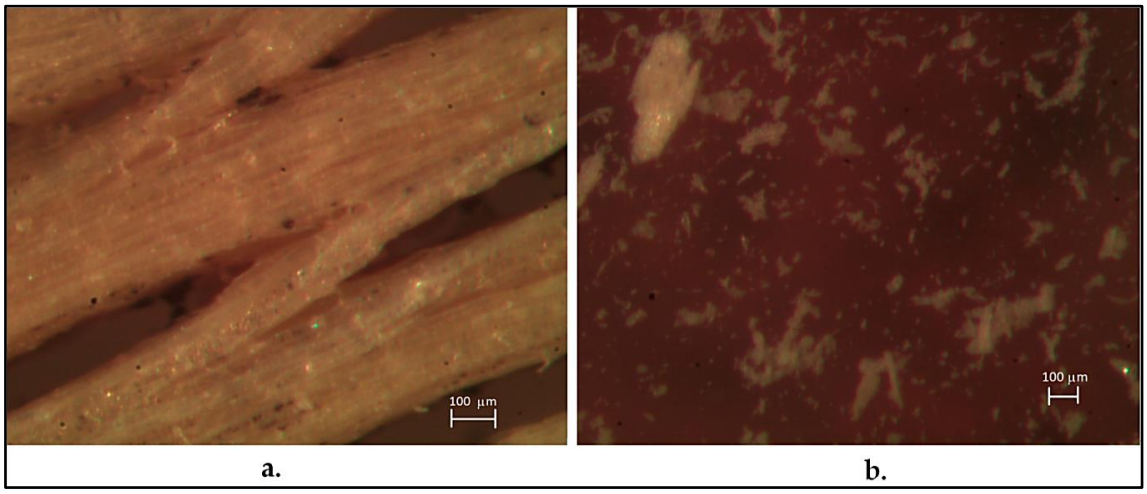

Figure 3. (a) Fibers as received after cleaning; (b) fibers after mashing in ball mill

The aspect of the samples before and after DSC analysis is reported in Figure 4. A qualitative observation allows reasoning on the fact that the least evidence of changing aspect of the material after DSC is observed in the case of composite B, yet this can also be due to the larger thickness, which has been obtained by a longer time mixing, which possibly introduced a larger amount of air in the composite. In the other cases, the color modification due to the temperature cycle is very evident. The respective heat flow curves obtained with temperature increase are reported in Figure 5, where the change in specific heat capacity due to the glass transition phenomenon is not apparent. In thermoplastic starches, glass transition temperature is normally supposed to be between 50 and 70 °C, although with large dependence on the type of starch used and on the amount of glycerol introduced [15]. The first heating cycle, which was performed on the material, did only allow observing a large peak roughly representing its progressive melting. This occurred since there is some previous thermal history of the material, linked to its production, which needs to be eliminated with some thermal cycling to perform a possible measurement of glass transition temperature of TPS. This measurement often proved difficult dealing with TPS blends or composites for its possible superposition with the more obvious peak correlated with melting [16]. The information obtained by this preliminary investigation is useful regardless to suggest whether the introduction of fibers can improve the maximum temperature for use of TPS, which is presently confined at temperatures not above around 50 °C, or not. The data reported in curves in Figure 5 suggest that an increase of melting temperature is only obtained for composites B, where a displacement of around 20 °C of the heat flow peak from the region of 90–95 °C to around 115 °C. This is likely to be connected with the larger thickness of the composite, as reported in Table 1, where the effect of the dry nopal fibers in delaying mechanical collapse due to heating applied is visible.

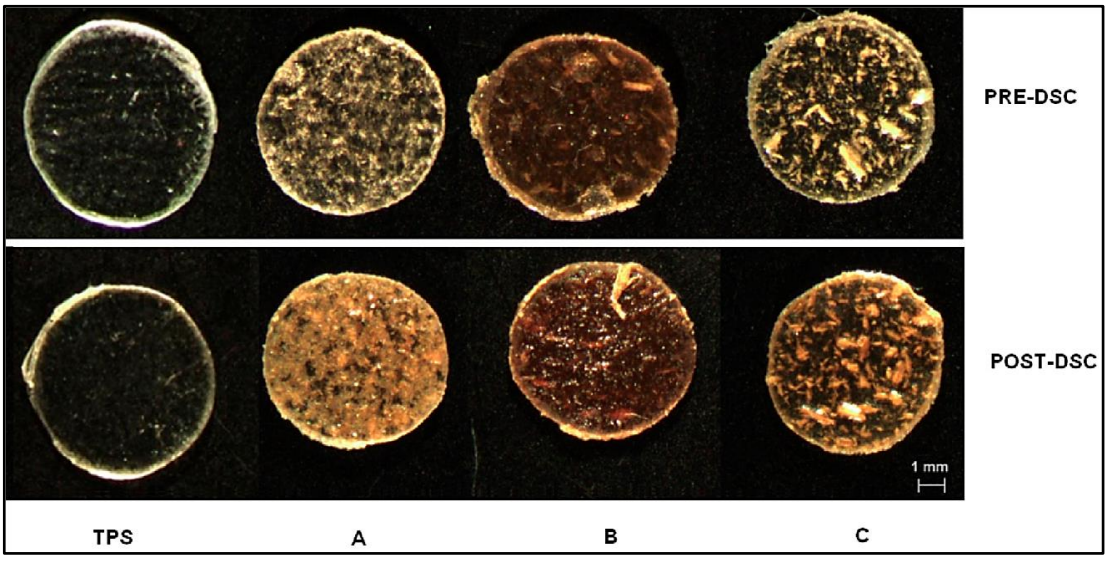

Figure 4. Samples of TPS and TPS–dry nopal composites (type A, B and C, respectively) pre- and post-differential scanning calorimetry (DSC) analysis

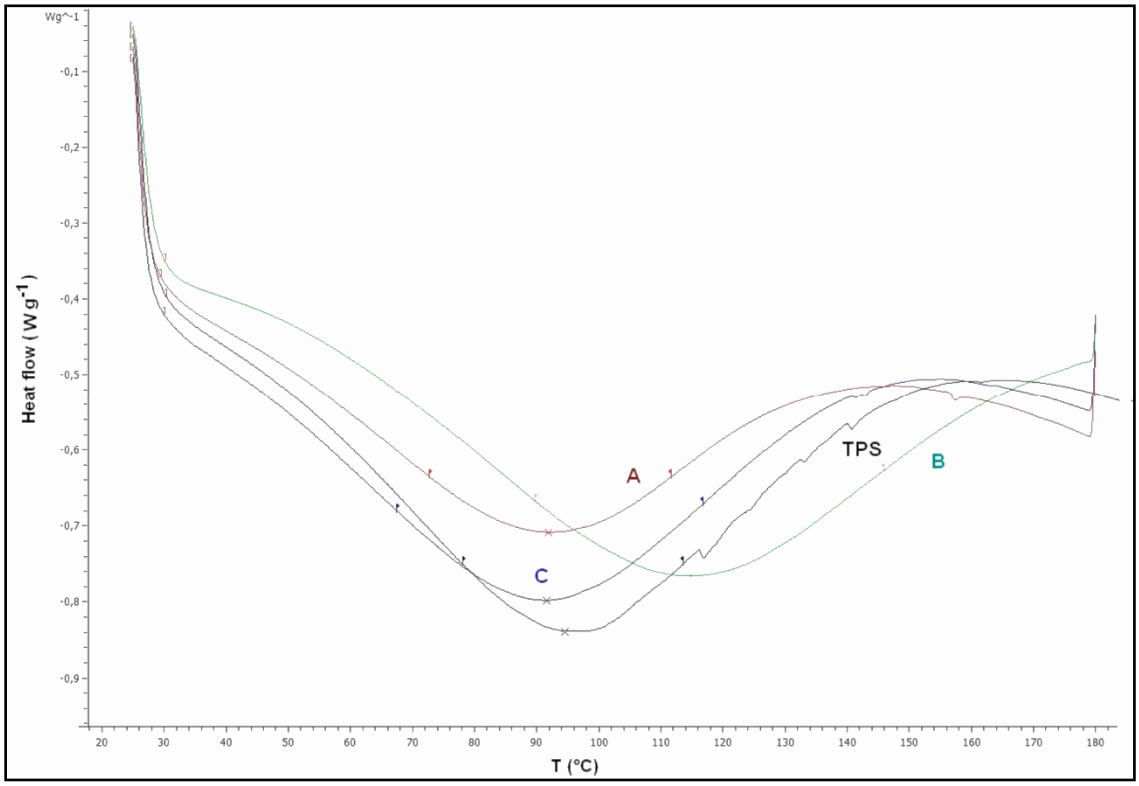

Figure 5. DSC curves for TPS and the three composites with dry nopal fibers (type A, B and C, respectively)

Table 1 – Thickness of thermoplastic starch (TPS) and TPS-dry nopal fiber composites

Material	Thickness (mm)
TPS	0.125 ± 0.015
TPS + FIBERS A	0.157 ± 0.013
TPS + FIBERS B	0.438 ± 0.035
TPS + FIBERS C	0.156 ± 0.008

As regards tensile characterization, the results showed a considerable decrease in terms of maximum stress as well as maximum strain for all the composites with respect to pure TPS, as reported in Table 2. The single curves obtained sample by sample (not less than 5 samples per series were tested) are shown in Figure 6. This decrease, which leads as a whole to a higher rigidity of the composites, can be attributed to the random distribution and the large dimensional scattering of the dry nopal filler after grinding. This situation could be possibly improved in the future either by working on a more effective mixing procedure or by chemically improving the compatibility between the fibers and the polymer; in the case of TPS, the composition could be optimized according to its adhesion with a single fiber once the latter is clearly isolated [17]. It can be observed in particular that in composite C, the variability of strain is very large. This has been attributed to the lower amount of fibers introduced, which therefore gives more importance to the orientation and morphology of the fibers in the composite. It can be also suggested that the use of dry fibers, possibly with different ages of collection, would equally strongly affect the strain of the composite with an effect not negligible in

comparison with the one of the amount of plasticizer used, in this case glycerol [18]. Given the evolution of stress–strain curves in the sense of the very limited presence of any really elastic zone, it was considered not very realistic to measure a precise value of Young's modulus, although in general terms, this can be suggested to be in the region of few MPa and with not very large variations between the three types of composites produced.

Table 2 – Tensile tests results for pure TPS and its composites

Material	Max. stress (MPa)	Max. strain (%)
TPS	3.75 ± 1.16	23.4 ± 8.3
TPS-A	1.06 ± 0.17	9.2 ± 1.8
TPS-B	1.52 ± 0.35	14 ± 1.6
TPS-C	1.45 ± 0.78	17.5 ± 14.1

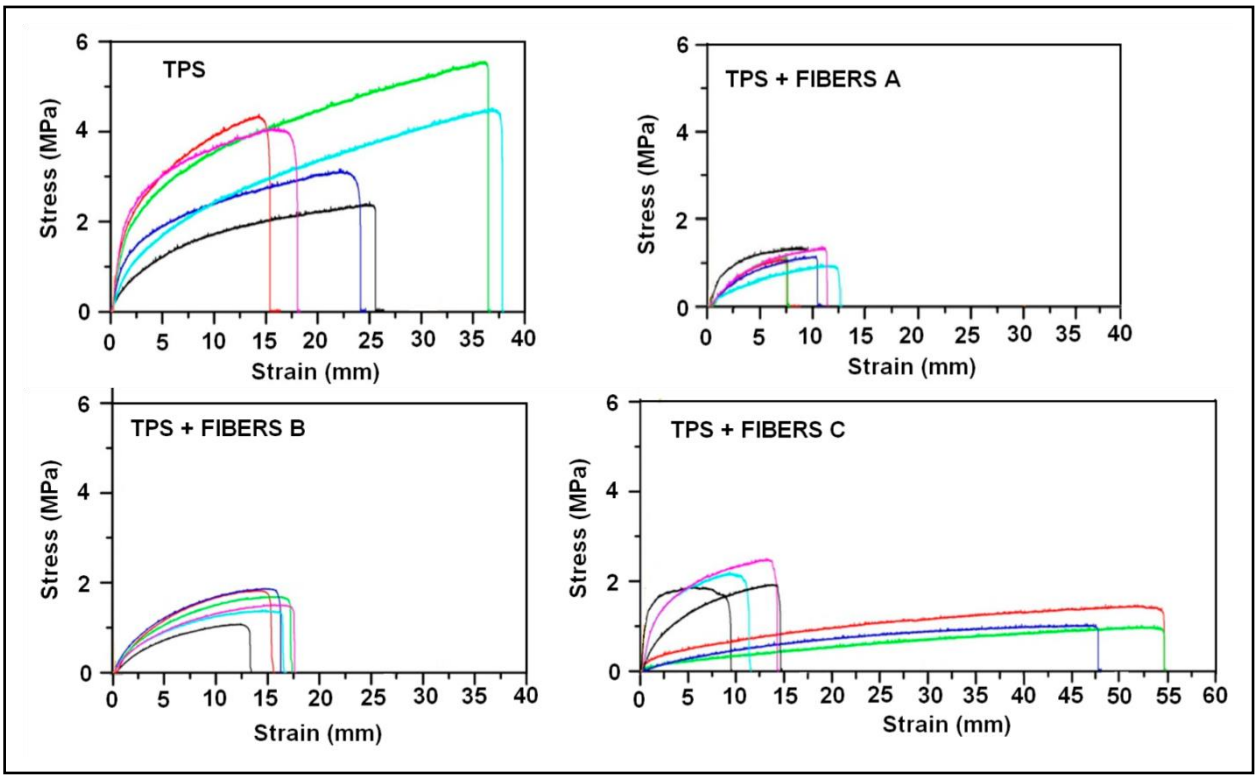

Figure 6. Tensile curves of thermoplastic starch (TPS) and its composites with dry nopal fibers (colors represent the curves for the different samples tested)

After unloading the materials, the recovery of the final strain was also observed, whose data are illustrated in Table 3. In pure TPS, this was very variable, in some cases leading to the material continuing to elongate after the removal of the load, resulting in a negative strain recovery value. As a whole, the recovery process appeared rather erratic in TPS, due to the simple fabrication process adopted, which represented an obvious limit for the material. Also in composite A, residual deformation was very limited, whereas some residual deformation was observed for the other composites, more predictable for composite B and more variable for composite C.

Table 3 – Values of post-tensile non-recovered strain for pure TPS and its composites

Material	Non-Recovered Strain (%)
TPS	-0.4 ± 1.5
TPS-A	0.9 ± 0.7
TPS-B	5 ± 0.5
TPS-C	3.4 ± 2.5

Fracture surfaces, reported in Figure 7, highlight that all materials are quite fragile. However, on one side, the fracture of TPS is abrupt and of a totally brittle nature, while some crack deviation is present in composites, due to the insertion of the fibers. In general terms, this process appears more uniform in composite A. On the other side, composite B typically shows also transverse cracks before failure, which is a sign of enhanced rigidity, but on the other side, it may indicate limited toughness, and composite C tends toward some inflection during loading. The fibrous material was proved to have an apparent density around 0.5 g/cm^3, which was deemed to reduce the TPS one, evaluated to be in the region of 0.95 ± 0.05 g/cm^3, albeit in a very limited way, due to the small amount of fibers introduced and the variability of the measurements taken.

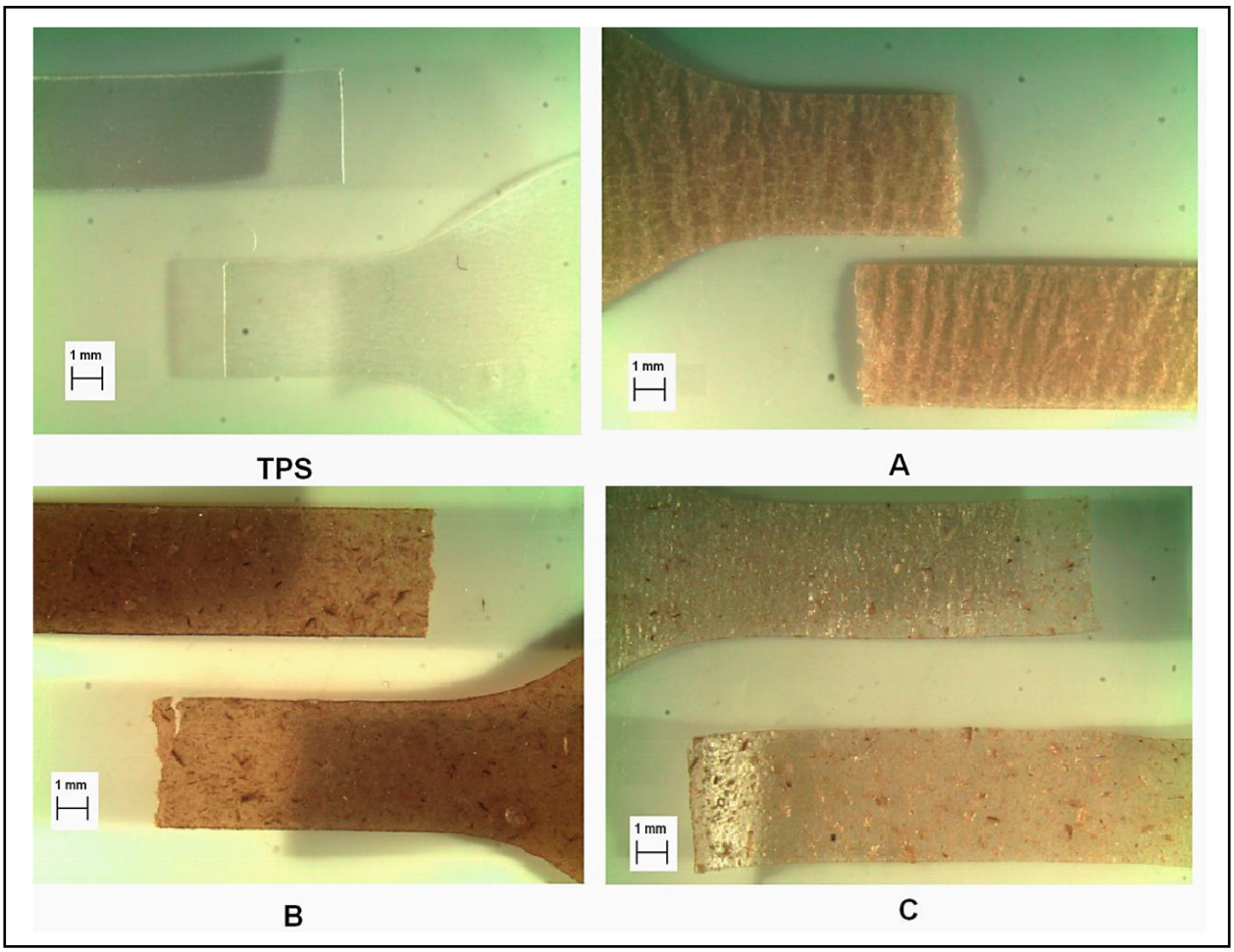

Figure 7. Tensile fractured samples of pure TPS and TPS–dry nopal fiber composites (type A, B and C, respectively)

For better insight into the characteristics of the composites, SEM images of the surfaces are offered in Figure 8. With respect to the bare TPS, the composites noticeably show higher porosity, with considerable variability as well. Average porosity value, in all cases higher than 10% over the surface, does not give significant indications, because voids appear to be concentrated mainly in some critical regions. However, the comparison between the three composites offers some suggestions—in particular, limited mixing time, together with the large amount of fibers generated in composite A, and some separation between TPS and the filler, especially when the latter is in the form of a powder. As a whole, the most compact composite surface is offered by composite B. Energy-dispersive X-ray spectrometry (EDS) analysis suggested that in the surface of composite B, salt deposits are present, which include a number of elements apart from the expected calcium, namely, aluminum, silicon, potassium, iron, and in some cases also titanium. This suggests that the improved mixing allows salts present in nopal fibers to surface. On the other side, it is proposed that some of these elements, which are not typically present in nopal, such as titanium, would need to be verified as regards their presence in soil and possible pollution [19]. The presence of irregularities and cavities is also revealed in composite C, where even more elongated nopal fibers show separation problems.

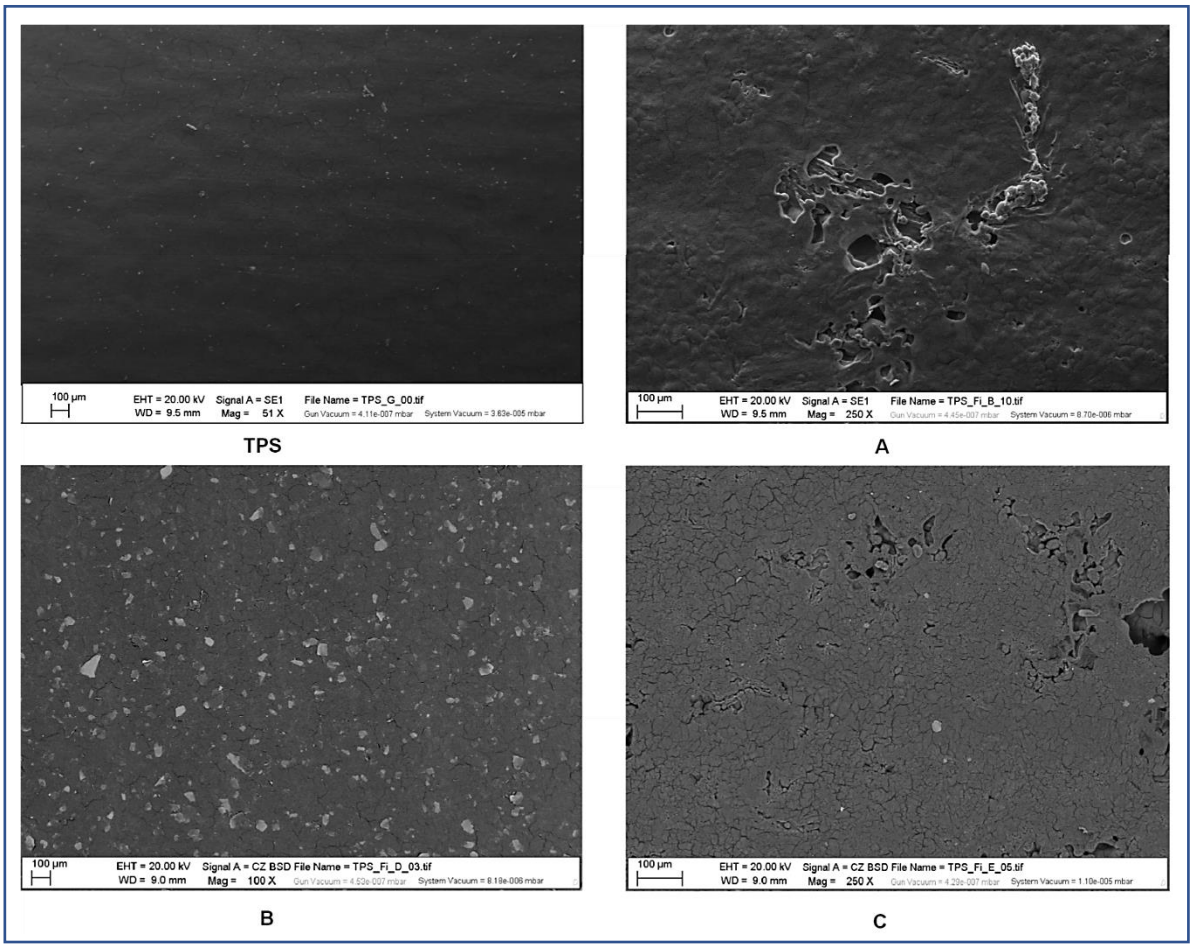

Figure 8. SEM images of thermoplastic starch (TPS) and its composites with dry nopal fibers (type A, B and C, respectively)

4. Conclusions

This preliminary work on the introduction of dry opuntia fibers (maximum amount 16 wt %) in an expressly prepared thermoplastic starch (TPS) led to some interesting observations on the possibilities and limits of application of this common garden waste as the filler of a purposely prepared biodegradable polymer.

More specifically, some critical points are observed in terms of possible improvement of fiber mixing so that their addition would not result in a substantial decrease of mechanical properties. On the other side, it is suggested that inserting a considerable amount of fibers in a TPS composite of thickness exceeding a few mm may lead to some improvement in the melting temperature with respect to bare TPS, provided that the mixing before material production is increased.

Future work would need to include the further characterization of opuntia fibers also in terms of their adhesion to the matrix, once inserted in variable morphology and with a very scattered aspect ratio.

Conflicts of Interest

The authors declare no conflict of interest.

Funding

The financial support of Fondazione CARIFAC (Fondazione Cassa di Risparmio di Fabriano e Cupramontana) is gratefully acknowledged, as regards in particular the PhD grant assigned to Mr. Fabrizio Scognamiglio.

References

1. Sáenz, C.; Sepúlveda, E.; Matsuhiro, B. Opuntia spp mucilage's: A functional component with industrial perspectives. *J. Arid Environ.* 2004, *57*, 275–290.
2. Ayadi, M.A.; Abdelmaksoud, W.; Ennouri, M.; Attia, H. Cladodes from opuntia ficus indica as a source of dietary fiber: Effect on dough characteristics and cake making. *Ind. Crop. Prod.* 2009, *30*, 40–47. [CrossRef]
3. Curvelo, A.A.S.; de Carvalho, A.J.F.; Agnelli, J.A.M. Thermoplastic starch-cellulosic fibers composites: Preliminary results. *Carbohydr. Polym.* 2001, *45*, 183–188. [CrossRef]
4. Malainine, M.E.; Mahrouz, M.; Dufresne, A. Thermoplastic nanocomposites based on cellulose microfibrils from opuntia ficus-indica parenchyma cell. *Compos. Sci. Technol.* 2005, *65*, 1520–1526. [CrossRef]

5. Greco, A.; Gennaro, R.; Timo, A.; Bonfantini, F.; Maffezzoli, A. A comparative study between bio-composites obtained with opuntia ficus indica cladodes and flax fibers. *J. Polym. Environ.* 2013, *21*, 910–916. [CrossRef]
6. Scognamiglio, F.; Santulli, C.; Roselli, G. Extraction of cellulose nanocrystals (NCC) from cotton waste and morphology of NCC obtained with different alkali neutralization. *Curr. J. Appl. Sci. Technol.* 2019, *36*, 1–8. [CrossRef]
7. Rodríguez-Garcia, M.E.; de Lira, C.; Hernández-Becerra, E.; Cornejo-Villegas, M.A.; Palacios-Fonseca, A.J.; Rojas-Molina, I.; Reynoso, R.; Quintero, L.C.; Del-Real, A.; Zepeda, T.A.; et al. Physicochemical characterization of nopal pads (Opuntia ficus indica) and dry vacuum nopal powders as a function of the maturation. *Plant Foods Hum. Nutr.* 2007, *62*, 107–112. [CrossRef] [PubMed]
8. De Rosa, I.M.; Iannoni, A.; Kenny, J.M.; Puglia, D.; Santulli, C.; Sarasini, F.; Terenzi, A. Poly(lactic acid)/phormium tenax composites: Morphology and thermo-mechanical behavior. *Polym. Compos.* 2011, *32*, 1362–1368. [CrossRef]
9. Troiano, M.; Santulli, C.; Roselli, G.; Di Girolami, G.; Cinaglia, P.; Gkrilla, A. DIY bioplastics from peanut hulls waste in a starch-milk based matrix. *FME Trans.* 2018, *46*, 503–512. [CrossRef]
10. Caliendo, C.; Langella, C.; Santulli, C.; Bove, A. Hand orthosis designed and produced in DIY biocomposites from agrowaste. *Des. Health* 2018, *2*, 211–235. [CrossRef]
11. Santulli, C. Natural Fiber-Reinforced Composites, chapter 12. In *Biomass, Biopolymer-Based Materials, and Bioenergy*; Verma, D., Fortunati, E., Jain, S., Zhang, X., Eds.; Woodhead Publishing: Cambridge, UK, 2019; pp. 225–238.
12. Sarasini, F.; Fiore, V. A systematic literature review on less common natural fibres and their biocomposites. *J. Clean. Prod.* 2018, *195*, 240–267. [CrossRef]
13. Navya Geethika, V.; Durga Prasada Rao, V.; Mahaboob Ali, S.K.R.S.; Saqheeb Ali, S.K.M.Z.M. Study of tensile and flexural strengths of cocoa and Opuntia fibre reinforced hybrid composites. *ASSRG Int. J. Mech. Eng. (SSRG-IJME)* 2017, Special Issue May 2017. 291–295.
14. Scaffaro, R.; Maio, A.; Gulino, E.F.; Megna, B. Structure-property relationship of PLA-Opuntia Ficus Indica biocomposites. *Composites* 2019, *167 Pt B*, 199–206. [CrossRef]
15. Forssell, P.M.; Mikkilä, J.M.; Moates, G.K.; Parker, R. Phase and glass transition behaviour of concentrated barley starch-glycerol-water mixtures, a model for thermoplastic starch. *Carbohydr. Polym.* 1997, *34*, 275–282. [CrossRef]
16. Averous, L.; Moro, L.; Dole, P.; Fringant, C. Properties of thermoplastic blends: Starch—Polycaprolactone. *Polymer* 2000, *41*, 4157–4167. [CrossRef]

17. Zhou, Y.; Fan, M.; Chen, L. Interface and bonding mechanisms of plant fibre composites: An overview. *Composites* 2016, *101 Pt B*, 31–45. [CrossRef]
18. Pushpadass, H.A.; Hanna, M.A. Age-induced changes in the microstructure and selected properties of extruded starch films plasticized with glycerol and stearic acid. *Ind. Eng. Chem. Res.* 2009, *48*, 8457–8463. [CrossRef]
19. Hernández-Urbiola, M.I.; Contreras-Padilla, M.; Pérez-Torrero, E.; Hernández-Quevedo, G.; Rojas-Molina, J.I.; Cortes, M.E.; Rodríguez-García, M.E. Study of nutritional composition of nopal (Opuntia ficus indica cv. Redonda) at different maturity stages. *Open Nutr. J.* 2010, *4*, 11–16. [CrossRef]

Appendix to NOPAL

Regarding the introduction of Opuntia mucilage into modern Paper materials, carried out at the Cartiere Miliani in Fabriano (Italy), it involved several materials, methods and techniques:

I. Three procedures adopted to extract the mucilage from the raw material obtained from the cladode (for detailed information about each process, please refer to the here presented 2nd Article):

- Maceration 1:1 (MA1): parenchymal material (g) - distilled water (ml) proportion of 1:1; maceration time: 24 hours in the dark;
- Maceration 1:9 (MA9): parenchymal material (g) - distilled water (ml) proportion of 1:9; maceration time: 72 hours in the dark;
- Mechanical (ME).

II. Zeta potencial analysis: addition of OFI mucilage (MA1, MA9 and ME) to the pulp without additives, in order to verify the possible zeta potential variation. For each Nopal solution there was an increase in absolute value: this result was considered of interest to substitute OFI mucilage for Carboxymethil Cellulose (CMC, an effective papermaking additive used in many procedures such as pigment coating, adding in the pulp and surface sizing, with good water-retaining property, dispersibility and shear thinning).

III. Introduction of Nopal solution (MA1, MA9 and ME) into the pulp (200 g) containing Kymene wet-strength additives (family of products proven to significantly improve the wet strenght of paper). Exploiting natural tendency of Nopal to replace CMC, it was added until a zeta potencial default value was reached (MA1: 7 ml; MA9: 3 ml; ME: 10 ml). The following steps were paper sheet forming and its mechanical characterization (double fold test, Table 1).

IV. Surface treatment: two different types of paper supports, one previously impregnated with poly(vinylalcohol) (PVA) and one untreated, were immersed in OFI mucilage (MA1, MA9 and ME) heating to 60 °C, and then dried in an oven at 105 °C for 1 minute; a mechanical (double fold test, Table 2) and morphological (optical microscopy) characterization of the sheets was performed, in order to evaluate the effects of Nopal introduction.

Table 1 – Number of double folds (*d*) for paper samples after the introduction of OFI mucilage into the pulp (containing Kymene additives)

Sample	*d*
Paper (Kymene + CMC)	1600
Paper (Kymene + MA1 solution)	1460
Paper (Kymene + MA9 solution)	1500
Paper (Kymene + ME solution)	1350

Table 2 – Number of double folds (*d*) for paper samples (with and without PVA) immersed in OFI mucilage

Sample	*d*
Paper	820
Paper + MA1 solution	920
Paper + MA9 solution	850
Paper + ME solution	960
Paper (PVA)	3940
Paper (PVA) + MA1 solution	2320
Paper (PVA) + MA9 solution	2465
Paper (PVA) + ME solution	2660

The tests highlighted that the contribution of Nopal to the mechanical resistance of modern Paper (introduction into the pulp and surface treatment of the sheet) was negative. Nevertheless, it should be emphasized that the results obtained on Paper without additives (Table 2) were quite appreciable, as confirmed by optical microscopy analysis, which evidenced an increment of the cohesion of fibers after the introduction of OFI mucilage. This outcome was considered of interest to evaluate the application of Nopal for the restoration of ancient Paper, so as to substitute this natural product for the synthetic PVA actually utilized in this field. In addition, future studies should investigate the possible use of Nopal (opportunely modified), which guarantees a large and reasonably constant availability, as a promising substitute of the expensive CMC, achieving several benefits in terms of cost, sustainability and fully compatibility of the additives utilized in moder papermaking.

Characterization of Handmade Papers (13th–15th century) from Camerino and Fabriano (Marche, Italy)

Journal of Cultural Heritage

Noemi Proietti[a], Graziella Roselli[b*], Donatella Capitani[a], Claudio Pettinari[c], Stefania Pucciarelli[d], Sara Basileo[b], Fabrizio Scognamiglio[e]

a Anna Laura Segre NMR Laboratory, Institute for Biological Systems, National Research Council of Italy, Area della Ricerca di Roma1, 00015 Monterotondo, Italy

b School of Science and Technology, University of Camerino, Via S. Agostino 1, 62032 Camerino, Italy

c School of Pharmacy, University of Camerino, Via Madonna delle Carceri 9, 62032 Camerino, Italy

d School of Biosciences and Veterinary Medicine, University of Camerino, Via Gentile III Da Varano, 62032 Camerino, Italy

e School of Science and Technology, Technologies and Diagnostics for Conservation and Restoration Laboratory, University of Camerino, Via Pacifici Mazzoni 2, 63100 Ascoli Piceno, Italy

* Corresponding author. E-mail: graziella.roselli@unicam.it

Regarding the contribution of the PhD student Fabrizio Scognamiglio to the presented article, he managed the literature search and performed SEM, FTIR, SDS-PAGE pre-treatment and, in collaboration with the Institute of Chemical Methodologies IMC of the National Research Council of Italy CNR in Rome (Italy), NMR analysis. FS also commented on experiment results and wrote the first draft of the paper.

Original Article

Abstract

The dispute over the paternity of western paper is a longstanding problem. In Italy, a country that has a long tradition of papermaking, many cities compete for the leadership in the production of this material; on the other hand, several studies attribute to Fabriano (13th century), a little center in Marche region, the birth of modern paper and its diffusion throughout Europe.

During the 14thcentury, the nearby town of Camerino imposed itself on the paper market, triggering a historic rivalry with the manufacture of Fabriano. As scientific studies on these different productions are missing, a comparative, multidisciplinary investigation has been carried out to characterize a set of thirteenth-fifteenth century handmade papers from Camerino-Fabriano area.

Several analytical techniques – some non-invasive such as Fourier-transform infrared spectroscopy (FTIR) and portable magnetic resonance (unilateral NMR), joined to microdestructive ones such as scanning electron microscopy (SEM), 13C CPMAS NMR spectroscopy, thermo-gravimetric analysis (TGA), sodium dodecyl sulphate-polyacrylamide gel electrophoresis (SDS-PAGE) and reverse-phase liquid chromatography (RP-HPLC) – have been employed in order to study the morphology of the paper documents, to identify the substances used in production process and to define their preservation state. Moreover principal component analysis (PCA) has been applied to the spectroscopic data, allowing the clustering of Fabriano documents with respect to Camerino ones and dividing the samples in two sets.

This work improves and confirms knowledges on paper production in Marche region, and the experimental data collected highlight similarities and differences between Camerino and Fabriano manufactures.

Keywords: ancient paper analysis; 13C CPMAS NMR spectroscopy; unilateral NMR; SEM; SDS-PAGE; PCA

1. Introduction

Paper art, handed down from Chinese people to Arabs in the 8th century, after a millennial intercontinental journey reached the West, Mediterranean Europe.

In Muslim Spain, it spread without undergoing any substantial technical-qualitative change. Instead in Italy, where paper was obtained by Arab methods too– in Sicily, in Amalfi (Campania) and Genoa (Liguria), in Veneto, Tuscany and in Marche regions – there was a technological evolution leading to the production of a new type of paper that gradually replaced the oriental one and maintained its quality characteristics unchanged for centuries. This type of production is known as: "the manufactured western paper".

This process began in the early years of the second half of the 13th century and lasted for several decades. During this period many innovations were introduced in papermaking, first of all the use of animal glue instead of starch one, to ensure the durability of the final product and the proper impermeability to ink.

Even if it seems difficult to establish which Italian region gave birth to western paper, recent historiographical studies [1, 2] identify Fabriano (13th century) as the centre which promoted the manufacturing revolution leadingto modern paper, and its spreads in Italy and later throughout Europe.

At the beginning of the 14th century Camerino (another town in Marche region) thanks to the quality of its product simposed itself on the paper market, becoming the only competitor of Fabriano. Analysis of historical sources confirms that the two towns adopted diversified but complementary production choices: Fabriano was oriented towards the production of very fine paper destined for narrow market, including the book one [3]; otherwise in Camerino increased the production of medium-high quality products, destined for wider consumption [4].

With the aim to compare these different manufactures a multianalytical approach was applied on samples from Camerino-Fabriano area, for obtaining a large amount of information.

2. Research Aims

In this study a multi-analytical approach was used to perform a diagnostic analysis of the group of paper samples from Camerino and Fabriano (13th-15th century). Making use of different types of analytical techniques, it was possible to investigate common and dissimilar aspects between the different manufactures of Marche region. The choice to use a multidisciplinary approach and carry out a wide range of characterization analyzes of the analyzed paper fragments is certainly original and is due to the need to proceed with comparative studies between two extremely similar materials produced in the same historical period in the attemp to gather and compare any little detectable difference.

3. Materials and Methods

Twenty-one documents (13th-15th century) coming from Camerino and Fabriano were selected to investigate the different manufactures of handmade papers (fig.1, Table 1).

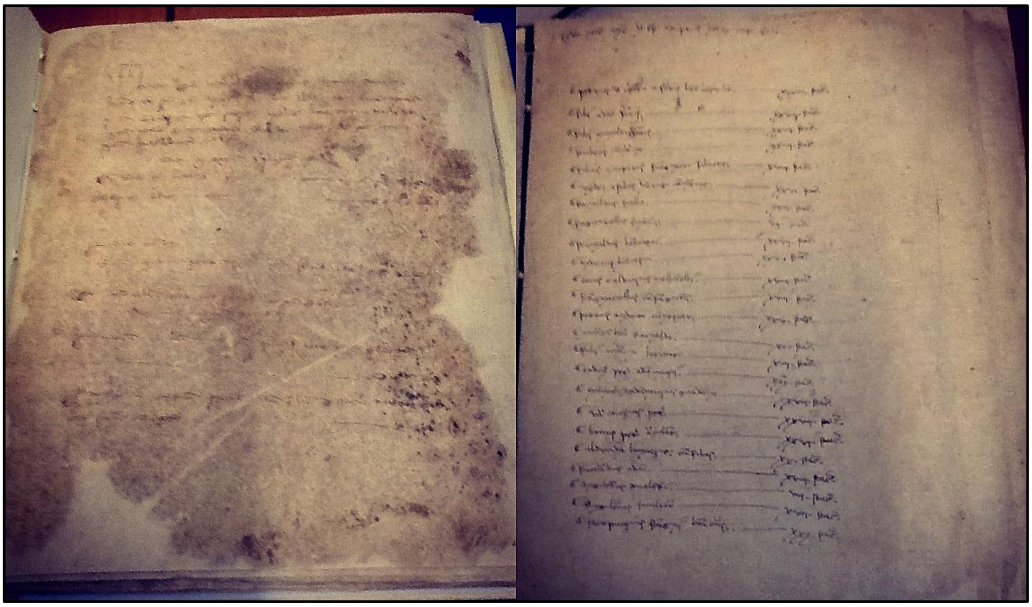

Fig. 1 – Paper documents from Camerino: left, sample 6; right, sample 7

Table 1 – Samples of paper coming from Camerino-Fabriano area (13th-15thcentury)

Sample ID	Paper document		Provenance – Date
1	Register of notaries – Camerino		Camerino – 1385 et seq
	Notary Giacomo Pucciarelli	Protocol 3956	
	Quinternions not collated	Two small unwritten paper fragments	
2	Register of notaries – Camerino		Camerino – 1387
	Notary Zuzio di Giovanni di Vestignano	Protocol 4008	
	Quinternions not collated	Four small paper fragments; one of them presents red stains produced by molds	
3	Old Cadastres of Camerino		Camerino – 1401
	Piece no. 2		
	Quinternions not collated	Four small unwritten paper fragments; one of them yellowed due to oxidation	
4	Old Cadastres of Camerino		Camerino – Ante 1435
	Piece no. 4		
	Quinternions not collated	One fragment related to paper 4-131	
5	Municipal register of Camerino		Camerino – 1464
	Borders with Foligno	b.n. 7	
	Sewn volume	Three small unwritten paper fragments	
6	Volume no. 1		Camerino – 1264
	Liber licentiarum Comunis Sancti Genesii del tempo del podestà Gentile da Varano		
	Restored		

7	Volume no. 8 Criminal Trials Manuscript Restored	Camerino – 1298
8	Fragment attached to the Protocol of Notary Berretta, volume 1279	Fabriano – 1283
9	Fragment attached to the Protocol of Notary Berretta, volume 1279	Fabriano – 1286
10	Fragment attached to the Protocol of Notary Berretta, volume 1279	Fabriano – 1301
11	Registers of the merchant Lodovico di Ambrogio di Bonaventura Volume 1352	Fabriano – 14th century
12	Registers of the merchant Lodovico di Ambrogio di Bonaventura Volume 1354	Fabriano – 14th century
13	Registers of the merchant Lodovico di Ambrogio di Bonaventura Volume 1355	Fabriano – 14th century
14	Registers of the merchant Lodovico di Ambrogio di Bonaventura Volume 1356	Fabriano – 14th century
15	Letter from Venice (Paoluccio di maestro Paolo di Camerino) to Pisa (Francesco di Marco Datini and Manno d'Albizo degli Agli)	Camerino - January 13th, 1395 (= 1396 of venetian year)
16	Letter from Venice (Paoluccio di maestro Paolo di Camerino) to Mallorca (Francesco di Marco Datini and Cristofano di Bartolo) String 1082 Codex 124240	Camerino - April 7th, 1397
17	Letter from Venice (Paoluccio di maestro Paolo di Camerino) to Mallorca (Francesco di Marco Datini and Cristofano di Bartolo) String 1082 Codex 124257	Camerino - March 29th, 1399
18	Letter from Bruges (Salvestro Mannini and brothers) to Florence (Francesco di Marco Datini) String 648 Codex 929177	Camerino – May, 1392
19	Letter from Fabriano (Meo di Venanzio) to Pisa (Francesco di Marco Datini and Manni d'Albizo degli Agli) String 443 Codex 504337	Fabriano - November 5th, 1400
20	Letter from Fabriano (Meo di Venanzio and Gregorio del Pace and companions) to Pisa (Manno d'Albizo degli Agli) String 443 Codex 504341	Fabriano - February 29th, 1400
21	Letter from Bruges (Luigi and Salvestro Mannini) to Florence(Francesco di Marco Datini) String 648 Codex 700898	Camerino - 1391

In order to identify areas showing effects of external agents and to select those ones to be analyzed, the paper samples were preliminary inspected in laboratory, both by naked eye and by a stereomicroscope Olympus SZX12 with digital image acquisition. In order to study the morphology of materials, to identify the substances utilized in production process and to define the preservation state of the paper samples, multiple analytical techniques, some non-invasive such as FTIR and

unilateral NMR, were combined with micro-destructive ones such as SEM, 13C CPMAS NMR spectroscopy, TGA, SDS-PAGE and RP-HPLC.

3.1 SEM

To explore the micromorphology, small fragments detached from some documents (11, 12, 13, 14, 16, 17, 19, 20 and 21) were firstly metalized and successively investigated by SEM, a Stereoscan S-360 of Cambridge Instrument (Somerville, MA, USA) with the accelerating voltage set to 15÷20 kV.

3.2 FTIR & TGA

FTIR analysis was carried out with a Perkin Elmer Spectrum 100 used in ATR mode (Total Reflected Reflectance), performing three acquisitions for each sample. The technique was applied to the handmade papers under study and two different cellulose samples, one treated with animal gelatin and the other one with gelatin and Tylose. It allowed to obtain preliminary information on fillers and adhesives utilized in paper manufactures, then confirmed by results of TGA and SDS-PAGE analysis. TGA analysis was performed with a Perkin Elmer STA (Simultaneous Thermal Analyzer) 6000 under nitrogen atmosphere. Three samples were analyzed: 19, 21 and a sample of pure cellulose used as standard.

3.3 SDS-PAGE & RP-HPLC

Small fragments (samples 17 and 20) were pre-treated in order to extract any protein material and later subjected to electrophoretic and chromatographic analysis. This procedure also involved two samples of cellulose treated with animal gelatin.

The SDS-PAGE analysis was carried out utilizing a 12% polyacrylamide gel run at 200 V constant voltage. The staining was made with the Silver Staining method, which is based on the interaction between proteins and silver nitrate with subsequent reduction, and allows to identify quantities in the nanogram range. The materials were weighed and soaked in an extraction buffer (1:1, 10 ml for 10 mg of sample) containing water, trifluoroacetic acid [TFA, 0.1%] and acetonitrile [25%]; then, they were pounded with a pestle, sonicated for 5 minutes (MSE Soniprep, power: medium, amplitude: 4) and centrifuged at 15,000 xg for 5 minutes.

The RP-HPLCwas performed with a ProSphere C4-300 Alltech Column (300 Å, 150 x 4.6 mm,5µm) and a linear gradient formed by a buffer A (H2O, TFA [0.1%]) and a buffer B (H2O, TFA [0.1%], and acetonitrile [90%]). The instrument was an Agilent 1100 with a diode-array detector, which allows to record UV spectrum for any eluted analyte of a chromatographic peak.

3.4 AMINO ACID COMPOSITION

Amino acid composition analysis of proteins present in the samples was performed by automated Edman degradation with a protein sequencer (Applied Biosystems, Foster City, California) through a full derivatization/hydrolysis cycle. Phenylisothiocyanate labels N-terminus of the given peptide, forms a cyclical compound, then under acidic conditions the labeled amino acid is cleaved away from the peptide and treated further in acid to form a more stable phenylthiohydantoin (PTH)-amino acid (AA) derivative. The PTH-AA derivatives were then identified by using online RP-HPLC. In order to disclose the presence of peptides deriving from animal gelatin in ancient paper, the same procedure was applied to 20 mg of two different samples: cellulose treated with commercial gelatin and sample 17 from Camerino.

3.5 NMR

3.5.1 Unilateral NMR

Measurements were carried out at 18.153 MHz with a unilateral NMR instrument from Bruker Biospin Italy. The operating probe has a penetration depth of about 0.1 cm inside. The maximum signal was obtained with a pulse width of 3 μs and the dead time was less than 15 μs. The spin– spin relaxation times T2 were measured with the CPMG sequence according to a previously published procedure [5, 6]. With this portable instrumentation a fully non-invasive analysis of the samples was carried out. The echo decays obtained applying the CPMG sequence were fit to the equation:

$$Y = \sum_i W_i \, exp\left[\frac{-t}{T_{2_i}}\right]$$

where *i* is the number of components, W*i* is the weight of the *i* component and T_{2i} is the spin-spin relaxation time of the i component. A regularized inverse Laplace transformation [7] was applied to invert the CPMG decay using a software implemented within the Matlab (MathWorks) software. After the transformation, data were represented as a distribution of relaxation times. In this representation, the maxima (peaks) of the distribution are centered at the corresponding most probable T_2 values, whereas peak areas correspond to the relative spin populations.

3.5.2 Solid-state ^{13}C CPMAS NMR spectroscopy

^{13}C CPMAS NMR spectra were carried out on a Bruker Advance III spectrometer operating at the proton frequency of 400.13 MHz on samples 2, 3, 4, 11, 12, 13, 14, 17, 18 and 19. Samples were

finely cut and packed into 4 mm zirconia rotors with an available volume reduced to 25 μl and sealed with Kel-F caps. The spin rate was 12 KHz. The contact time for the cross polarization was 1.5 ms, the recycle delay was 3 s, and the ^{1}H $\pi/2$ pulse width was 3.5 μs. The cross-polarization was achieved applying the variable spin-lock sequence RAMP–CPMAS [8, 9], the RAMP was applied on the ^{1}H channel, and during the contact time the amplitude of the RAMP was increased from 50 to 100% of the maximum value. Spectra were acquired with a time domain of 1024 data points were zero filled and Fourier transformed with a size of 4096 data points applying an exponential multiplication with a line broadening of 8 Hz.

The deconvolution of ^{13}C CP-MAS spectra was performed using the dm2004 program [10]. Each resonance was modelled by the following parameters: amplitude, position, width at half height and gaussian line shape. Applying the best fit procedure, the area and the chemical shift of all resonances were obtained. The sum of the integral of all resonances in each spectrum was normalized to 100.

3.6 PRINCIPAL COMPONENT ANALYSIS

Principal component analysis was applied to NMR spectral data. The statistical processing of NMR data was performed using Microsoft Office Excel 2003 and Excel macros for PCA written by Tom Thurston [11]. Before the application of PCA the absolute intensities of 3746 points in NMR spectra were normalized to obtain the same total integral value (10000) for all the samples. PCA was applied to mean-centred 3746 variables.

4. Results and Discussion

4.1 SEM

The morphological characterization carried out by electron microscopy highlighted some differences between the paper manufactures in Marche region. Firstly, in Camerino samples fibers show a greater uniformity (fig. 2-a) respect to Fabriano ones, where a lower refining of raw materials can be assumed [12]. In the handmade papers from Fabriano, there is an inhomogeneous distribution of the glue: this could have been caused by the application method that is the immersion of the sheet in a bath of hot gelatin [13], with consequent heterogeneous absorption by the fibers (fig. 2-b). In all samples from Camerino fibers appear fractured, probably as a consequence of material aging. Otherwise, in Fabriano documents there is a disarrangement of fibers structure reasonably due to a different and more vigorous mechanical treatment of the primary rags in the papermaking process. Indeed, comparing the SEM images of the fibers with those relating to fatigue and abrasion tests recorded on cotton and linen fibers, it can be seen that these are very different from those related to deterioration due to aging observed for example on archaeological textile fibers [14]. Similarities can be observed

with the morphologies of the breaks in the fibers of fabrics coming from a collection of linen sheets and dresses, which had been in regular use for about 40 years, and these were examined using microscopical analysis that revealed complex changes in both yarn and fibre structure, and it is probable that these changes, resulting from abrasive action, leading to fibre fatigue and 'brush ends' and an extended fatigue damage is also resulting in fibre loss, thin places and broken threads. On the other hand, the morphological image of aged flax fibers without having suffered mechanical stress is very different, as shown by a number of small fragments of fabric from the tomb of Tutankhamun under SEM examination. The fragment of shawl showed no signs of wear and the individual fibres, which appear to be flax, have suffered a concertina-type deformation, which seems to be associated with length shrinkage[14], (fig. 2-c,d).

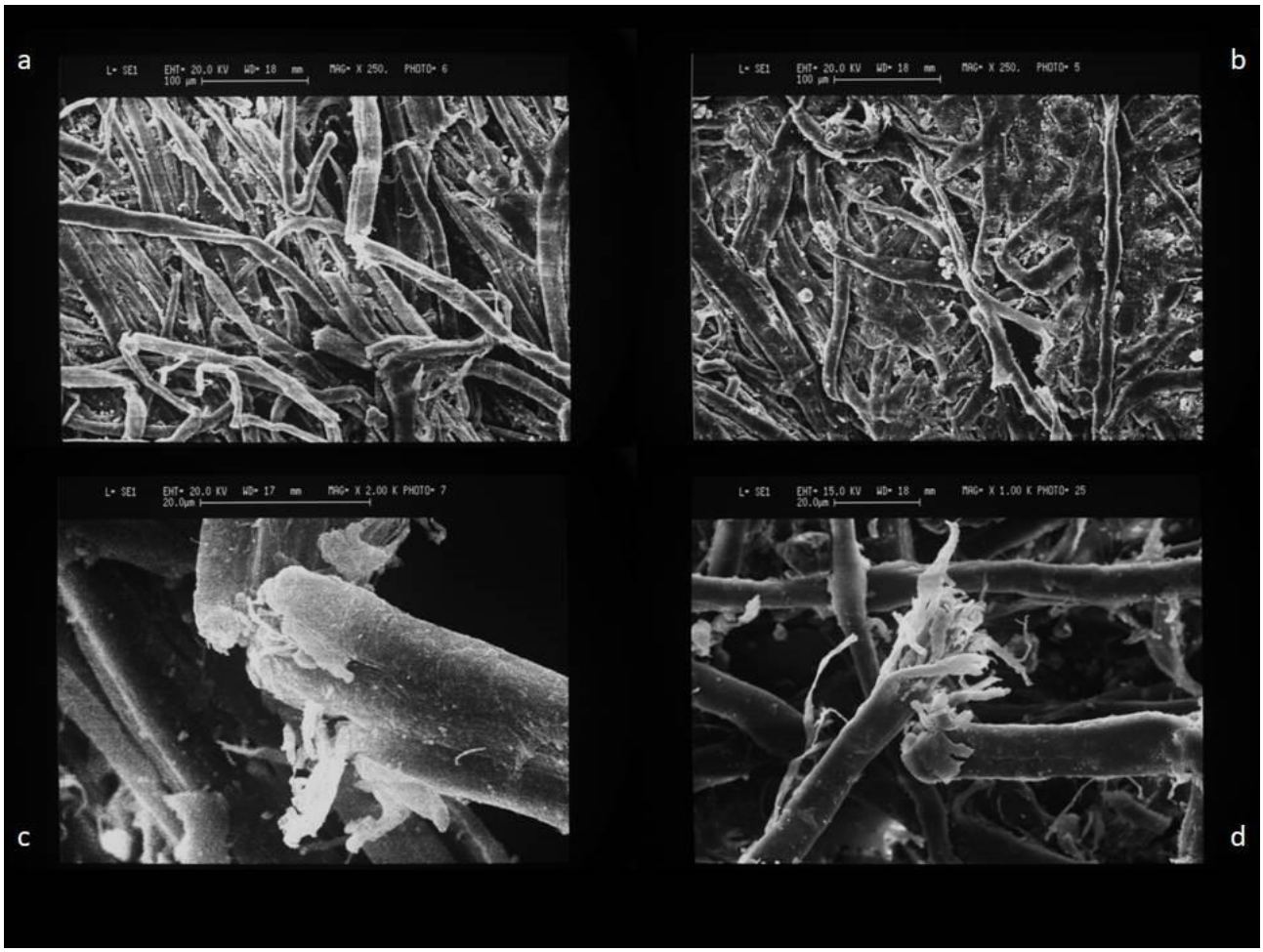

Fig. 2 – SEM images: a) sample 16 (Camerino), b) sample 19 (Fabriano), c) sample 16 (Camerino), d) sample 14 (Fabriano)

4.2 FTIR & TGA

The organic and inorganic substances which can contribute to the composition of paper are manifold: cellulose, starch, lignin, gelatin, rosin, synthetic adhesives, inks, fillers etc. FTIR spectroscopy, with

the employment of other complementary techniques, allows the identification of most of these components through the study of their characteristic absorption frequencies, thus avoiding or limiting the use of destructive analyses. Table 2 shows the typical bands and functional groups of cellulose, hemicellulose and lignin [15, 16].

Table 2 – Absorption Bands in the IR Spectra of cellulose, hemicellulose and lignin

Frequency [cm^{-1}]	**Functional groups**
3600-3000	OH stretching
2860-2970	C-H_n stretching
1700-1730	
1510-1560	C=O stretching
1600-1650	H_2O bending
1632	C=C
1613, 1450	C=C stretching
1470-1430	O-CH_3
1440-1400	OH bending
1402	CH bending
1370; 1335; 1316	CCH-COH bending
1232	C-O-C stretching
1215	C-O stretching
1170, 1082	C-O-C stretching vibration
1108	OH association
1060	C-O stretching and C-O deformation
700-900	C-H
700-400	C-C stretching

In this study, FTIR analysis of the paper samples, on the one hand excluded the presence of starch adhesive, identified through the peak at 998 cm^{-1}, on the other hand highlighted the possible use of animal gelatin, recognizable by the characteristic signals of the peptide bond at about 1520 cm^{-1} and 1670 cm^{-1}[15, 17]. As for samples 6 and 7, the identification of a protein-based glue is doubtful: considering that they are restored documents, however, this could be due to the presence of Tylose – a cellulose ether used as adhesive in restoration – which might not make gelatin peaks more visible. This hypothesis seems to be confirmed by the spectra of cellulose samples treated with animal gelatin and Tylose: in fig. 3 we note a general attenuation of the IR signals for the sample prepared with the addition of the cellulose ether, even in the region which corresponds to peptide bond absorption.

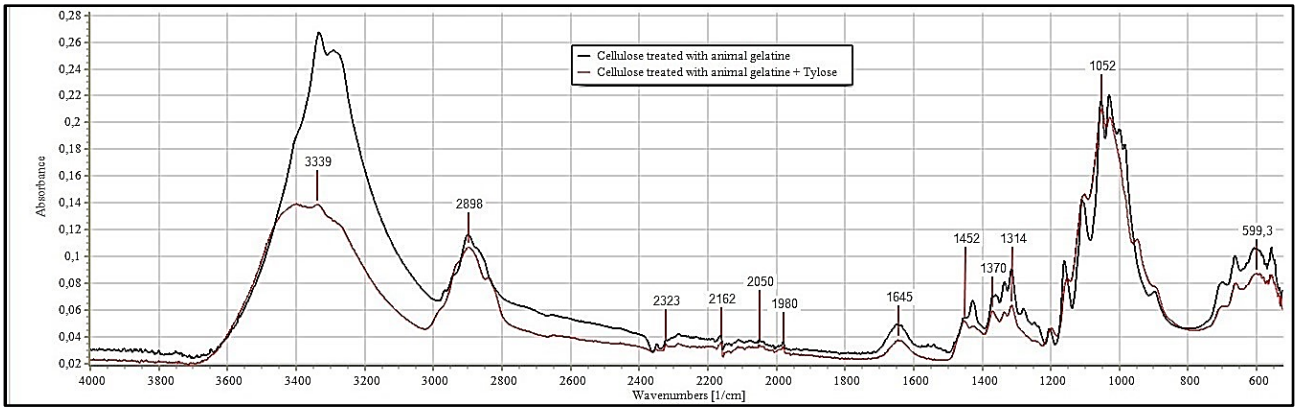

Fig. 3 – FTIR spectra of cellulose samples: black, cellulose treated with animal gelatin; red, cellulose treated with animal gelatin and Tylose

About the identification of the filler utilized in the papermaking process, all the examined documents show a weak signal at 1410-1430 cm^{-1}, characteristic of the use of alkali carbonates [15]. The presence of calcium carbonate, in particular, was confirmed by recording of its second characteristic peak at 875 cm^{-1}. The thermogravigrams of the analyzed paper fragments show four peaks: the first, at 100 °C, is due to the loss of samples moisture content; the second peak, between 380 and 400 °C, indicates the decomposition of cellulose; the third, at 500 °C, is attributed to the combustion of organic compounds; finally, the fourth and last peak, between 750 and 800 °C, indicates the transformation of carbonate compounds into the corresponding monoxides, thus confirming their presence as deduced from FTIR analysis [18].

4.3 SDS-PAGE & RP-HPLC

The electrophoretic analysis confirmed the hypothesis – corroborated by literature [2,19] – on the useof a protein-based glue in the paper manufactures of Marche region: in both samples from Camerino and Fabriano, survey results show the presence of proteins similar to those extracted from cellulose treated with animal gelatin, as can be seen by comparing protein pattern of lanes 2, 3, 4 and 5, with evident low molecular weight bands (< 10000 Da) and weak high molecular weight ones (>40000 Da) (fig. 4).

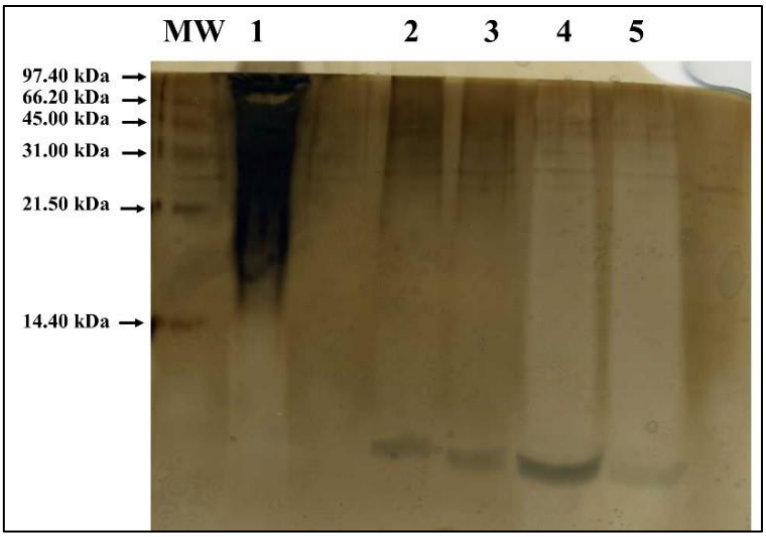

Fig. 4 – Silver-stained SDS-PAGE pattern of proteins extracted from cellulose treated with animal gelatin (lanes 2 and 3) and from paper samples 17 (lane 4, Camerino) and 20 (lane 5, Fabriano). In lane 1 gelatin treated with extraction buffer has been loaded

About RP-HPLC results, both samples investigated show chromatographic peaks with UV spectra characteristic of protein material, with a maximum at about 220 nm, identifying the peptide bond, and another one at 280 nm, due to the presence of aromatic amino acid residues.

4.4 AMINO ACID COMPOSITION

The results shown in fig. 5 represent a comparison of the percentage of each aminoacid residue relative to the total residues, detected in the cellulose treated with gelatin and in the paper document 17.

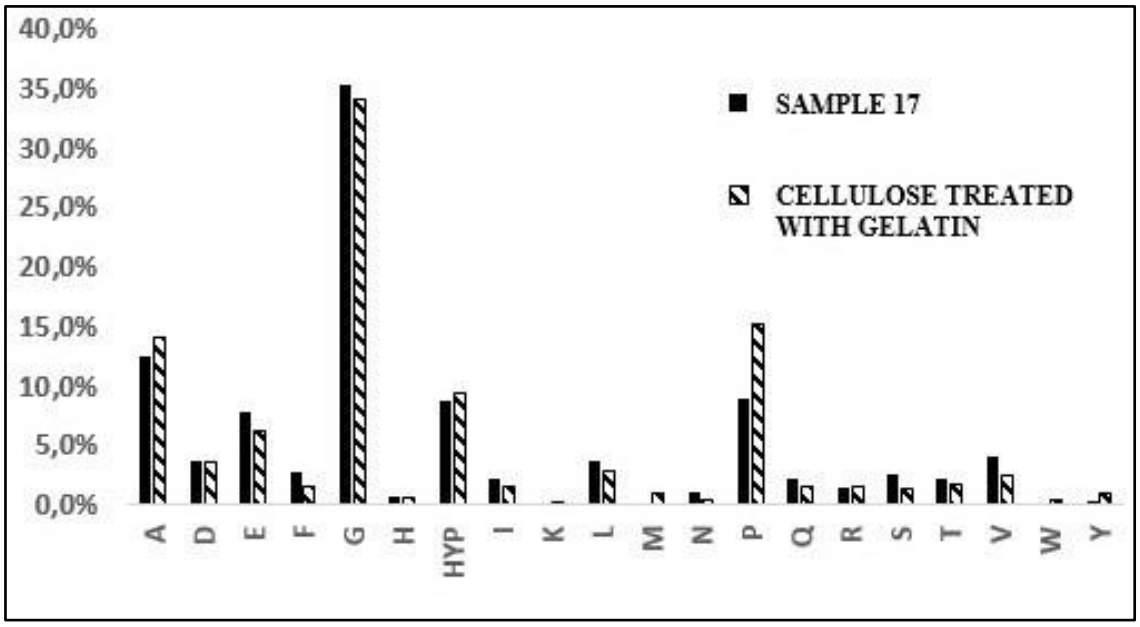

Fig. 5 – Aminoacid composition of sample 17 from Camerino and cellulose treated with commercial gelatin, expressed as relative percentage on total residues

The detection of hydroxyproline in both samples indicates the presence of collagen derived gelatin. The aminoacidic profile of the two analyzed samples is indeed very similar, with the characteristic pattern represented by glycine (G), hydroxyproline (HYP), proline (P), typical of collagen, and the absence of cysteine [20, 21]. Gelatin is the product of collagen partial hydrolysis either in acid or alkaline environment; the product is a group of denatured different peptides with gel and gluing properties. The procedure used for gelatin extraction and the kind of animal source can determine some differences in the relative percentage of aminoacid, but the characteristic signature of collagen is conserved. The high abundance of alanine is also a characteristic of collagen.

4.5 NMR

4.5.1 Unilateral NMR

Unilateral NMR allows to perform a fully non-destructive and non-invasive analysis providing diagnostic information on a wide range of materials of interest in the field of cultural heritage [22-24].

It is possible to measure directly on the object without sampling. The measuring probe consists of a small magnet that generates a magnetic field outside the magnet itself. Unlike conventional NMR techniques, in unilateral NMR, the measurement is carried out applying the probe head to one side of the object, thus completely circumventing the problem of size and sampling of the object being studied. The experiments carried out allow to measure the hydrogen content present in the material, the longitudinal (T_1) and the transverse relaxation time (T_2). These parameters may be related to the degradation state of the material under consideration. In a previous study it was reported that, in particular T_2, can be considered a degradation index in paper conservation studies. The recent development of portable instruments has made it possible to exploit this method of investigation to study in a completely non-invasive and non-destructive way historical documents for which also the sampling of small quantities of paper must be absolutely avoided [24, 25]. T_1 and T_2 relaxation times depend on the water confined in the matrix under investigation, therefore on the size of the domains themselves. The measurement of relaxation times obtained by unilateral NMR on a good quality paper sample, made of pure cellulose, shows two T_2 relaxation time distributions (fig. 6).

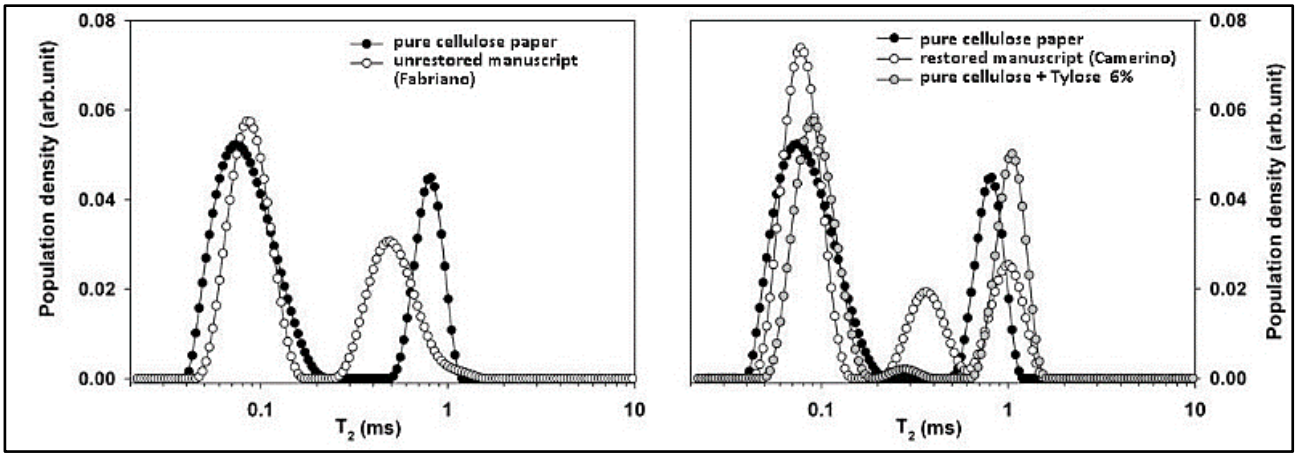

Fig. 6 – T_2 relaxation times distribution: left, comparison between pure cellulose paper and an unrestored manuscript (Fabriano); right, comparison among pure cellulose paper, pure cellulose paper treated with Tylose 6%, restored manuscript (Camerino)

The shorter component of T_2 is about 0.08 ms and is due to water strongly bound to the cellulose and hemicellulose chains; the longer component of about 0.9-1.0 ms is ascribable to water found in larger domains of cellulose. The same figure shows the distribution of the relaxation times T_2 obtained for a Fabriano manuscript that has not been restored. According to the literature, the ancient manuscript shows the shortening of the longer component of T_2 as a result of degradation. Measurements of relaxation times were also carried out on manuscripts from Camerino, which were subjected to restoration and reintegration of really damaged pages. In this case, the measurement has yielded more difficult results to interpret. Fig. 6 shows the distribution of relaxation times obtained on a deteriorated and reintegrated page (white symbols). The distribution of relaxation times shows three peaks, two of which are superimposable to those obtained by measuring the restoration card used for reintegration (black symbols). The interpretation of the peak of intermediate T_2 (about 0.38 ms) has not yet been clarified. One hypothesis was to attribute this peak to the substance used to adhere the restoration card to the manuscript, Tylose. The same figure shows the distribution of relaxation times obtained on a standard of pure cellulose paper treated with Tylose (gray symbols). In this last sample, the distribution of T2 relaxation times also shows a third intermediate peak, of lesser intensity recorded on the manuscript, which is probably due to water bound to Tylose.

4.5.2 Solid-state ^{13}C CPMAS NMR spectroscopy

Solid state ^{13}C CPMAS NMR spectroscopy is a versatile tool for morphology studies of cellulose based materials. The ^{13}C CPMAS spectrum of the paper may be actually considered as the "fingerprint" of the solid component of paper, allowing the recognition of the type of cellulose, the determination of the crystalline/amorphous ratio, the detection of the possible presence of hemicellulose, cellulose oligomers, and non-cellulosic compounds such as organic additives present

in the material. These molecular properties strongly influence the chemical, physical, and mechanical characteristics of a cellulose material and are, thus, of interest for detecting changes induced in the solid matrix of the paper due to the ageing processes. The ^{13}C CP-MAS spectrum of paper made by pure cellulose only, used as cellulose standard sample, is shown in fig. 7-a.

The spectrum of cellulose exhibits easily separable resonances from crystalline and less-ordered domains for the C_4 and C_6 atoms of the glucose unit. In particular resonances at 90.3 and 66.8 ppm labelled as C_{4c} and C_{6c} are respectively due to C_4 and C_6 of the crystalline phase, whereas those at 85.4 and 64.5 labelled as C_{4a} and C_{6a} are respectively due to C_4 and C_6 of the amorphous phase of the cellulose. Highly informative region in ^{13}C spectrum is the signal from C_4 carbon. Information extracted from this region can be used to determine the crystallinity of cellulose, *CI*, calculated by dividing the area of the crystalline peak C_{4c} by the total area assigned to the C_4 peak (C_{4c}+C_{4a}) [26]:

$$CI = C_{4c}/(C_{4c}+C_{4a})$$

The resonance at about 106 ppm ascribed to C_1, reveals the presence of two crystalline forms, namely I_α and I_β. It is well known that cellulose can occur in four polymorphic varieties denoted as I, II, III and IV [27]. As generally accepted, the native cellulose I crystallizes in two forms labelled as I_α and I_β, whose differ in hydrogen bonding patterns only while the backbone conformations are nearly identical [28, 29].

The information extracted from C_1 can be used to evaluate the ratio R= I_α /I_β, which depends on the origin of cellulose [30].

With the aim of evaluating differences among ancient samples coming from different manufacturing areas (Camerino and Fabriano), ^{13}C CPMAS NMR analysis was carried out on samples 2, 3, 4, 17 and 18 belonging to Camerino area and 11, 12, 13, 14 and 19 belonging to Fabriano area. In fig. 7 a selection of solid state spectra are reported for both series. Clear differences are evident between Fabriano and Camerino samples, in particular Fabriano samples show broader resonances and a different ratio between the two crystalline polymorphous forms, I_α and I_β compared to that of Camerino samples.

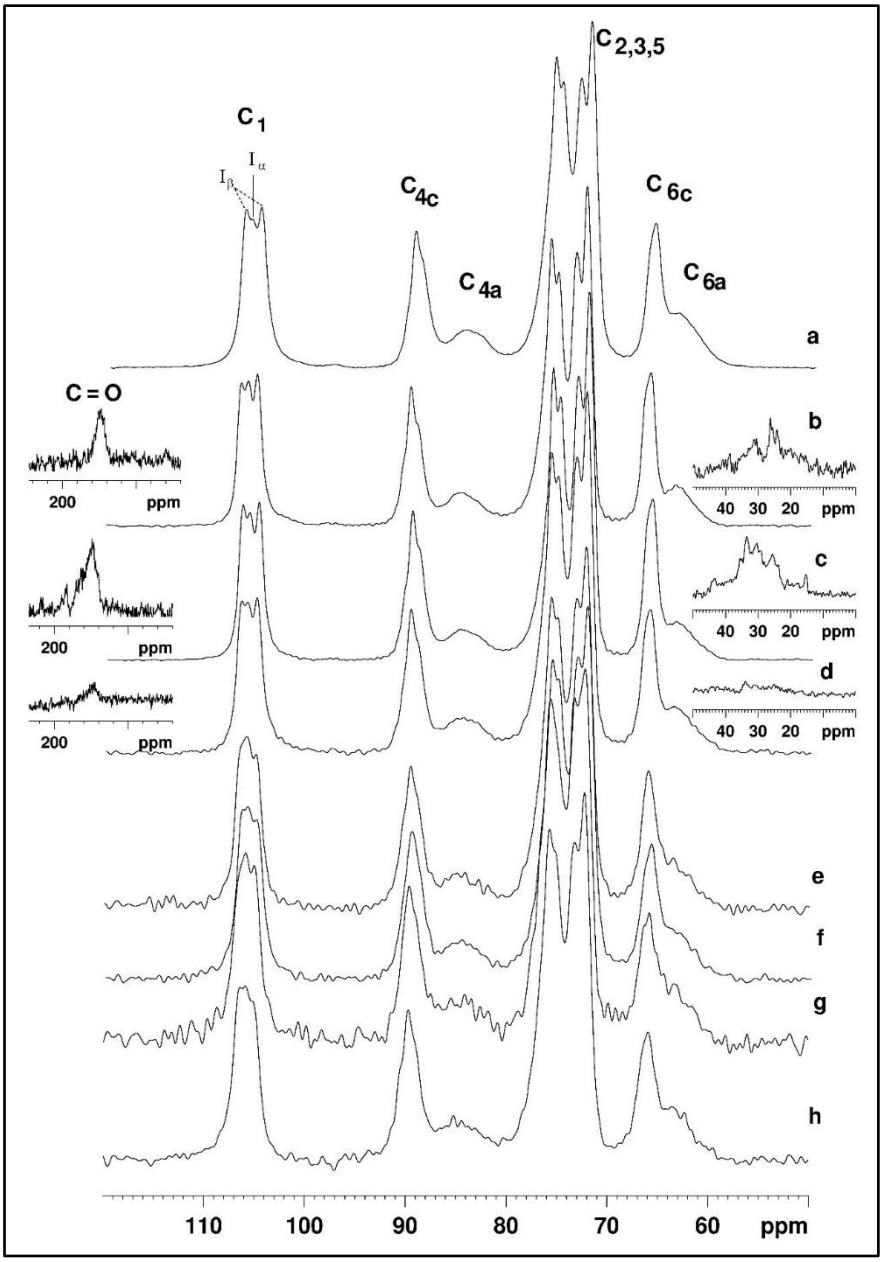

Fig. 7 – ^{13}C CPMAS NMR spectra of a) reference pure cellulose paper, b) sample 2 (Camerino), c) sample 3 (Camerino), d) sample 4 (Camerino), e) sample 11 (Fabriano), f) sample 12 (Fabriano), g) sample 13 (Fabriano), h) sample 14 (Fabriano)

The resolution of ^{13}C CPMAS NMR spectra is adequate enough to allow chemically equivalent carbons from different magnetic environments to be separated, however special processing techniques like deconvolution are needed to fully interpret the overlapping lines. From the full deconvolution of the spectra the integrals of the resonances can be obtained, allowing a quantitative evaluation of the modifications occurring in the cellulose matrix for the two series.

For this study the relevant integrals of the resonances are: the integral of the broad shoulder between 90 and 100 ppm that gives the amount of cellulose oligomers due to the depolymerization of cellulose; the ratio between the integrals between of the I_α and I_β that gives information about the origin of the

cellulose; the ratio between the integrals of C_{4c} and C_{4a} that gives the crystalline/amorphous ratio and the integrals of the resonance of carboxyl groups. The integrals obtained from the deconvolution procedure applied to the ancient papers are reported in Table 3. In the same table the integral value obtained for the standard sample paper is also reported. In all ancient samples a very small quantity of the oligomers was found, indicating a general good state of conservation of the paper.

Table 3 – Integrals (%) of resonances obtained applying the deconvolution procedure to ^{13}C CPMAS spectra of Camerino and Fabriano paper samples

Sample ID	I_α	I_β	oligo	C_{4c}	C_{4a}	C_{235}	C_{6c}	C_{6a}	C=O	C Aliphatic	$CI = \frac{C_{4c}}{C_{4a}+C_{4c}}$	$R = \frac{I_\alpha}{I_\beta}$
Standard	3.0	13.6	nd	9.0	6.6	52.5	10.3	4.3	nd	nd	0.57	0.22
2	3.5	12.7	0.2	9.7	4.8	48.8	8.6	5.0	2.1	2.0	0.67	0.27
3	3.2	12.2	0.1	9.9	4.9	46.6	9.0	4.7	2.9	5.0	0.67	0.27
4	2.9	12.4	1.1	9.3	6.3	45.9	6.6	5.1	1.5	4	0.59	0.23
17	3.2	13.8	0.9	13.1	4.7	50.9	7.3	6.6	nd	nd	0.73	0.24
18-21	3.0	12.6	0.1	9.0	5.8	50.6	6.9	6.4	0.7	2.5	0.61	0.24
11	5.2	11.4	0.5	10.5	6.0	49.4	8.3	6.2	nd	nd	0.63	0.45
12	4.6	11.2	0.3	11.4	4.9	47.8	7.5	6.1	1.2	nd	0.70	0.41
13	4.9	12.1	0.8	11.0	3.9	49.5	6.9	4.5	nd	nd	0.74	0.40
14	4.6	10.9	0.2	10.3	5.5	47.2	7.2	7.1	0.8	nd	0.65	0.42
19	4.4	11.0	0.4	9.5	3.8	46.6	7.4	7.3	nd	nd	0.71	0.40

The *CI* (crystallinity index), was 0.57 for reference paper sample, whereas it increased in all Camerino and Fabriano samples, with values ranging between 0.6-0.65 up to 0.73 for sample 17 and 0.74 for sample 13. However, slightly higher values were observed for Fabriano samples. The actual mechanism and reason for the observed line narrowing and relative crystalline signal enhancement remains largely unknown.

However hydrolytic degradation has historically been looked upon as the most important reason for the breakdown of cellulose during the ageing of paper [31]. What is important in this context is that the degradation processes are often very strongly related, both the acid and the oxidation hydrolysis. Acid hydrolysis leads similarly to the forming of reducing end-groups which can easily be oxidized to carboxyl groups, which induce autohydrolytic breakdown of the cellulose.

Cross-linking of the cellulose through the formation of e.g. hemiacetal bonds (acid catalyzed reaction) has an embrittling effect as does crystallization (induced through hydrolysis) or relaxation of the free volume of the amorphous cellulose (natural physical ageing of polymers) [31]. In addition also Park et al. suggested that amorphous components become more ordered upon hydration [27].

Therefore *CI* can be used as an index that parameterizes the degradation process in Fabriano and Camerino samples, and can be ascribed to a hydrolysis reaction induced by favorable microclimatic conditions.

The behavior of the ratio R between the two crystalline polymorphous forms, I_α and I_β was found to be very peculiar. Such a ratio is calculated by the integrals obtained from the deconvolution of C_1 resonance.

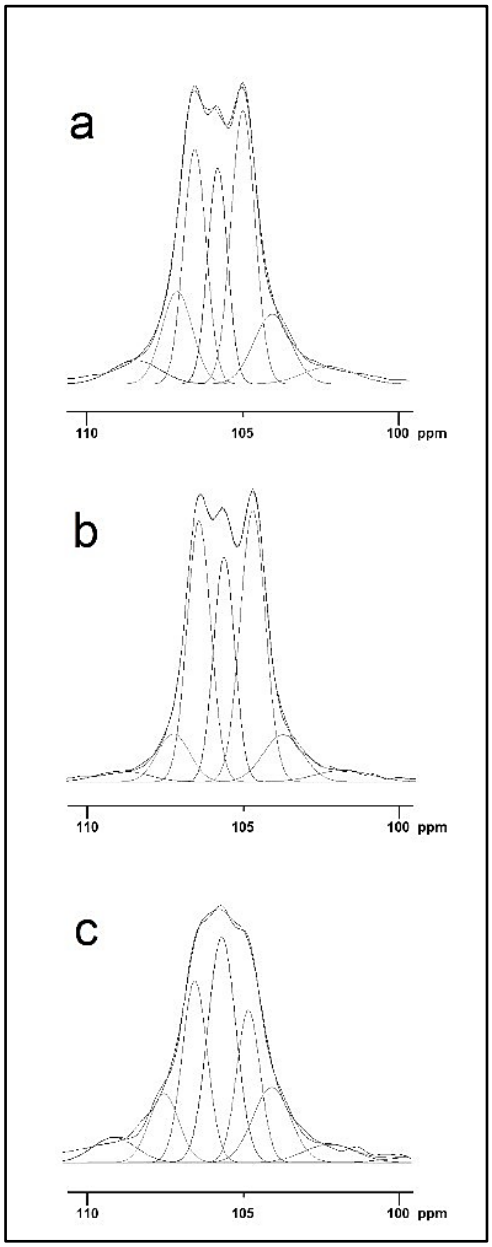

Fig. 8 – Details of deconvolution of C_1 resonance of ^{13}C CPMAS NMR experimental spectra of a) pure cellulose paper sample; b) sample 3 (Camerino); c) sample 11 (Fabriano)

In fig. 8 a detail of deconvolution of C_1 resonance obtained for reference paper, sample 3 (Camerino) and sample 11 (Fabriano) is reported. As shown, the profile of the C_1 resonance is characterized by three sharp resonances centered at 106.6, 105.8 and 105 ppm and two very broad bands at 107 and 104 ppm. The central sharp resonance at 105.8 is due to I_α, whereas the two lateral sharp resonances at 106.6 and 105 ppm are due to I_β. In the pure cellulose paper this ratio is 0.22, and in Camerino paper samples the integral ratio R (I_α /I_β) is around 0.25. These values are very similar to those

reported in literature for higher plant celluloses [32]. On the contrary for Fabriano samples an increase of integral due to I_α is observed (fig. 8-c). For all these samples a value of R of 0.4-0.45 is found. In fig. 9 the ratio R as a function of all examined samples is reported.

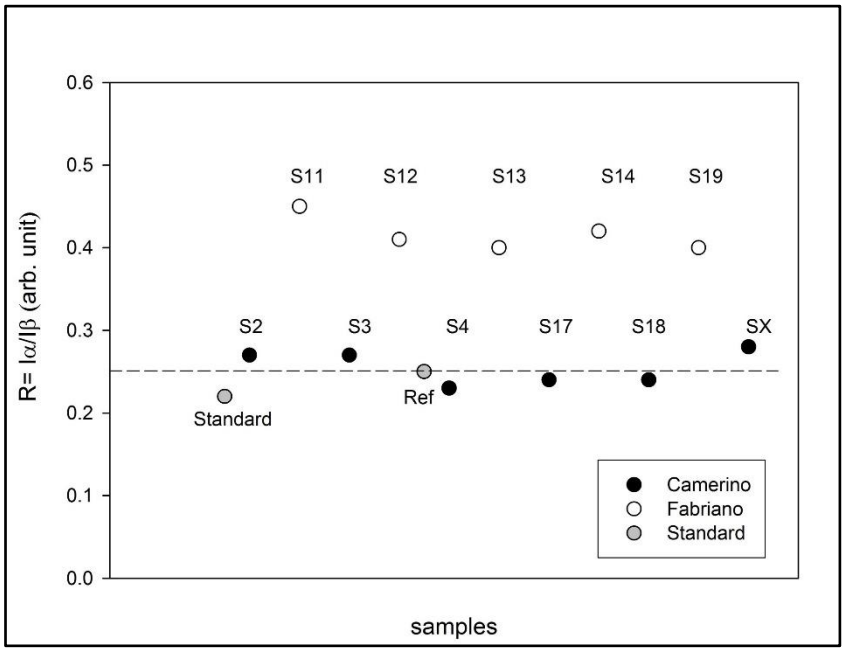

Fig. 9 – (R= I_α / I_β) Ratio of the integrals I_α and I_β obtained from deconvolution of C_1 resonances of ^{13}C CPMAS NMR paper samples spectra

Finally, a weak carbonyl band at around 176 ppm, due to oxidative degradation phenomena, was always observed in the samples from Camerino and in samples 12 and 14 coming from Fabriano. A weak resonance band ranging from 10 to 50 ppm, attributable to aliphatic compounds, was also found in some Camerino samples.

4.6 PRINCIPAL COMPONENT ANALYSIS

Principal component analysis can be applied to the spectroscopic data to enhance the discriminant power of this analytical technique on spectral data. PCA is a statistical method to reduce the multidimensionality of the experimental data. It is a statistical procedure that applies an orthogonal transformation of data to transform a set of possibly correlated variables into a set of values of linearly uncorrelated variables called principal components. This transformation is defined in such a way that the first principal component accounts for a such of the variability in the data as possible; and succeeding component in turn has the highest variance possible under the constraint that is orthogonal to the preceding components. Each resulting vectors is a linear combination of the variable containing *n* observation. The resulting vectors (each being a linear combination of the variables and containing *n* observations) are an uncorrelated orthogonal basis set.

PCA has been widely used in medicine and in food matrices [33], and recently it was applied to discriminate data obtained from ambers and fossil resins, coming from different geographical areas [34].

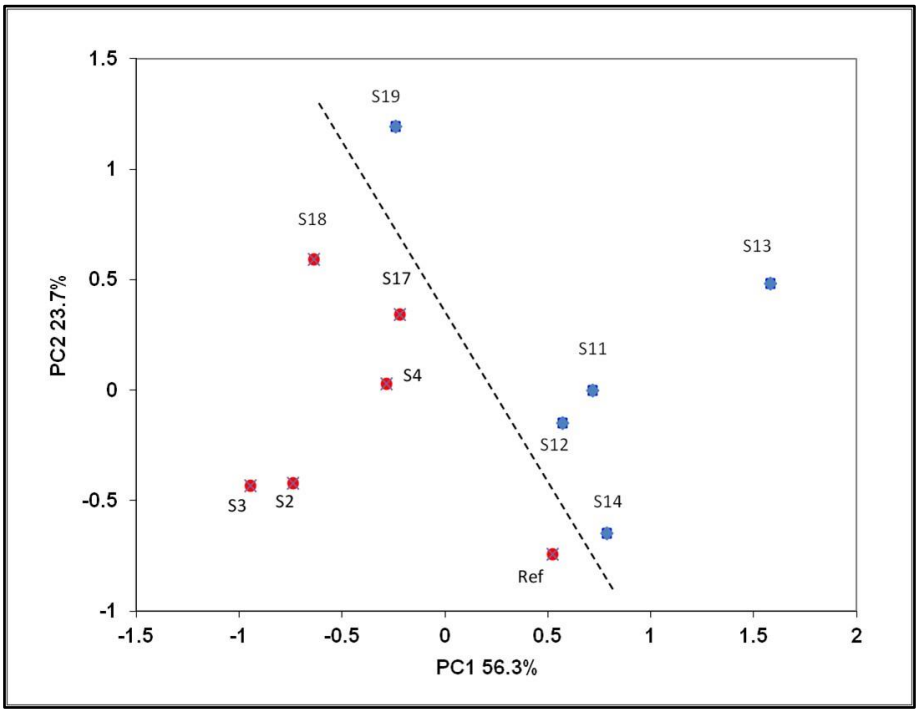

Fig. 10 – Principal component analysis (PCA) of ^{13}C CPMAS NMR spectroscopic data: scores of the principal component variables PC1 and PC2

Fig. 10 shows the scores of the PCs obtained applying the PCA to ^{13}C CPMAS NMR spectral data. The first two PCs account for 80% of the variability within the data, PC1 providing for 56.3% and PC2 for 23.7%. Principal component PC1 allows the clustering of Fabriano samples with respect to Camerino ones and divides all documents in two sets.

Conclusions

In this study a multi-analytical approach was used to perform a diagnostic analysis of a group of paper samples from Camerino and Fabriano (13th-15th century). Making use of different types of analytical techniques, it was possible to investigate common and dissimilar aspects between the different manufactures of Marche region. The morphological characterization carried out by SEM highlighted some differences between handmade papers from Camerino-Fabriano area. In Camerino samples fibers appear fractured, probably as a consequence of material aging, whereas in Fabriano there is a disarrangement of fibers structure probably due to a different and more vigorous mechanical treatment. An inhomogeneous distribution of the glue, probably caused by the application method, was found.

FTIR spectroscopy excluded the presence of starch adhesive and highlighted the possible use of animal gelatin in both areas. Moreover, the technique allowed to identify the filler utilized in the papermaking process by the characteristic range of alkali carbonates, as confirmed also by TGA analysis.

SDS-PAGE and RP-HPLC confirmed the hypothesis on the use of a protein-based glue in both documents from Camerino and Fabriano. In the amino acidic profile of a sample from Camerino, the detection of hydroxyproline and alanine indicated the presence of collagen derived gelatin.

In addition, the paper samples were also evaluated and characterized by NMR.

Using portable NMR was possible to establish the state of conservation of the handmade papers from Camerino and Fabriano. Moreover, it was possible to detect the presence of organic substances on the surface of restored paper probably due to Tylose, a medium used to adhere the restoration card to the manuscript. ^{13}C CPMAS Spectroscopy provided very valuable information about the cellulosic support. The spectrum of cellulose exhibits easily separable resonances from crystalline and less-ordered domains. Highly informative region in ^{13}C spectrum is the signal from C_4 carbon, from which information can be extracted to determine the crystallinity of cellulose, *CI*, whose value was found higher in Fabriano and Camerino samples respect those found in reference paper sample. These increase of crystallinity can be ascribed to the hydrolytic degradation process.

The resonance at about 106 ppm ascribed to C_1, revealed the presence of two crystalline forms, namely I_α and I_β. The information extracted from C_1 were used to evaluate the ratio $R= I_\alpha /I_\beta$, which depends on the origin of cellulose. Different values of $R= I_\alpha /I_\beta$ were found in the Fabriano and Camerino samples. Finally differences between the paper manufactures were evidenced by applying PCA analysis to the spectroscopic NMR data, which allowed the clustering of Fabriano samples with respect to Camerino ones and divided all documents in two sets.

The choice to use a multidisciplinary approach and carry out a wide range of characterization analyzes of the analyzed paper fragments is certainly original and is due to the need to proceed with comparative studies between two extremely similar materials produced in the same historical period. This type of study carried out on similar materials and present in trace (glue) requires in fact the collection of data coming from different analytical techniques that allow an integrated comparison to evaluate the minimal differences or similarities recorded to compare the two different manufactures.

Acknowledgements

The analysed paper documents have been kindly made available by the Section of the State Archive of Camerino, the Municipal Historical Archive of Fabriano and the State Archive of Prato.

The assistance of Dr.A. Amici, Dr.G. Castagnari, Dr. P. Di Martino, Dr. E. Di Stefano, Dr. M. Minicucci, Dr. L. Petetta, Dr. M. Ricciutelli and Dr. S. Tiberi is gratefully acknowledged.

Declarations of interest: none.

This research did not receive any specific grant from funding agencies in the public, commercial, or not-for-profit sectors.

References

1. Gasparinetti, Carta, cartiere e cartai fabrianesi, estratto da Il Risorgimento grafico 9-10 settembre-ottobre 1938, Milano 1939, pp. 373-431.
2. G. Castagnari, Le origini della carta occidentale nelle valli appenniniche delle Marche centrali da una indagine archivistica, in Alle origini della carta occidentale: tecniche, produzioni, mercati (secoli XIII-XV), Atti del Convegno, Camerino, 4 ottobre 2013, pp. 9-34.
3. S. RodgersAlbro, Searching for Fabriano paper in the library of Congress, in G. Castagnari, a cura di, Impiego delle tecniche, cit., pp. 193-224.
4. E. Di Stefano, Proiezione europea e mediterranea della carta di Camerino-Pioraco e di Fabriano all'apogeo dello sviluppo medievale (secoli XIV-XV), in Alle origini della carta occidentale: tecniche, produzioni, mercati (secoli XIII-XV), Atti del Convegno, Camerino, 4 ottobre 2013, pp. 35-62.
5. N. Proietti, D. Capitani, E. Pedemonte, B. Blümich, A.L. Segre, Monitoring degradation in paper: non-invasive analysis by unilateral NMR. Part II, Journal of Magnetic Resonance, Volume 170, (2004), pp. 113-120.
6. K. Castro, N. Proietti, E. Princi, S. Pessanha, M.L. Carvalho, S. Vicini, D. Capitani, J.M. Madariaga, Analysis of a coloured Dutch map from the eighteenth century: the need for a multi-analytical spectroscopic approach using portable instrumentation, Analytica chimica acta, 623 (2), (2008), pp. 187-194.
7. W.H. Press, S.A. Teukolsky,W.T. Vetterling, B.P. Flannery, Numerical Recipes in Chemistry, Cambridge University Press: Cambridge, UK, 1994.
8. G. Metz, X. Wu, S.O Smith, Ramped-amplitude cross polarization in magic-angle-spinning NMR, Journal of Magnetic Resonance, Series A 110 (2), (1994), pp. 219-227.
9. R.L. Cook, C.H. Langford, R. Yamdagni, C.M. Preston, Magic Angle Spinning 13C NMR Procedure for the Study of Humic Materials, Analytical Chemistry, Volume 68, Issue 22, (1996), pp. 3979-3986.

10. D. Massiot, F. Fayon, M. Capron, I. King, S. Le Calvè, B. Alonso, JO. Durand, B. Bujoli, Z. Gan, G. Hoatson, Modelling one- and two-dimensional solid-state NMR spectra, Magnetic resonance in chemistry, 40 (1), (2002), pp.70-76.
11. R.G. Brereton, Chemometrics: Data Analysis for the Laboratory and Chemical Plant, Wiley: Chichester, UK, 2003, pp. 449-456.
12. E. Pedemonte, a cura di, La carta: storia, produzione, degrado, restauro, Marsilio Ed.: Venezia, 2008.
13. O. Emery, a cura di, L'arte della carta a Fabriano, Jesi, 1978.
14. J.W.S. Hearle, B. Lomas, W.D. Cooke, Atlas of Fibre Fracture and Damage to Textiles, 2nd Edition, Woodhead Publishing: Cambridge, UK, 1998.
15. V. Librando, Z. Minniti, S. Lorusso, Ancient and modern paper characterization by FTIR and Micro-Raman spectroscopy, Conservation Science in Cultural Heritage, 11, (2011), pp. 249-263.
16. P. Calvini, A. Gorassini, R. Chiggiato, Fourier-Transform Infrared Analysis of some Japanese Papers, Restaurator, 27, (2006), pp. 81-89.
17. V. Librando, S. Lorusso, Z. Minniti, Ancient and Modern Paper Characterization by FTIR and Micro-Raman Spectroscopy, Conservation Science in Cultural Heritage, 11, (2011), pp. 249-268.
18. H.G. Wiedemann, J.R. Günter, H.R. Oswald, Investigation of ancient and new Japanese papers, Termochimica acta, 282, (1996), pp. 453-459.
19. E. Di Stefano, La carta marchigiana sul mercato europeo e il caso di Camerino nei secoli XIV-XV, in Proposte e ricerche, 54, 2005, p. 198, nota 15.
20. J.E. Eastoe, The amino acid composition of mammalian collagen and gelatin, Biochemical Journal, 61 (4), (1955), pp. 589-600.
21. M. Gauza-Włodarczyk, L. Kubisz, D. Włodarczyk, Amino acid composition in determination of collagen origin andassessment of physical factors effects, International Journal of Biological Macromolecules, 104, (2017), pp. 987–991.
22. B. Blümich, S. Anferova, S. Sharma, A.L. Segre, C. Federici, Degradation of historical paper: nondestructive analysis by the NMR-MOUSE, Journal of Magnetic Resonance, 161 (2), (2003), pp. 204-209.
23. N. Proietti, D. Capitani, E. Rossi, S. Cozzolino, A.L. Segre, Unilateral NMR study of a XVI century wall painted, Journal of Magnetic Resonance, 186 (2), (2007), pp. 311-318.
24. K. Castro, S. Pessanha, N. Proietti, E. Princi, D. Capitani, M.L. Carvalho, J.M. Madariaga, Non-invasive and non-destructive NMR, Raman and XRF analysis of a Blaeucoloured map from the seventeenth century, Analytical and bioanalytical chemistry, 391 (1), (2008), pp. 433-441.

25. D. Capitani, M.C. Emanuele, A.L. Segre, C. Fanelli, A.A. Fabbri, D. Attanasio, B. Focher, G. Capretti, Early detection of enzymatic attack on paper by NMR relaxometry, EPR spectroscopy and Xray powder spectra, Nordic Pulp and Paper Research Journal, 13, (1998), pp. 95-100.
26. P.T. Larsson, K. Wickholm, T. Iversen, A CP/MAS C-13 NMR investigation of molecular ordering in celluloses, Carbohydrate Research,302 (1-2), (1997), pp.19-25.
27. S. Park, J.O. Baker, E.H. Himmel, P.A. Parilla, D.K. Johnson, Cellulose crystallinity index: measurement techniques and their impact on interpreting cellulase performance, Biotechnology for Biofuels, 2010, 3:10.
28. J.H. Wiley, R.H. Atalla, Raman Spectra of Celluloses, in R.H. Atalla, The Structures of Cellulose. Characterization of the solid states, ACS Symposium Series 340, American Chemical Society: Washington, DC, 1987, pp. 151-168.
29. J. Sugiyama, J. Persson, H Chanzy, Combined infrared and electron diffraction study of the polymorphism of native celluloses, Macromolecules, 24, (1990), 2461.
30. R.H. Atalla, D.L. Vanderhart, Native cellulose: a composite of two distinct crystalline forms, Science, 223 (4633), (1984), pp. 283–285.
31. C. Fellers, T.Iversen, T.Lindström, T. Nilsson, M.Rigdahl, Ageing/Degradation of Paper - A literature survey,FoU-projektet for papperskonservering Report No. 1E, ISSN 0284-5636, Stockholm, September 1989.
32. G. Zuckerstätter, G. Schild, P. Wollboldt, T. Röder, H.K. Weber, H. Sixta, The elucidation of cellulose supramolecular structure by 13C CP-MAS NMR, LenzingerBerichte, 87, (2009), pp. 38-46.
33. L. Mannina, A.P. Sobolev, S. Viel, Liquid state 1H high field NMR in food analysis, Progress in Nuclear Magnetic Resonance Spectroscopy, 66, (2012), pp. 1-39.
34. G. Barone, D. Capitani, P. Mazzoleni, N. Proietti, S. Raneri, U. Longobardo, V. Di Tullio, 13C Solid State Nuclear Magnetic Resonance and m-Raman Spectroscopic Characterization of Sicilian Amber, Applied Spectroscopy, 70(8), (2016), pp. 1346–1355.

Mortar analysis of historic buildings damaged by recent earthquakes in Italy

The European Physical Journal Plus

G. Roselli[1]*, D. Mirabile Gattia[2], O. AlShawa[3], P. Cinaglia[4], G. Di Girolami[4], C. Francola[3], F. Persia[2], E. Petrucci[5], R. Piloni[1], F. Scognamiglio[4], L. Sorrentino[3], S. Zamponi[1], and D. Liberatore[3]

1 School of Science and Technology, Chemistry Division, University of Camerino, Via S. Agostino 1, 62032 Camerino, Italy

2 Department of Sustainability SSPT - ENEA - CR Casaccia, Via Anguillarese 301, 00123 Rome, Italy

3 Department of Structural and Geotechnical Engineering, "Sapienza" University of Rome, Rome, Italy

4 School of Science and Technology, Technologies and Diagnostics for Conservation and Restoration Laboratory, University of Camerino, Via Pacifici Mazzoni 2, 63100 Ascoli Piceno, Italy

5 School of Architecture and Design, University of Camerino, 63100 Ascoli Piceno, Italy

* Corresponding author. E-mail: graziella.roselli@unicam.it

Regarding the contribution of the PhD student Fabrizio Scognamiglio to the presented article, he managed the literature search and performed mortar sampling, MO inspection, sieving process, particle-size analysis, XRD, SEM and microanalysis, DSC, FT-IR analysis. FS also commented on experimental results and managed writing-original draft and writing-review preparations.

Regular Article

Abstract

The paper presents an experimental study on mortar samples taken from historic and monumental buildings damaged or collapsed following the seismic events in Central Italy (2016-2017). Sixty-one samples were analysed via a set of diagnostic investigations to characterize the mortar and correlate it with the performance of the masonry. The techniques used were: X-ray diffraction, scanning electron microscopy and microanalysis, differential scanning calorimetry, calcimetry, Fourier-transform infrared spectroscopy, soluble salt analysis by conductimetry and dosage of anionic species by ion chromatography, particle-size analysis, direct shear. Microstructural characterization of the mortars revealed differences in mortar composition depending on their provenance. In particular the samples from Norcia contained large quantities of calcite while in the mortars from Pretare, dolomite was identified. In the case of Amatrice, only a few samples showed crystalline phases and compounds ascribable to binders. These results were largely confirmed by the other chemical and physical analysis performed, and mechanical tests also demonstrated low cohesion. The tests showed that in almost all the samples, poor quality mortars were used, and, in some cases, underachieving binder mortar.

1. Introduction

In 2016 and early 2017, some dramatic earthquakes severely damaged, and in some cases destroyed, several small towns in Central Italy, causing the loss of human lives and the destruction of old historic town centres. A very high number of buildings were badly damaged in an extended area that includes portions of the Abruzzo, Lazio, Marche and Umbria regions [1]. Figures 1 and 2 detail earthquakes of magnitude greater than 3.5 occurring between 2015 and 2018, originating respectively in Southern Europe, and in Central Italy.

Fig. 1. Earthquakes in Southern Europe from 2015 to March 2018, magnitude greater than 3.5 [2]

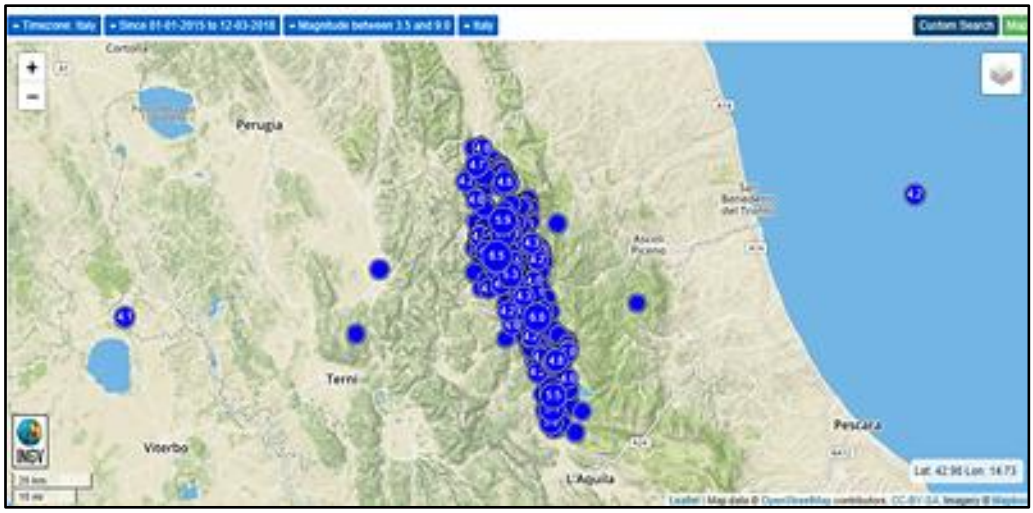

Fig. 2. Earthquakes in Central Italy from 2015 to March 2018, magnitude greater than 3.5 [2]

In past centuries, in these regions, construction activity was characterized by the use of local materials and workforce. Until the 1960s, the most common source for such building materials was an area of the Apennines characterized by the outcrop of turbiditic sandstone (Laga Flysch, Messinian), limestone and pelagic marly limestone of the UmbroMarchigiana series (Mesozoic) [3].

Damage to architectural heritage has shown construction defects, dating back to the original buildings or transformations due to environmental factors and natural aging. For these reasons, it is necessary to investigate in depth the nature of the building system, focusing on the masonry and mortars that contribute to the durability of the overall construction.

The structural behaviour of masonry, particularly under seismic actions, is strongly influenced by masonry bond and mortar quality. Typically, the collapse of existing masonry structures is triggered by: disintegration, out-of-plane mechanisms (overturning or bending), and in-plane mechanisms (shear or bending). Usually, disintegration is the most dangerous mechanism in rubble masonry with two or three leaves, and in the absence of transverse connections (headers). In such conditions, and with the action of eventual external solicitations, the separation between the leaves and the partial or total collapse of the construction occurs. Good quality mortar is essential to delaying/preventing the separation of leaves.

Building constructions in Italian historic centres are largely characterized by load-bearing walls, whose masonry does not always follow the rule of the art [4–6]. In fact, the masonry construction techniques used in these areas show some deficiencies such as: the presence of mixed materials (sandstone and limestone, usually mined in the area around the building site), the use of undressed or rounded units, an inconsistent or weakly cemented nucleus. Material quality and appropriate bond are basic requirements for defining well-executed masonry walls. Geometry, size and type of units, cross-connections, bond (with horizontal bed joints and the correct stagger of head joints), quantity

and quality of mortar, the presence of an inner nucleus, are important details which have to be considered in the analysis of old masonry.

The wall structure does not always display good box-like behaviour, by means of effective connections between walls, and robust horizontal structures connected to vertical structures. Walls show numerous openings, without or with deformed timber lintels. Moreover, renovations carried out after earthquakes occurring in the same area in the last decades of the 20th century modified the structural performance.

Some buildings have particular construction systems, related to the seismic history of the sites. In 1859, a strong earthquake caused victims and numerous collapses in some parts of the old town of Norcia, and the Papal States issued a rather effective regulation. The Regolamento required: use of dressed units (river ovoid units were forbidden); control of mortar production (clear sand and lime binder); connections at walls intersections; minimum thickness of wall (recommended tapered vertical cross section). Then, the 1979 Valnerina earthquake damaged other parts of the historic centre, and was followed by interventions to strengthen many buildings.

One of the techniques used was cementitious plaster reinforced with carbon steel welded meshes. This intervention is controversial because of the durability and effect of moisture and salt on existing materials, but it has avoided masonry disintegration, making Norcia a successful case of combined pre-modern and recent regulations [7].

Examples of masonry walls found in little villages in Central Italy can be seen in fig. 3, wherein both internal and external load-bearing panels are shown. Masonry is characterized by material variability (river pebbles, sandstone, travertine), rough-hewn or uneven-size units, irregular bed joints. Sometimes, in order to regularize the courses, timber elements (dormienti) or longer units were inserted. Within the wall thickness there are few bond units (diatoni) and the nucleus is completely inconsistent.

With the aim of gaining a better understanding of masonry damaging mechanisms, in particular those related to mortars used in these constructions, a series of diagnostic investigations were carried out on a set of mortars collected from collapsed buildings.

Fig. 3. Walls in Pretare (Arquata del Tronto, Marche)

2. Experimental Methods

Mortar was sampled in different sites located in Central Italy (table 1 and fig. 4), namely 20 in Lazio, 16 in Marche and 25 in Umbria. Materials were collected from collapsed masonry located in accessible sites or, otherwise, under the supervision of firefighters and civil protection officers. First of all, the site was visually inspected in order to select sampling points that were significant from a structural point of view. All the samples consist of mortar with bedding function. Sampling activity was carried out in a way that avoided contamination from other materials, such as stones, bricks, plasters, modern cements etc.

At the time of sampling, a record card was filled in with date, location, type of building, point of sampling, and sample quantity (estimated).

Table 1 – Mortar samples

Region	Settlement ID	Settlement	Municipality	Sample IDs
LAZIO	1	Accumoli	Accumoli	1
	2	Santa Maria delle Coste	Accumoli	2
	3	Amatrice	Amatrice	3
	4	Capricchia	Amatrice	4, 5
	5	Casale	Amatrice	6
	6	Cascello	Amatrice	7, 8
	7	Cossito	Amatrice	9, 10
	8	Prato	Amatrice	11
	9	Preta	Amatrice	12-14
	10	Saletta	Amatrice	15
	11	San Capone	Amatrice	16, 17
	12	Sommati	Amatrice	18
	13	Torrita	Amatrice	19
	14	Voceto	Amatrice	20
MARCHE	15	Borgo	Arquata del Tronto	21-26
	16	Pretare	Arquata del Tronto	27-35
	17	Trisungo	Arquata del Tronto	36
UMBRIA	18	Ancarano	Norcia	37
	19	Campi di Norcia	Norcia	38-49
	20	Norcia	Norcia	50-60
	21	Piedivalle	Norcia	61

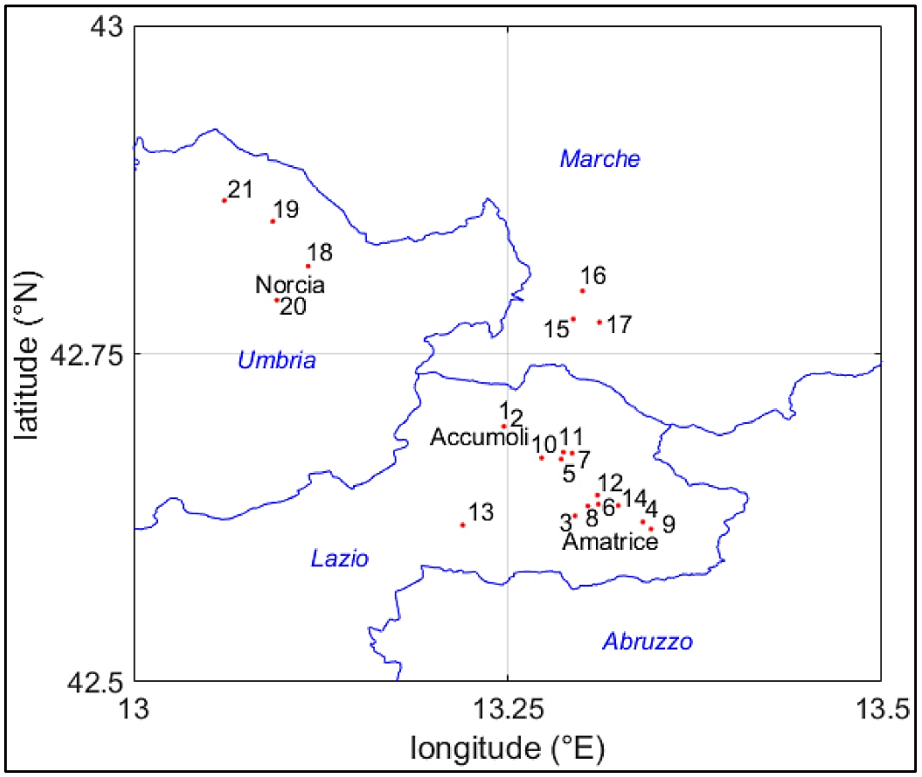

Fig. 4. Location of mortar sample sites

An integrated analytical approach was considered so as to obtain a large amount of information and correlate the composition and mechanical behaviour of the mortars with the performance of the

masonry. First, the samples collected were inspected in the laboratory, both with the naked eye and a stereomicroscope Olympus SZ × 12 with digital image acquisition, in order to remove possible spurious impurities, such as wood or coal, and to exclude samples that displayed the effects of external agents. Then, to evaluate grain size distribution, the samples were first roughly cracked into smaller pieces and successively they were sieved. Different mechanical treatments were performed in dry conditions and the material passing through the sieve was weighted and recovered [8]. Particle-size analysis was carried out using the following sieves: 2.000, 1.000, 0.500, 0.250, 0.106, 0.063mm.

X-ray diffraction (XRD) was performed with a Smartlab Rigaku powder diffractometer, with graphite monochromator in the diffracted beam, operated at 40kV and 30mA. A suitable quantity of mortar, in the form of fine powder, was laid on a zero-background sample holder. Patterns were obtained from 2 to 90 2θ degree, at steps of 0.04 2θ degree and 12s per step. Material passing 0.063mm sieve further milled in an agate mortar was used for XRD analysis, in order to identify the mineralogical phases present in the samples [9,10].

A scanning electron microscope (SEM) EVO MA15 equipped with energy dispersive spectroscopy (EDS) was used to study the morphology of the different fractions constituting the mortars and to perform microanalysis.

Differential scanning calorimetry (DSC) was performed with a Mettler Toledo HPDSC with a temperature programmed to run from room temperature to 650 °C at a heating rate of 5K/min and 50ml/min of Ar flux. The technique makes it possible, by simply heating the sample in a wide temperature range, generally from room temperature to 650 °C, to reveal the heat involved in eventual decompositions or transformations, as phase ones, in a small quantity of samples in solid or even liquid form.

Analysis by Fourier-Transform Infrared Spectroscopy (FT-IR) was carried out on mortar samples ground in a agate mortar and then passed completely through a 0.125mm sieve. A Perkin Elmer Spectrum 100 was used in attenuated total reflectance (ATR) mode. For each sample two acquisitions were performed.

Calcimetry was performed, using the gas-volumetric Dietrich-Fruheling method. The sample was ground manually with an agate mortar until it could be completely passed through a 0.063mm sieve, then dried into a thermobalance at 60 °C up to constant mass. The sample was treated with a reagent

based on hydrochloric acid, which decomposes the carbonates present by CO_2 development, as regulated by UNI 11140: 2004. This technique made it possible to evaluate with greater precision, than through analysis in FT-IR spectroscopy ATR, the quantity of carbonates present in the samples.

Soluble salt analysis by conductimetry and measurement of anionic species by ion chromatography were carried out. From the conductivity value of the solutions - the formula indicated in the DIMOS document, part II module 3, ICR, 1978 was applied - the percentage of soluble salts present in the samples was estimated. Analysis of soluble salts procedure (UNI 11087: 2003) was followed: the sample was dried in an oven at 60 °C for about 24h, then ground manually within an agate mortar until it completely passed through a 0.125mm sieve. The samples were weighed (95mg up to 105mg) and treated in a thermobalance at a temperature of 60 °C up to a constant mass. One hundred ml of bidistilled H2O, whose conductivity was previously measured, were added to the sample and placed in a flat-bottomed glass container. The container was hermetically sealed to prevent evaporation and slowly stirred for 2h. Then, residuals were left to deposit for about 30min. Finally, conductivity was measured with a XS Multiparameter, model PC 70. The suspension obtained was then filtered (black band filter) and the solution was used for the measurements of the single ionic species by ion chromatography.

Ion chromatograms were recorded with a Metrohm Ion Chromatograph 761 Compact with chemical integrated Metrohm suppressor module (MSM) and a METROSEP A Supp. 5 150/4.0 separation column. A conductivity detector was used to identify the main anionic species present in the mortar solution. Introduction volume was typically 1.5ml and the loop volume was 20µl. Sartorius 0.45µm RC-Membrane PP-Housing filters were used to remove particles. Three repetitions for each analysis were performed.

Direct shear test was performed on the fraction of non-cohesive samples with particle-size less than or equal to 2mm. For each sample, three levels of normal stress were applied: σn = 0.05, 0.10, 0.20 MPa. For each normal stress level, a cyclic test provided the maximum (τ_{max}) and the residual (τ_{res}) shear stresses. Based on direct shear test, cohesion *c* and friction coefficient μ were determined.

3. Results and Discussion

3.1 Sieving process and grain size distribution

Curves in fig. 5 show the preponderance of a coarse fraction in mortars from Umbria, in particular those from Norcia, contrary to a fine fraction in samples from Marche, especially from Pretare.

Particle-size analysis highlighted the great compositional variability of the sampled mortars, not only between different regions but also within the same regional context, reflecting the extreme typicality of each of the small towns of Central Italy and possibly of each building site, if not of each mortar batch.

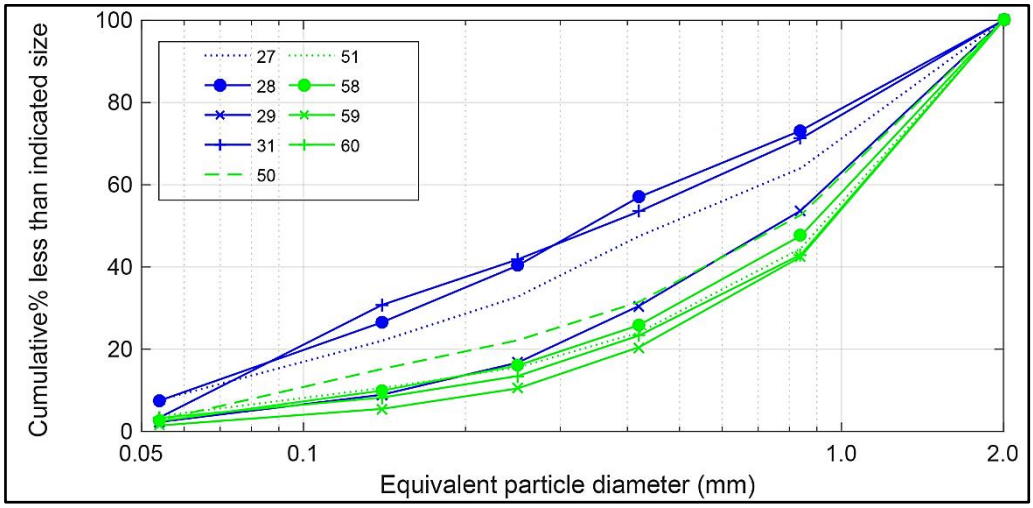

Fig. 5. Particle-size analysis

3.2 X-Ray diffraction

Figure 6 shows typical X-ray diffractograms of mortars from settlements in the municipality of Amatrice.

XRD showed that the main phases present in these samples are quartz, phyllosilicates and feldspars, whereas few samples contained calcite or other traces of different binders. The samples from the area of Amatrice display crystalline phases related mainly to inert fractions of the mortar.

Differently from Amatrice, samples from Norcia showed the presence of large quantities of calcite, quartz, traces of phyllosilicates (in particular clinochlore) and in some samples, gypsum (fig. 7).

Differently from Amatrice and Norcia, dolomite was found in the mortars from Pretare and Borgo. Figure 8 shows X-ray diffractograms of samples from the churches of Saints Peter and Paul (Borgo, 21, 24), Saint Francis (Borgo, 22, 25–26), and Saint Rocco (Pretare, 27–28). In all these samples, large quantities of dolomite were found, together with calcite, quartz, phyllosilicates and feldspars.

X-ray diffraction is a technique that can discern among crystalline phases but not distinguish among $CaCO_3$ due to inert or binder fraction. However in mortars, lower concentrations of $CaCO_3$ (15–20% of the whole sample) could be related to the binder, whereas high concentrations (80 to 100%) could be associated to aggregate [11].

The mortars sampled in Pretare and neighbouring areas showed the presence of dolomite, calcite and quartz with some feldspars and phyllosilicates. Dolomite in these mortars was probably used as

aggregate rather than binder. In fact hydromagnesite, $Mg_5(CO_3)_4(OH)_2 \cdot 4H_2O$, which is the main product resulting from the curing of magnesian lime mortars, is not present in these samples. This phase presents a fine plate-like aspect and its formation is directly correlated to mortar mechanical strength [12]. It has been said that dolomitic mortars are not recommended in dry areas, as shrinkage and pore networks negatively impact water transfer. Moreover, calcareous aggregate is preferred to dolomitic aggregate, as it results in better mortar cohesion [13]. The materials used to prepare the mortars analysed were probably extracted from quarries near the corresponding settlements. In a future work, sampling from known quarries will be performed in order to link digging site to construction site.

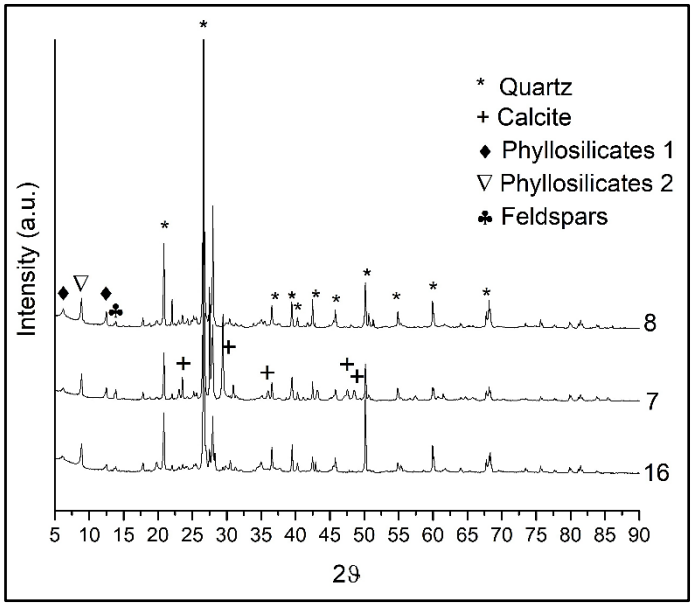

Fig. 6. XRD patterns of some samples from settlements in the municipality of Amatrice

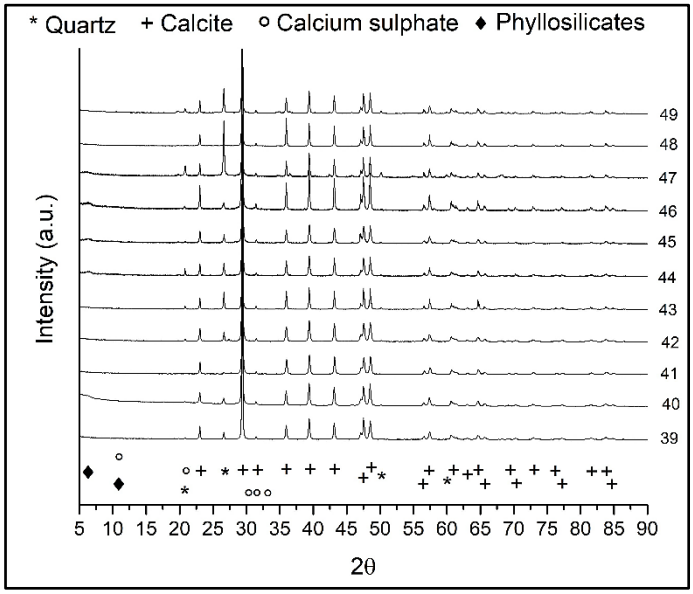

Fig. 7. XRD patterns of samples from Saint Salvatore Church in Campi di Norcia

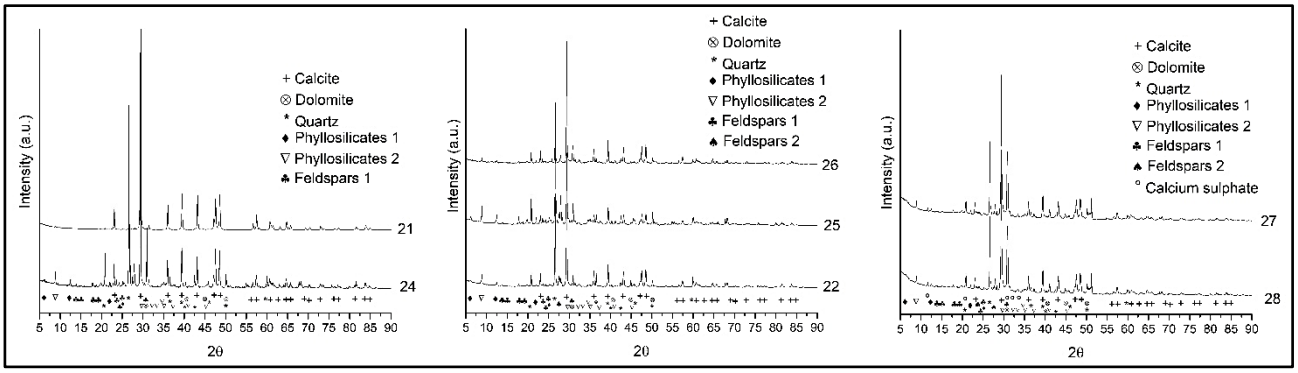

Fig. 8. X-Ray diffractograms of samples from the churches of Saints Peter and Paul (Borgo, 21, 24), Saint Francis (Borgo, 22, 25-26), Saint Rocco (Pretare, 27-28)

3.3 Scanning electron microscopy and microanalysis

SEM-EDS was used for the microstructural characterization of the fraction constituting the mortar and for microanalysis, with the aim of evaluating differences among the samples from various regions.

Figure 9 shows a representative selected set of SEM images of the samples (a) 7, (b) 3, (c) 27 and (d) 44, respectively, from Cascello, Amatrice, Pretare and Norcia. The numbers refer to EDS point analysis and the results are summarized below:

a) 1: Si, O; 2: Si, O, Al, Na, K, Ca; 3: Si, O, and traces of Al, K and Fe; 4: Si, O, Al and K, and traces of Na; 5: Si, O, Al, K, and traces of Mg, Na, Fe
b) 1-10: Si, O; 11: Si, O, and traces of Mg, Al, K; 12: Si, O, K, Al, Mg, and traces of Fe
c) 1: Ca, C, O, and traces of Mg, Fe; 2: Ca, Mg, C, O, Si; 3: Ca, C, O, and traces of Mg, Al, Si; 4: Ca, C, O, and small quantities of Mg and Si
d) 1: Si, O; 2: Si, O; 3: Si, O, Ca, C, and traces of Mg, Al, K; 4: Ca, C, O, and a few traces of Al, Mg, Si, K, and Fe; 5: Ca, C, O, and traces of Mg

EDS results are largely in agreement with those obtained by X-ray diffraction. The large presence of Si, Al, K, Mg, Na and O can be ascribed to the presence of feldspars and phyllosilicates in these samples. Moreover, it should be noticed that some samples observed present fractions containing mainly Ca, C and O and which can be correlated to calcite phase, in particular in samples from Norcia and Pretare. In this last case, high quantities of Mg can also be detected, together with Ca, C and O. These results could reinforce the hypothesis that calcite and dolomite were used also as inert materials in the mortar preparation.

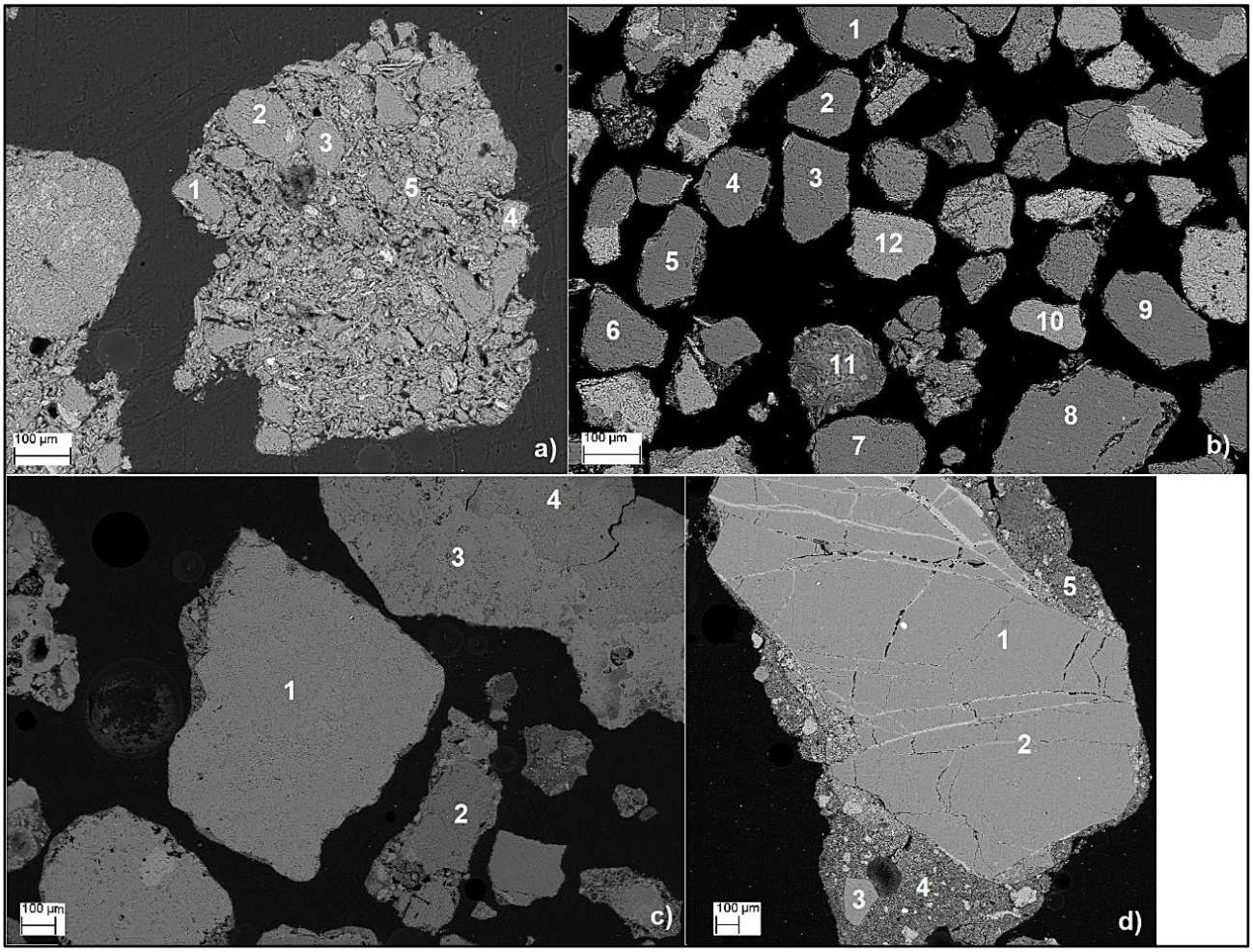

Fig. 9. Scanning electron microscope images of samples from a) Cascello (7, Amatrice), b) Amatrice (3), c) Pretare (27, Arquata del Tronto) and d) Norcia (44)

3.4 Differential scanning calorimetry

DSC was used with the aim of detecting possible amorphous, inorganic or organic compounds. Figure 10 shows differential scanning calorimetric curves of samples from the church of Saint Francis in Borgo, together with a pure $CaCO_3$ reference curve. The graphs demonstrate low quantity of water adsorbed in the samples (< 1%) in the range from room temperature to 120 °C, and some exothermic phenomena which could be correlated to dolomite decomposition (400–500 °C), which takes place at different temperatures [14,15]. Confirming XRD results, quartz is still present in these samples, as evident from the alpha to beta inversion at 573 °C.

Air lime and dolomitic mortars are low hygroscopic, and this feature allows them to be identified [10]. In the samples analysed, the water adsorbed, which is lost in the heating process, is lower than 1%.

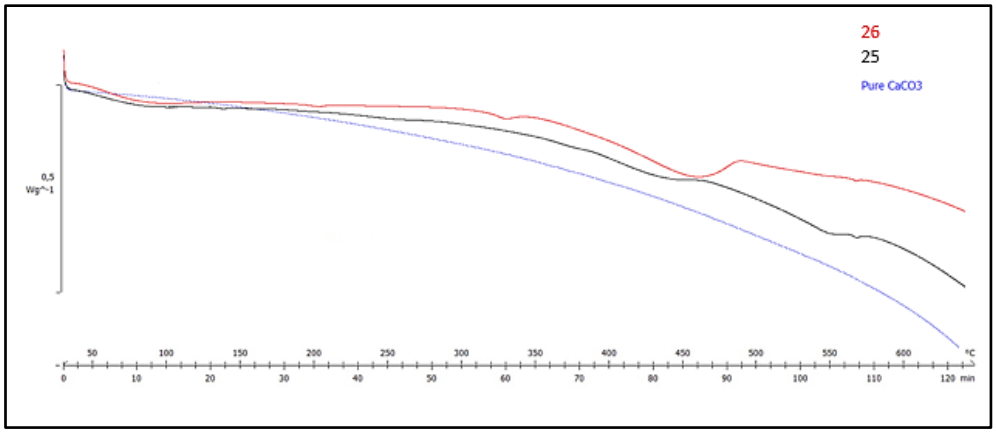

Fig. 10. Differential scanning calorimetric curves of samples from the church of Saint Francis in Borgo. $CaCO_3$ curve is shown as reference

3.5 Fourier-transform infrared spectroscopy

FT-IR analysis made it possible to have an overview of the composition of the mortars [16] and, with regard to carbonates, silicates and sulphates, the intensity of their stretching signals were used to obtain a semi-quantitative evaluation (table 2). Table 2 allows us to draw the following considerations:

- most of the samples from Amatrice (Lazio) did not display the characteristic signals of carbonates but only those of silicates;
- mortars collected in the settlements of the municipalities of Arquata del Tronto (Marche) and Norcia (Umbria) show intense signals of carbonates and, in some cases, also of silicates.

Table 2 - FT-IR results from Lazio (Sample ID: 1 to 20), Marche (Sample ID: 21 to 36) and Umbria (Sample ID: 39 to 61) regions. The number of 'x' indicates the intensity of the stretching signals of carbonates, silicates and sulphates

Sample ID	FT-IR			Sample ID	FT-IR			Sample ID	FT-IR		
	CO_3^{2-}	SiO_4^{4-}	SO_4^{2-}		CO_3^{2-}	SiO_4^{4-}	SO_4^{2-}		CO_3^{2-}	SiO_4^{4-}	SO_4^{2-}
1	xxx	xx		20	(x)	xxx		42	xxx	x	
2				21	xxx			43	xxx	(x)	
3	xx	xxx		22	xxx	xx		44	xxx	(x)	
4	xxx	xxx		23	xxx[a]	xx		45	xxx	x	
5		xxx		24	xxx	xxx		46	xxx	x	
6		xxx		25	xxx	xx[b]		47	xxx	xx	
7	xx	xxx		26	xxx	x[b]		48	xxx	xx	
8		xxx		27	xxx[a]	x		49	xxx	x	
9		xxx		28	xxx[a]	x		50	xxx	x	
10	(x)	xxx		29	xxx[a]	(x)		52	xxx	(x)	
11	(x)	xxx		30	xxx[a]	x		53	xxx	x	
12	x	xxx		32	xxx[a]	x		54	xxx	x	
13	x	xxx		33	xxx	x		55	xxx	x	
14	x	xxx		34	xxx	x		56	xxx	xx	
15				35	xxx[a]	(x)		57	xxx	x	
16		xxx		36	xxx	xx[b]		58			
17	(x)	xxx		39	xxx	(x)		59			
18		xxx		40	xxx	x		60			
19		xxx		41	xxx			61	xxx	x	

a Presence of dolomite, in addition to calcite
b Presence of kaolinite, in addition to quartz

3.6 Calcimetry

With regard to the eighteen samples from Amatrice, twelve of them have very low carbonate content. This indicates that the mortar is characterized by the absence of binder, as evidenced by XRD.
Most samples from Norcia and Arquata del Tronto, however, have a percentage of carbonates higher than 30%. More than two thirds of the samples (25 out of 36) have a percentage of carbonates well above 50%, indicating that carbonates, too, were used as aggregates, while in the case of Amatrice, a silicatic type of aggregate is present.

3.7 Soluble salt analysis by conductimetry and dosage of anionic species by ion chromatography

As can be seen in table 3, the percentage of soluble salts in most Amatrice mortars is below 3%, with the exception of samples 4 and 11, which are barely above. The mortars of Arquata and Norcia are, instead, characterized by values between 2 and 10%. Concerning the concentration of the various anionic species (table 3), the following considerations can be made:

- the sulphates were present in low quantities, below 3ppm (except for samples 1, 3, 28 and 36);
- the presence of chlorides in the samples is negligible: only four samples exceed 2ppm (11, 33, 36, 45);
- regarding nitrates, there is a very heterogeneous situation: most of the samples show negligible concentrations (lower than 2ppm) except for twelve samples with higher concentrations;
- the presence of fluorides and phosphates was not detected (except for sample 3).

Figure 11 shows a representative chromatogram for the anions detected in sample 45.

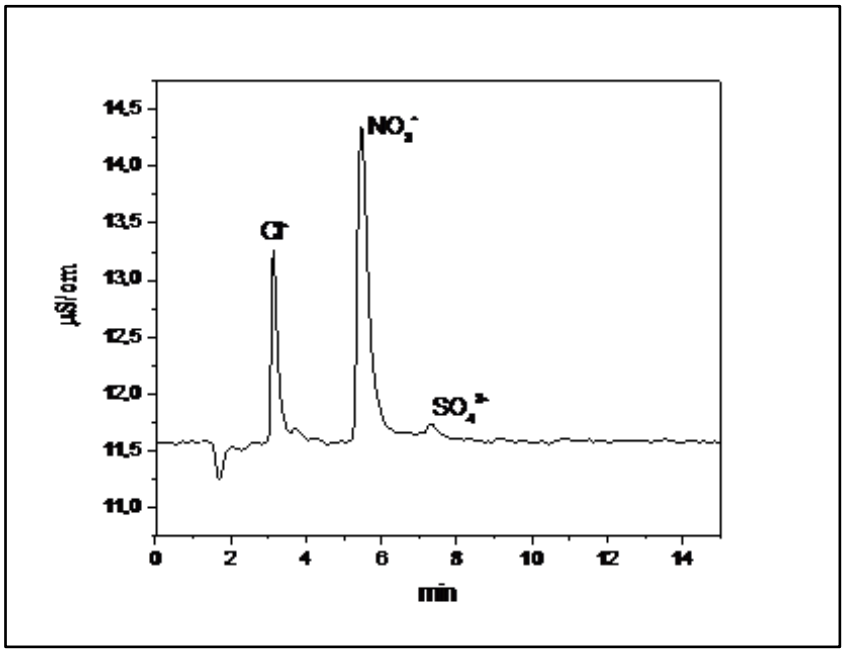

Fig. 11. Anion chromatogram for sample 45. Injection volume: 20µl; eluent: 2 mmol/l $NaHCO_3$ / 1.3 mmol/l Na_2CO_3 in dist. H_2O with the addition of 1% of CH_3CN; flow: 1 ml/min

Table 3 – Percentage of Soluble Salts (SS) and concentration of anionic species (average value of three measurements) in the samples from Lazio (Sample ID: 1 to 20), Marche (Sample ID: 21 to 36) and Umbria (Sample ID: 39 to 61) regions

Sample ID	Conductivity [µS]	SS [%]	F^-	Cl^-	NO_3^-	PO_4^{3-}	SO_4^{2-}
					[ppm]		
1	64	3.99	-	1.31±0.10	3.31±0.17	-	9.32±0.07
3	47	2.96	0.53	0.35±0.02	-	1.36	3.41±0.24
4	51.3	3.05	-	2.01±0.06	3.82±0.10	-	1.16±0.12
5	29.5	1.71	-	0.15	0.16	-	2.15
6	17.4	1.06	-	0.39±0.03	0.74±0.08	-	0.66±0.19
7	45	2.67	-	0.43±0.04	-	-	0.51±0.11
8	7.8	0.40	-	0.42±0.02	-	-	0.63±0.11
9	15.6	0.89	-	0.49±0.02	0.71±0.14	-	>0.5
10	33.3	2.06	-	0.42±0.03	0.74±0.12	-	>0.5
11	45	3.00	-	3.10±0.10	8.50±0.28	-	0.52
12	39	2.48	-	0.40±0.02	0.40±0.01	-	-
13	35.2	2.23	-	0.34±0.02	-	-	>0.5
14	42.2	2.59	-	0.59±0.01	2.73±0.34	-	1.05±0.10
16	18	1.04	-	0.52±0.07	0.91±0.12	-	0.71±0.07
17	44	2.81	-	1.18±0.12	-	-	1.36±0.14
18	19.7	1.20	-	0.47±0.04	0.53±0.19	-	>0.5
19	21	1.19	-	0.42±0.05	-	-	0.56±0.10
20	38.3	2.21	-	0.43±0.03	1.80±0.27	-	>0.5
21	45.3	2.91	-	0.43±0.02	0.647026	-	>0.5
22	92	5.90	-	0.98±0.04	19.17±0.17	-	1.00±0.04
23	54	3.42	-	0.57±0.11	0.45	-	0.90±0.17
24	40.2	2.36	-	0.38±0.03	-	-	>0.5
25	56.3	3.64	-	0.83±4.6E-3	0.74	-	-
26	82.5	5.25	-	1.08±0.16	13.56±1.22	-	-
27	78.9	4.96	-	0.50±0.03	0.45±0.05	-	>0.5
28	65.2	3.97	-	1.04±0.17	1.50±0.29	-	8.84±1.05
29	125.4	8.27	-	0.33±5.17E-3	0.30±0.20	-	0.51±0.13
30	45.5	2.79	-	0.52±7.33E-3	-	-	0.67±0.05
32	61	4.12	-	0.50±0.07	1.15±0.20	-	0.92±0.10
33	158	10.03	-	2.57	13.14	-	0.65
35	66	3.99	-	0.59±0.09	0.24	-	1.07±0.12
36	93.5	5.91	-	5.00±0.05	13.70±1.79	-	3.87±0.64
39	44	2.61	-	0.42±0.02	0.56±0.10	-	0.47±0.04
40	44.4	2.57	-	0.42±0.04	0.49	-	>0.5
41	54.3	3.25	-	1.40±0.08	0.39±0.04	-	2.17±0.07
42	39.5	2.41	-	0.42±9.17E-4	-	-	>0.5
43	39	2.37	-	0.34±3.67E-4	0.36±0.04	-	>0.5
44	48	2.92	-	0.89±0.08	1.06±0.24	-	1.18±0.21
45	80	4.73	-	3.87±0.08	17.01±0.84	-	>0.5
46	40	2.40	-	0.59±0.13	0.31±0.02	-	0.60±0.09
47	62	3.81	-	2.03±0.13	5.81±0.20	-	0.75±0.13
48	43.5	2.60	-	0.46±0.02	-	-	-
49	43.9	2.61	-	0.48±0.03	0.46±0.10	-	>0.5
50	40	2.45					
52	51.7	3.08	-	0.47±0.03	1.39±0.24	-	0.53±0.13
53	45	2.73	-	2.06±0.05	1.13±0.04	-	0.77±0.18
54	56.6	3.64	-	1.96±0.05	6.10±0.56	-	1.76±0.12
55	39.5	2.63	-	0.46±0.02	-	-	0.58±0.13
56	44.4	2.71	-	0.48±0.03	0.32±0.02	-	0.64±0.25
57	45	2.79	-	0.51±4.59E-3	0.47±0.07	-	1.00±0.06
61	42.5	2.63	-	1.05±0.05	2.14±0.16	-	0.73±0.12

3.8 Direct shear

An example of shear stress *vs.* displacement curve is shown in fig. 12.

On the basis of a direct shear test, cohesion c and friction coefficient μ were determined. The results obtained for Norcia, using maximum shear stress, are shown in table 4 and fig. 13. As expected [4], cohesion and friction coefficient display a negative correlation.

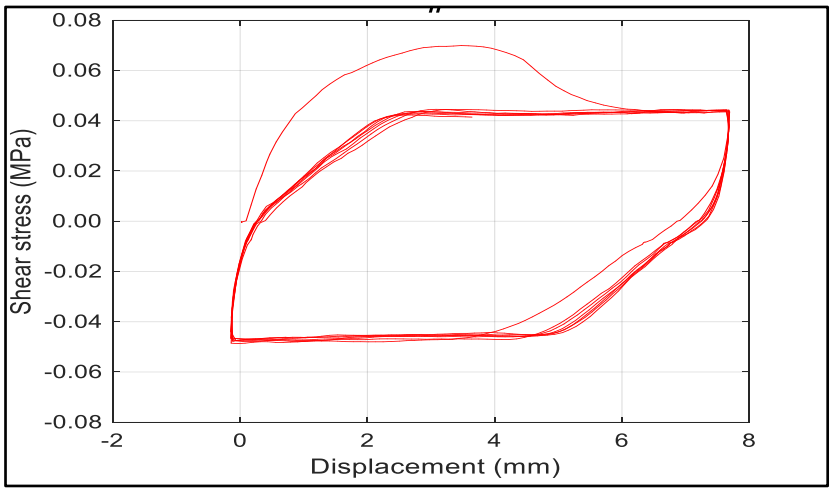

Fig. 12. Example of shear force *vs.* displacement curve (Sample 1, σ*n* = 0.05 MPa)

Table 4 – Synthesis of direct shear test (maximum shear stress, Norcia)

	***μ* [-]**	***c* [kPa]**
max	1.01	37.58
min	0.81	13.91
mean	0.90	26.74
std dev	0.08	8.45
CoV	0.09	0.32
R	-0.75	
R^2	0.57	

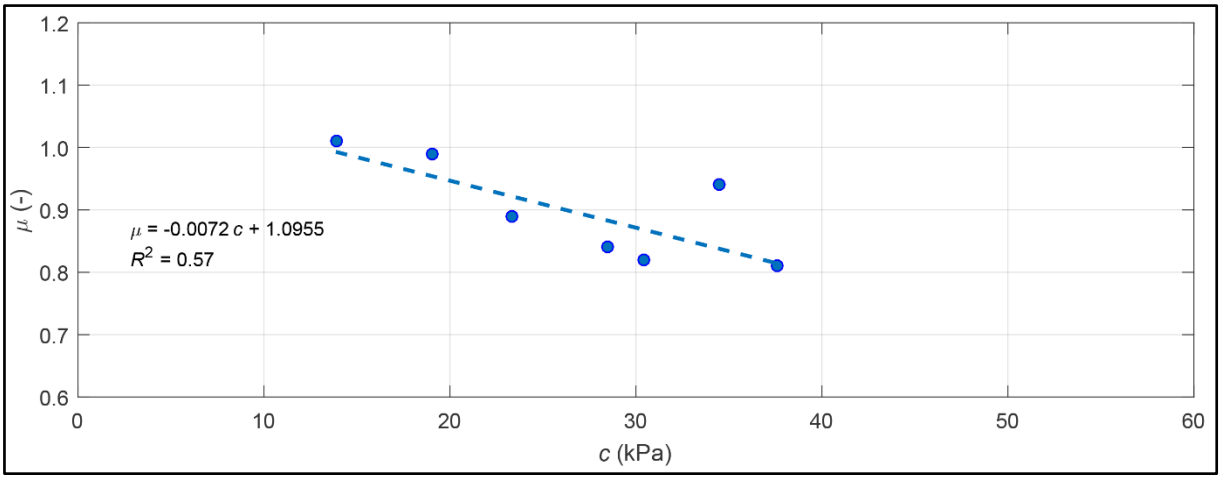

Fig. 13. Relation between cohesion and friction coefficient (maximum shear stress, Norcia)

3.9 Discussion

The extensive experimental analysis campaign performed for this work made it possible to define a rather clear scenario regarding the quality of bedding mortars used in masonries, mainly in the form of uneven stone walls with bearing function, from different old towns and their neighbourhoods in Central Italy. In particular, the mortars sampled revealed different compositions, which were verified by various methods. The samples from Norcia (Umbria) contained large quantities of calcite, while in those from Arquata del Tronto (Marche), dolomite was largely detected. In the case of Amatrice (Lazio), low quantities of binder were detected, consisting mainly of inert fractions, in particular quartz.

During sampling, these mortars were in the form of loose powder with few consistent portions. The primary materials used for the preparation of the mortars analysed were probably extracted locally considering the composition of the inert fractions and the presence of dolomite in the area of Arquata del Tronto. Pebbles which were quite rounded in shape could have been extracted from the river Tronto, which flows close to Arquata del Tronto and then on to Amatrice. The presence of similar feldspars and phyllosilicates in the mortars could be related to the presence of these minerals in the sands and pebbles derived from this river. In the case of Norcia, the large quantities of calcite detected in the mortars could be related to the use of limestones, not only for the preparation of slaked lime but also as inert material.

Future work will explore the provenance of construction materials typical of regions in Central Italy, since this work is primarily concerned with evaluating the properties of bedding mortars in terms of chemical and physical properties.

Conclusions

Mortar analyses are customary in the investigation of architectural heritage, aimed at defining historic construction stages, for instance by identifying inert and binder phase as well as the presence of additives. In the case of historical buildings, the investigation of construction materials is useful not only for simple identification but also to evaluate their vulnerability to external events, such as earthquakes.

In this work, mortar samples were studied to qualitatively and semi-quantitatively determine their composition, as well as some of their physical and mechanical properties, in order to correlate these values with the seismic damage surveyed. Sixty-one mortar samples were collected in buildings damaged by the 2016-2017 Central Italy earthquakes, and analysed using several diagnostic techniques, such as: particle-size analysis, X-ray diffraction, differential scanning calorimetry, calcimetry, Fourier-transform infrared spectroscopy, solute salt analysis, and direct shear.

Experimental results suggest the use of different materials, in particular mortars obtained from limestone in Umbria (Norcia), dolomitic limestone in Marche (Pretare), and a high quantity of quartz. A large number of samples from Amatrice had a fairly negligible carbonate content, the main component being quartz. This indicates that in these cases the mortars are characterized by the absence of a binder. Mechanical tests confirmed the poor performances of these mortars.

In future work, mortar will be produced in the laboratory, replicating observed compositions but manufacturing standard size specimens to be tested under bending and compression. Moreover, this work could form the basis of territorial seismic risk analyses, wherein vulnerability is also a function of surveyed mortar properties.

Additionally, correlations across regions and centuries could be proposed, based on a statistically robust database. Finally, data on mortar properties could be used in future conservation and restoration schemes, to enhance the compatibility of new and existing materials, and to direct priorities in intervention activity based on the identification of site vulnerability.

References

1. L. Sorrentino, S. Cattari, F. Da Porto, G. Magenes, A. Penna, Bull. Earthq. Eng. 17, 5583 (2019).
2. INGV – National Institute of Geophysics and Volcanology, http://cnt.rm.ingv.it.
3. U. Chiocchini, F. Castaldi, Hydrogeol. J. 19, 651 (2011).
4. D. Liberatore, N. Masini, L. Sorrentino, V. Racina, M. Sileo, O. AlShawa, L. Frezza, Constr. Build. Mater. 122, 810 (2016).
5. L. Restuccia, A. Lopez, G.A. Ferro, D. Liberatore, J.M. Tulliani, Fatigue Fract. Eng. Mater. Struct. 41, 119 (2018).
6. E. Petrucci, F. Di Lorenzo, La Storia si ripete: eventi sismici a Norcia fra distruzione e ricostruzione, in Reuso 2017, Sobre una Architectura Hecha de Tiempo - Metodologıa, Tecnica y Conservacion, Vol. 1 (Universidad De Granada, 2017) pp. 453–459.
7. R. Sisti, M. Di Ludovico, A. Borri, A. Prota, Bull. Earthq. Eng. 17, 5609 (2019).
8. C. Groot, G. Ashall, J. Hughes, Characterization of Old Mortars with Respect to their Repair, Final Report of RILEM TC 167-COM (1996).
9. C. Carrara, F. Persia, Indagini mineralogiche-petrografiche e di diffrazione dei raggi X sulle incrostazioni calcaree e sulle malte, in Gli acquedotti Claudio e Aniene Nuovo nell'area della Banca d'Italia in Via Tuscolana (Istituto Poligrafico e Zecca dello Stato, 2001) pp. 193–197.
10. V. Cardinale, F. Persia, L. Campanella, F. Cardellini, S. Omarini, Storia costruttiva del complesso monastico di San Vincenzo al Volturno attraverso la determinazione di differenze composizionali

nelle malte. Risultati preliminari, in Atti del 2° Congresso Nazionale AIAr (AIAr, 2002) pp. 505–513.
11. G. Chiari, M.L. Santarelli, G. Torraca, Mater. Struct. 2, 111 (1992).
12. R.M. Dheilly, A. Bouguerra, B. Beaudoin, J. Tudo, M. Queneudec, Mater. Sci. Eng. A 268, 127 (1999).
13. A. Arizzi, G. Cultrone, Cem. Concr. Res. 42, 818 (2012).
14. M. Olszak-Humienik, M. Jablonski, J. Therm. Anal. Calorim. 119, 2239 (2015).
15. L. Chever, S. Pav`ıa, R. Howard, Mater. Struct. 43, 283 (2010).
16. M. Gulmini, G. Roselli, F. Scognamiglio, G. Vaggelli, Appl. Phys. A 120, 1643 (2015).

Characterization of historical masonry mortar from sites damaged during the Central Italy 2016-2017 seismic sequence: the case study of Arquata del Tronto

Annals of Geophysics

Daniele Mirabile Gattia[1*], Graziella Roselli[2], Omar AlShawa[3], Paolo Cinaglia[4], Giuseppe Di Girolami[4], Cristina Francola[3], Franca Persia[1], Enrica Petrucci[5], Roberto Piloni[2], Fabrizio Scognamiglio[4], Luigi Sorrentino[3], Silvia Zamponi[2], Domenico Liberatore[3]

1 Department of Sustainability SSPT - ENEA - CR Casaccia, Rome, Italy

2 School of Science and Technology, Chemistry Division, University of Camerino, Camerino, Italy

3 Department of Structural and Geotechnical Engineering, "Sapienza" University of Rome, Rome, Italy

4 School of Science and Technology, Technologies and Diagnostics for Conservation and Restoration Laboratory, University of Camerino, Ascoli Piceno, Italy

5 School of Architecture and Design, University of Camerino, Ascoli Piceno, Italy

* Corresponding author. E-mail: daniele.mirabile@enea.it

Regarding the contribution of the PhD student Fabrizio Scognamiglio to the presented article, he managed the literature search and performed mortar sampling, MO inspection, sieving process, particle-size analysis, XRD and FT-IR analysis. FS also commented on experimental results and managed writing-original draft and writing-review preparations.

Abstract

Mortar quality is a fundamental parameter to take into account when studying the structural behavior of masonry, especially under seismic actions. Separation between the leaves of rubble masonry can occur, inducing the partial or total collapse of the construction. A good quality mortar is essential to delay/prevent the separation of leaves, but often, especially in ancient building with a cultural value, mor− tars have low binder capabilities.

The paper presents an experimental investigation on mortar specimens taken from buildings of a little municipality in Marche region, Arquata del Tronto, heavily damaged by recent earthquakes in Central Italy (2016−2017). Both diagnostic techniques as X−Ray diffrac− tion, Fourier−Transform infrared spectroscopy and calcimetry, and mechanical test as compression tests were carried out in order to cor− relate the obtained values with the performance of the original masonry.

Keywords: mortar; earthquakes; materials characterization; Arquata del Tronto; mechanical behaviour

1. Introduction

The damage caused by the 2016-2017 Central Italy earthquakes to architectural heritage in the municipalities of Marche region were very high. In Arquata del Tronto, a small town in the province of Ascoli Piceno, the earthquakes caused collapses and damage of churches, monuments and cultural heritage, as well of buildings in small neighboring villages.

From the macro-seismic point of view the municipality of Arquata, as well as the other localities in the same area, was historically subjected to significant earthquakes interspersed with periods of seismic inactivity: as shown in Table 1, in which only recent seismic events with a level of damage greater than or equal to the VI MCS are reported, it is possible to note that a long period of calm goes from the shock on May 12th, 1730 (VII-VIII MCS) to that on July ^{4th}, 1916 (VII MCS).

The shock on August 24th, 2016 caused damage associated to the IX degree of the MCS. Although damage was more severe in the surrounding villages, only a few buildings collapsed in the main square, whereas all the others were damaged. With the event on October 30th of the same year (Figure 1) the scenario changed radically: Arquata was completely destroyed. The Italian Army and the firefighters started the debris removal and the realization of a *tabula rasa* in all the Arquata promontory.

Table 3 – Recent earthquakes in Central Italy with a level of damage greater than or equal to the VI MCS [Locati et al., 2016; Albini et al., 2016]

MCS ≥ VI	Date	Epicenter
IX	January 14th, 1703	Valnerina
VII-VIII	May 12th, 1730	Valnerina
VII	July 4th, 1916	Sibylline Mountains
VI	April 7th, 1930	Sibylline Mountains
VI	December 19th, 1941	Sibylline Mountains
VI	January 29th, 1943	Sibylline Mountains
VI	October 3rd, 1943	Area of Ascoli Piceno
VI-VII	September 5th, 1950	Gran Sasso d'Italia
VI-VII	November 26th, 1972	Southern Marche
VI	September 19th, 1979	Valnerina
VIII-IX	August 24th, 2016	Area of Amatrice

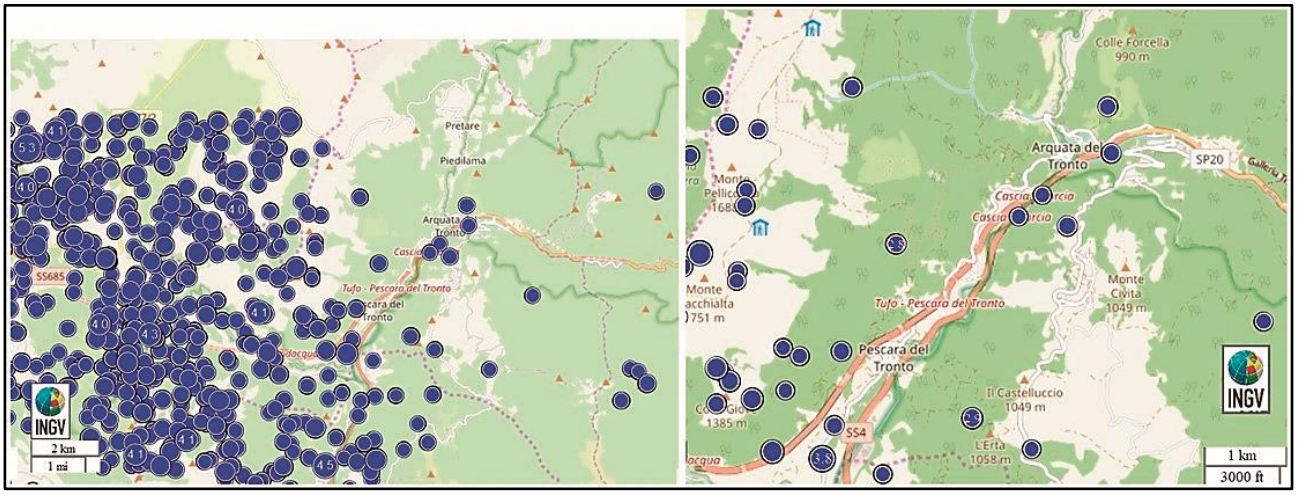

Fig. 1. Earthquakes registered, between 2016 and 2017, in the area surrounding Arquata del Tronto with magnitude higher than 2.5. The events of magnitude from 3.8 to 4.1 on October 30th, 2016 are shown. Left, larger scale; right, smaller scale (source: INGV[1])

The 2016 seismic sequence affected a portion of the Apennines characterized by the outcrop of turbiditic sandstones (Laga Flysch, Messinian), limestones and pelagic marly limestones of the Umbro-Marchigiana series (Mesozoic) (Figure 2). These lithologies are the most common construction material of the buildings erected until the sixties of the last century, as well as of all the

[1] Data and results published on this website by Istituto Nazionale di Geofisica e Vulcanologia (http://www.ingv.it/) are licensed under a Creative Commons Attribution 4.0 International License (http://creativecommons.org/licenses/by/4.0/). ISIDe Working Group at National Earthquake Center (http://cnt.rm.ingv.it/) benefited from funding provided by the Italian Presidenza del Consiglio dei Ministri, Dipartimento della Protezione Civile.

monumental buildings as churches, castles, towers and convents. An in-depth study on the architectural heritage in the territory of Arquata del Tronto shows that the masonry structures follow a building practice which changed during time, entailing substantial variations of their load bearing capacity. Local materials were used for masonry, with differences between the zones north and south of river Tronto. The southern zone is characterized by sandstone mixed with river pebbles, with rare brick units, whereas the northern zone by limestones added to masonry. The masonry fabric consists of irregularly rough-hewed units and chips of natural materials. The mortar is poor of lime and particularly crumbly. Irregularities are compensated by plentiful mortar. A limited compliance of the horizontal orientation can be observed. Sometimes the horizontality of courses is provided by the insertion of brick wedges. The offset of head joints is nearly absent. Several buildings are in complete abandonment since decades, and some of them were near collapse already before the earthquake. At the same time there are inhabited buildings in normal maintenance conditions, where relatively recent interventions were carried out, with ring beams and roofs in reinforced concrete, in some cases with smooth rebars, not linked each other and without hoops. As already observed after the 1997 Umbria-Marche earthquake and the 2009 L'Aquila earthquake, these intervention, without a proper consolidation of the vertical structure, usually entailed widespread collapses.

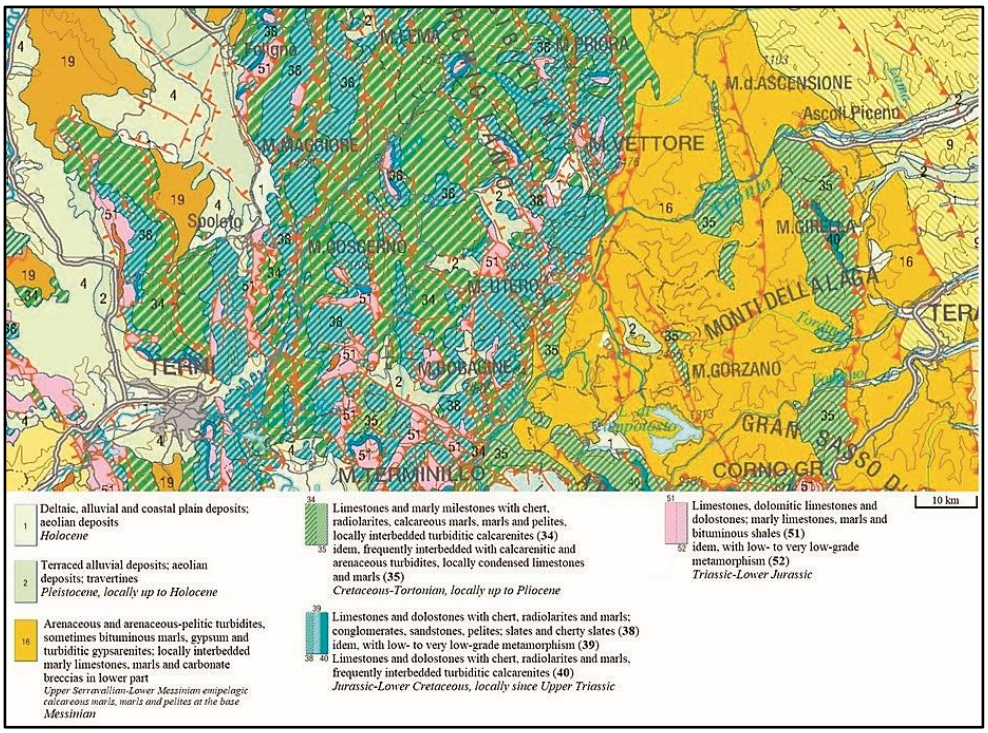

Fig. 2. Geological map (1:1000000) relative to Arquata del Tronto and surroundings (source: ISPRA – www.isprambiente.gov.it)

Although it is aware that the seismic effects on structures depend on a plurality of factors, like the energy released by the earthquake, the geological characteristics of the site, the type of foundation, the original materials and techniques, but also the state of conservation of the buildings and possible maintenance actions occurred during the time [Guidoboni and Ferrari, 2009], developing a methodology to define mortar quality would be very useful to interpret the mutual relationship and the correlation between earthquake and damage. With this aim, a sampling campaign in Arquata and its neighboring villages was carried out, in order to chemically and mechanically characterize the mortar and correlate the obtained values with the performance of the original masonry.

2. Experimental Setup or Method

Twenty-four mortar samples have been collected, under the supervision of firefighters, from historical and monumental buildings located in different settlements within the municipality of Arquata del Tronto (Table 2 and Figure 3). Sampling has been performed with care considering only bedding mortars from collapsed or partially collapsed buildings.

During sampling, for each mortar specimen a record card has been filled with: date, location, type of building, point of sampling, sample quantity (estimated).

Table 2 – Mortar samples from settlements within the municipality of Arquata del Tronto

Settlement	Sample ID
Arquata del Tronto	1
	2
	3
Borgo	4
	5
	6
	7
	8
	9
Camartina	10
	11
	12
	13
Faete	14
Pretare	15
	16
	17
	18
	19
	20
	21
	22
Trisungo	23
	24

Fig. 3. Mortar sampling campaign in Pretare − St. Rocco Church (Arquata del Tronto)

Firstly, an inspection of the samples collected has been carried out, in order to remove possible impurities and to exclude samples that presented effects of external agents. The inspection has been made in laboratory, both with naked eye and a stereomicroscope Olympus SZX12 with digital image acquisition.

Possible contaminations could be due to the collapse of the structure itself, causing contact with other materials, or from subsequent contact with external agents (natural or anthropic). For instance, some mortar samples have been excluded from the analysis as they presented the formation of plants probably due to exposure to a humid environment.

Then, to evaluate grain size distribution the samples have been firstly roughly cracked in smaller pieces and successively they have been sieved. Different mechanical treatments have been performed in dry conditions and the material passing through the sieve has been weighted and recovered [Groot et al., 1996]. Particle-size analysis was carried out using the following sieves: 2.000, 1.000, 0.500, 0.250, 0.106, 0.063 mm.

The samples were analysed by X-Ray diffraction in order to evaluate the type of binder and aggregate. This technique allows identifying crystalline phases, while the presence of amorphous phases generates broad halos in the pattern.

A SmartLab Rigaku powder diffractometer, equipped with Cu kα radiation source and a graphite monochromator in the diffracted beam, operated at 40kV and 30 mA, has been used. X-Ray diffraction powder patterns have been acquired within the angular range 2-90 2theta at a step size of 0.04 and 12 seconds per step. In order to enhance the binder fraction the disaggregated mortars have been sieved at 63 μm and the powder obtained has been successively grinded in order to further reduce particles dimensions [Carrara and Persia, 2001; Cardinale et al., 2002]. Some samples have been

analysed also after removal of larger inert coarser granule and refining the powders using an agate mortar [Chiari et al., 1993].

Analysis by Fourier-Transform Infrared Spectroscopy (FT-IR) was carried out on mortar samples ground in a agate mortar and then passed completely through a 125 μm sieve. A Perkin Elmer Spectrum 100 was used in ATR mode (Total Reflected Reflectance). For each sample two acquisitions were performed.

Calcimetry has been performed, using the gas-volumetric Dietrich-Fruhling method. The sample was ground manually with an agate mortar until it was completely passed through a 63 μm sieve, then dried into a thermobalance at 60 °C up to constant mass. The sample was treated with a reagent based on hydrochloric acid, which decomposes the carbonates present by CO_2 development, as regulated by UNI 11140: 2004. This technique allowed to evaluate with greater precision, compared to the analysis in FT-IR spectroscopy ATR, the quantity of carbonates present in the samples (uncertainty: ± 0.1%).

Soluble salt content was estimated by conductometric measurements. From the conductivity value of the solutions, the formula indicated in the DIMOS document, part II module 3, ICR, 1978 was applied, estimating the percentage of soluble salts present in the samples. Analysis of soluble salts (UNI 11087: 2003) was carried out as following: the sample was dried in an oven at 60 °C for about 24 h, then ground manually within an agate mortar until it was completely passed through a 125 μm sieve. The samples were weighed (95 mg up to 105 mg) and treated into a thermobalance at a temperature of 60 °C up to constant mass. 100 ml of bi-distilled H_2O, whose conductivity was previously measured, were added to the sample and placed in a flat-bottomed glass container. The container was hermetically sealed to prevent evaporation and slowly stirred for 2h; then residuals were left to deposit for about 30 min; finally, conductivity was measured with a XS Multiparameter, model PC 70 (resolution: 0.1 μS). The obtained suspension was then filtered (black band filter) and the solution was used for the measurements of the single ionic species by ionic chromatography.

Concentration of anions contained in mortar under study has been measured with a Metrohm Ion Chromatograph 761 Compact with chemical integrated Metrohm suppressor module (MSM) and METROSEP A Supp. 5 150/4.0 separation column. Injection volume was typically 1.5 ml and the loop volume was 20 μl. Sartorius 0.45 μm RC-Membrane PP-Housing filters were used to remove particles. Three repetition for each analysis were performed. The method of calibration curve with increasing concentrations of standards has been used to calculate the concentration of anions.

Prismatic specimens were obtained from field samples, the edges were measured, the top and bottom faces were covered with plaster and a compression test was performed. The tests were performed under displacement control at a speed of 0.54 mm/min. Strain was calculated dividing the relative

displacement between the load cell and the base plate by the initial distance. The measurement was not taken directly on the sample because of the large size of the aggregate. For each sample, the stress-strain curve was elaborated. The normalized compressive strength f_m was determined multiplying the nominal strength f by the shape factor δ:

$$f_m = \delta f \qquad (1)$$

The shape factor δ, which accounts for the sample geometry, was calculated according to [BS EN 772-1:2011 + A1:2015, 2015].

Since no standard is available for the determination of the modulus of elasticity of masonry mortar, that recommended for concrete was used [ASTM C 469 – 02, 2002]. Thus, the modulus of elasticity E is given by:

$$E = \frac{S_2 - S_1}{\varepsilon_2 - \varepsilon_1} \qquad (2)$$

where:

S_2 = 40% of the nominal compressive strength f S_1 = stress corresponding to strain ε_1

ε_2 = strain corresponding to stress S_2 ε_1 = 0.00005

As for the measurement of strain, the beginning of the test was identified when the load was monotonically increasing under a prescribed monotonically increasing displacement.

3. Results and Discussion

3.1 Sieving process and grain size distribution

Particle−size distribution highlighted the prepon− derance of a fine fraction in mortar samples, especially those from Pretare, as shown in Figure 4.

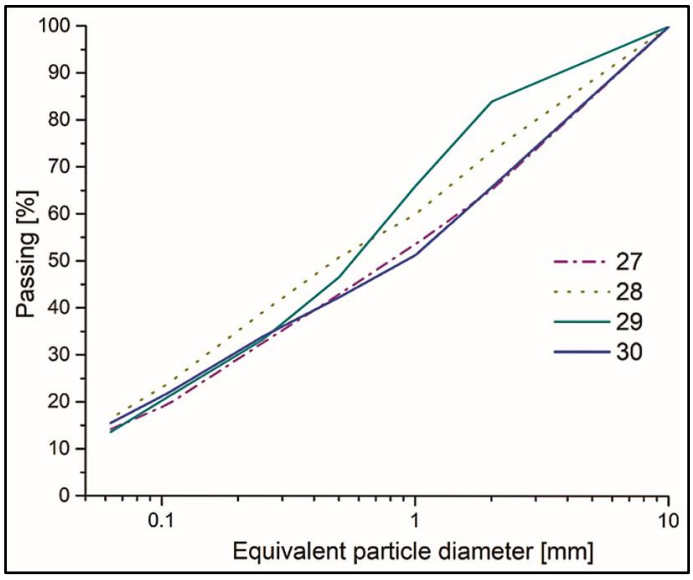

Fig. 4. Particle−size analysis

In some cases the finer fractions, smaller than 0.5 mm, constitute more than 40% of the entire aggregates.

3.2 X-Ray diffraction

In Figure 5 XRD patterns of mortars from Arquata del Tronto (1, 2, 3), Camartina (10, 11, 12, 13), Faete (14) and Trisungo (24) are shown. The samples from Arquata presented principally quartz, calcite, phyllosilicates, feldspars and dolomite, in particular in sample 2 and some traces of gypsum. Same phases were identified in the samples from Camartina, even if only traces of dolomite were present while gypsum was absent. Sample 11 from Camartina presented higher quantity of calcite with respect to the other samples. Material sampled in Faete revealed small quantity of calcite, being quartz the most abundant phase. The sample from Trisungo presented similar phases respect to those from Arquata but also gypsum and lower concentrations of calcite. It has to be noted that no crystalline phases related to hydraulic binders have been detected in all the samples investigated. X-Ray diffraction data could give important indication about binder and aggregates even if it should be considered that the detection limit of the technique is about 1 wt%. Moreover, eventual non crystalline phases deriving from carbonation and hardening, as amorphous calcium silica gel (C-S-H), deriving from hydration of cement, could not be detected. In some samples large quantities of calcite have been detected being probably related in part to aggregate fraction [Chiari et al., 1992].

The dolomite recognized in the samples was probably used as aggregate, because peaks related to hydromagnesite and hydrated magnesium carbonate hydroxide have not been detected in the XRD patterns. The presence of hydromagnesite deriving from mortars with binders deriving from dolomite as precursor is still controversial [Montoya et al., 2003].

As just stated above and referring to the geological map, the analysis of the materials sampled are in agreement with the hypothesis that the construction materials were extracted around these small towns.

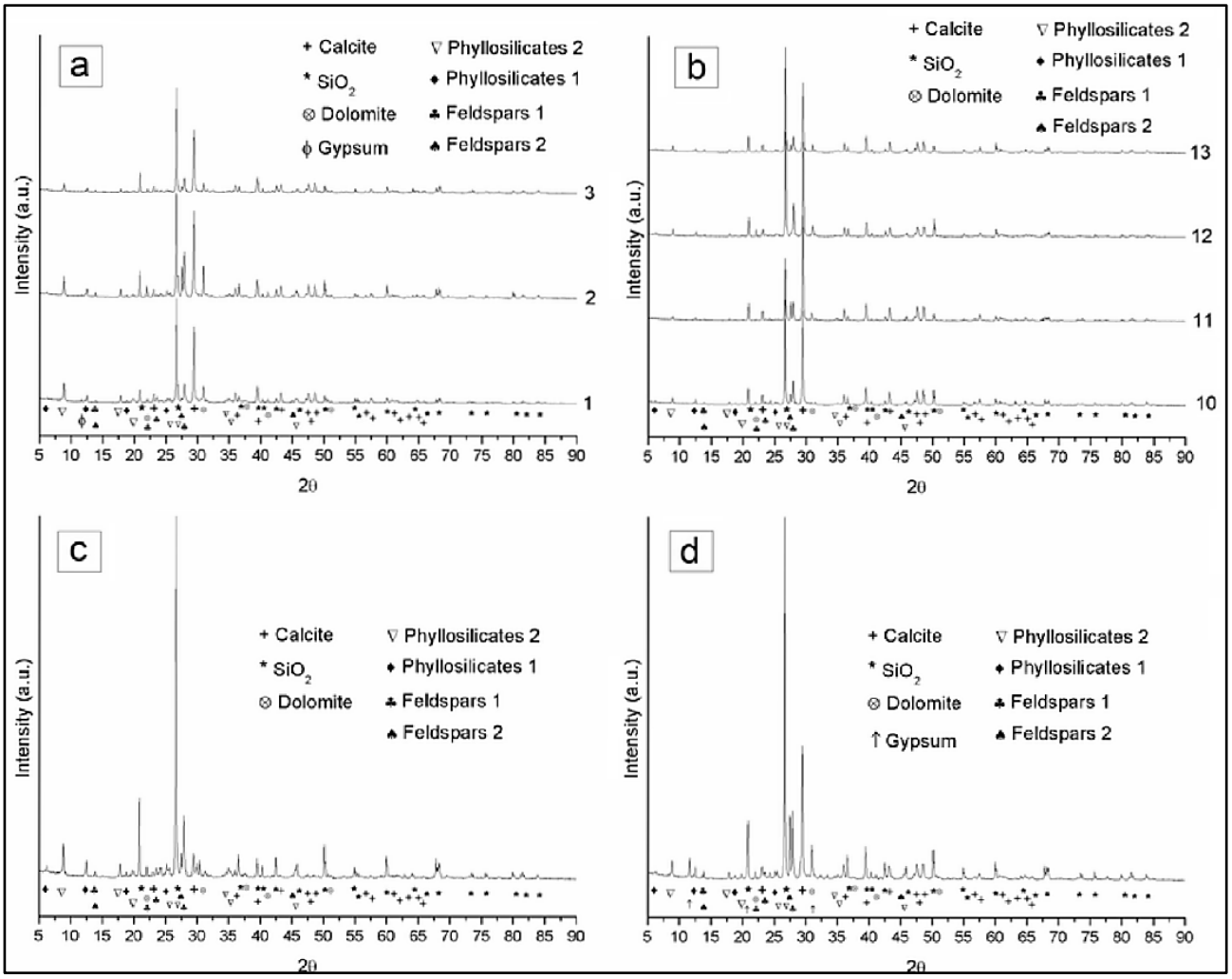

Fig. 5. XRD patterns of samples from a) Arquata del Tronto (1, 2, 3), b) Camartina (10, 11, 12, 13), c) Faete (14) and d) Trisungo (24)

3.3 Fourier-transform infrared spectroscopy, calcimetry, soluble salt analysis and dosage of anionic species

FT-IR analysis allowed to gain an overview of the composition of the mortars [Gulmini et al., 2015] and, relatively to carbonates, silicates and sulphates, the intensity of their stretching signals have been used to obtain a semi-quantitative evaluation (Table 3).

The most part of mortars collected show intense signals of carbonates, as confirmed by calcimetry: eighteen samples have a percentage of carbonates higher than 30%; eleven of them have a percentage well above 50% (table 3), indicating that the aggregate is partially made by carbonates. According to XRD results, in some specimens FTIR analysis highlighted the presence of dolomite.

Table 3 - FT-IR results and percentage of carbonates in mortars analyzed from settlements within the municipality of Arquata del Tronto. The intensity of the stretching signals of carbonates, silicates and sulphates is indicated by the number of 'x'

Settlement	Sample ID	FT-IR			Calcimetry [% of carbonates]
		CO_3^{2-}	SiO_4^{4-}	SO_4^{2-}	
Arquata del Tronto	1	xx*	xxx		26.5
	2	xx*	xx	(x)	21.1
	3	x	xx		16.5
Borgo	4	xxx			95.6
	5	xxx	xx		52.6
	6	xxx*	xx		51.9
	7	xxx	xxx		35.4
	8	xxx	xx**		32.9
	9	xxx	x**		62.2
Camartina	10	xxx	xx		50.0
	11	xxx	xx		50.9
	12	xxx	xx		44.5
	13	xxx	xxx		36.9
Faete	14	x	xxx		16.6
Pretare	15	xxx*	x		76.4
	16	xxx*	x		54.4
	17	xxx*	(x)		30.5
	18	xxx*	x		39.3
	19	xxx*	x		95.1
	20	xxx	x		76.7
	21	xxx	x		73.5
	22	xxx*	(x)		32.7
Trisungo	23	x	xx**		17.6
	24	x*	xxx	xx	11.0

* Presence of dolomite, in addition to calcite
** Presence of phyllosilicates, in addition to quartz

In regard to the soluble salt analysis by conductimetry, the mortars are characterized by percentages between 2 and 10%, with the exception of sample 24 (Table 4).

Concerning the concentration of the various anionic species (table 4), the following considerations can be made:

- the sulphates were present in low quantities, below 3 ppm (except for samples 2, 16, 23 and 24);
- the presence of chlorides in the samples is negligible: only two samples exceed 3 ppm (2 and 23);
- regarding nitrates there is a very heterogeneous situation, with values between 0,24 and 19,17 ppm;
- presence of fluorides and phosphates was not detected.

Table 4 – Percentage of Soluble Salts (SS) and concentration of anionic species (average value of three measurements and associated standard deviation) in mortars analyzed from settlements within the municipality of Arquata del Tronto

Settlement	Sample ID	Conductivity [µS]	SS [%]	F^-	Cl^-	NO_3^- [ppm]	PO_4^{3-}	SO_4^{2-}
Arquata del Tronto	1	62.1	4.1	-	2.11±0.12	2.64±0.36	-	2.18±0.21
	2	105.8	7.1	-	5.84±0.49	9.63±0.19	-	9.78±0.60
	3	62.5	4.2	-	1.07±0.07	-	-	1.72±0.25
Borgo	4	45.3	2.9	-	0.43±0.02	0.65±0.05	-	>0.5
	5	92.1	5.9	-	0.98±0.04	19.17±0.17	-	1.00±0.04
	6	54.3	3.4	-	0.57±0.11	0.45±0.05	-	0.90±0.17
	7	40.2	2.4	-	0.38±0.03	-	-	>0.5
	8	56.3	3.6	-	0.83±0.01	0.74±0.05	-	-
	9	82.5	5.2	-	1.08±0.16	13.56±1.22	-	-
Camartina	10	44.8	3.0	-	<0.25	-	-	<0.25
	11	52.0	3.4	-	<0.25	-	-	<0.25
	12	49.5	3.2	-	1.50±0.06	3.57±0.34	-	<0.25
	13	57.4	3.8	-	0.54±0.11	0.76±0.05	-	<0.25
Faete	14	67.5	4.4	-	2.43±0.31	3.10±0.56	-	-
Pretare	15	78.9	5.0	-	0.50±0.03	0.45±0.05	-	>0.5
	16	65.2	4.0	-	1.04±0.17	1.50±0.29	-	8.84±1.05
	17	125.4	8.3	-	0.33±0.01	0.30±0.20	-	0.51±0.13
	18	45.5	2.8	-	0.52±0.01	-	-	0.67±0.05
	19	61.1	4.1	-	0.50±0.07	1.15±0.20	-	0.92±0.10
	20	158.3	10.0	-	2.57±0.01	13.14±1.5	-	0.65±0.05
	21							
	22	66.2	4.0	-	0.59±0.09	0.24±0.05	-	1.07±0.12
Trisungo	23	93.5	5.9	-	5.00±0.05	13.70±1.79	-	3.87±0.64
	24	177.9	11.9	-	2.07±0.05	3.39±0.37	-	61.17±0.41

3.4 Compression Tests

Some samples, although containing calcite, presented poor compactness and they could be easily fragmented. Mechanical tests have been performed on the samples that presented the highest compactness and in particular those that could be cut to a shape suitable for tests without fragmentation. Two specimens were obtained from sample 17, collected at Pretare. The prismatic samples, tested in compression, are shown in Figure 6. Their dimensions are reported in Table 5, along with the corresponding shape factor. It is mandatory to emphasise that these specimens were obtained from a sample having an aboveaverage compactness compared to those collected in the municipality.

For sample 17.1, a first test was performed that did not reach failure, and a second test until failure. For sample 17.2, failure was reached at the first test. For each sample, the stress-strain curve is reported in Figures 7-8, along with a picture of the sample at the end of the test.

Fig. 6. Cubic samples obtained from sample 17: left, sample 17.1; right, sample 17.2

Table 5 – Characteristics of the samples tested in compression

Sample	Weight (g)	Length (mm)	Width (mm)	Cross-section area (mm^2)	Height (mm)	Density (kg/m^3)	Shape factor (-)
17.1	154	49	54	2660	45	1284	0.821
17.2	149	50	55	2739	44	1235	0.816

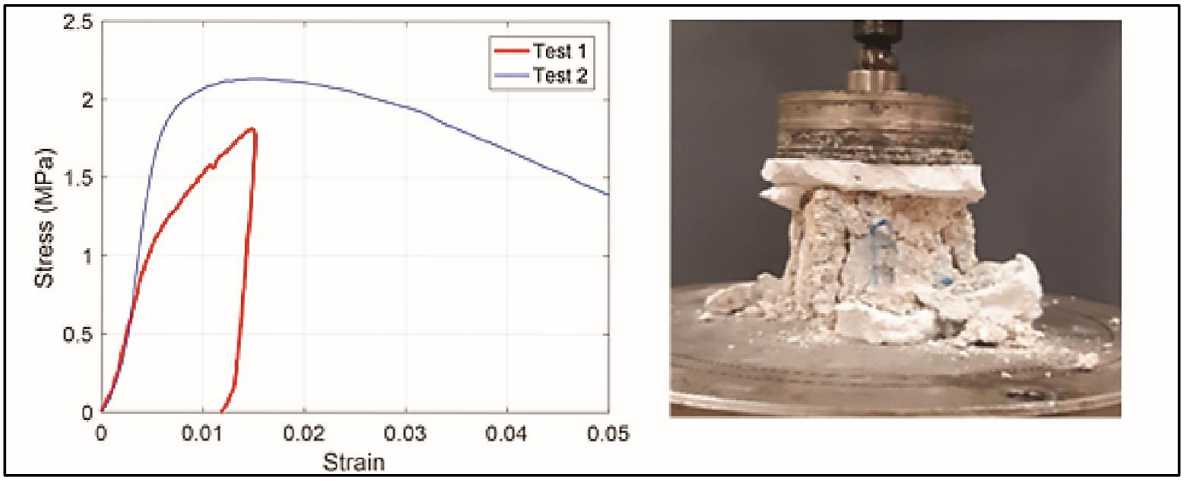

Fig. 7. Sample 17.1: left, stress−strain curve; right, sample at the end of the test

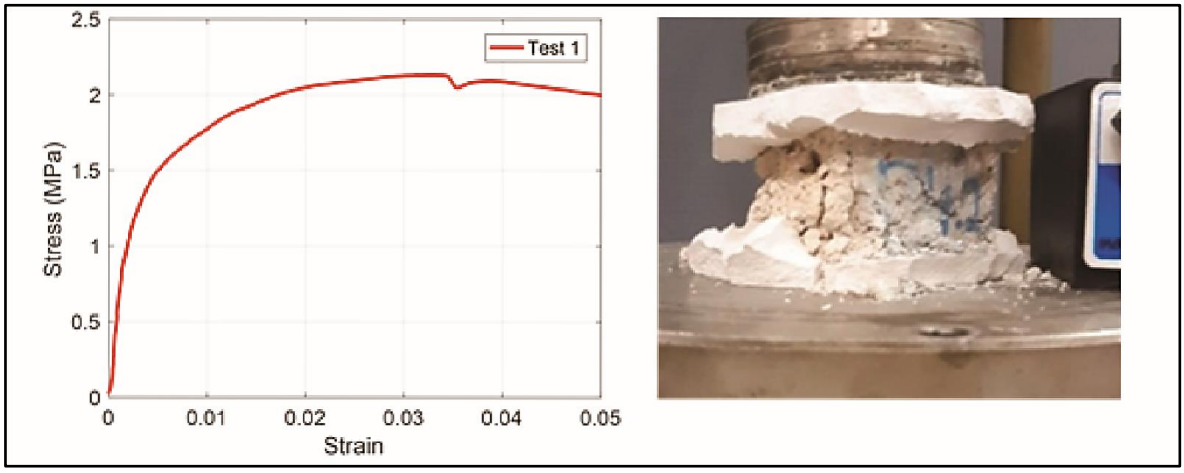

Fig. 8. Sample 17.2: left, stress−strain curve; right, sample at the end of the test

The normalized compressive strength f_m was calculated according to Eq. (1). The results are reported in Table 6, where, for the test that did not reach failure:

F_{max} = maximum load

σ_{max} = maximum stress

ε_{max} = strain at maximum stress

ε_r = residual strain

and, for the tests that reached failure:

F_u = ultimate load

f = nominal strength

ε_f = strain corresponding to ultimate load

Table 6 – Results of compression tests

Sample	**Failure**	F_{max} **(kN)**	σ_{max} **(MPa)**	ε_{max}	ε_r	F_u **(kN)**	f **(MPa)**	f_m **(MPa)**	ε_f
17.1	No	5.0	1.88	0.015	0.012	-	-	-	-
	Yes	-	-	-	-	5.8	2.18	1.79	0.015
17.2	Yes	-	-	-	-	6.0	2.19	1.79	0.035

The two samples highlight an almost perfect match in terms of strength, but a significant difference in terms of strain at ultimate load. Such difference could be ascribed to sample scatter, to disturbance introduced during sample preparation or, more likely, to the fact that sample 17.1 underwent a first test before the failure one. The strength value can be compared with the 60 values collected from literature in [Liberatore et al., 2014] for clay brickwork: there are six samples with a smaller strength (the smallest being 0.28 MPa). If the 42 sample of tuffwork in [Marotta et al., 2016] are considered, Arquata's samples are larger of just four values (minimum value 0.55 MPa). Additionally, it is worth emphasising that the current Italian building code [DMIT, 2018] prescribes a minimum strength of 2.5 MPa for ordinary loads (Sect. 11.10.2), and 5.0 MPa under earthquake loads (Sect. 7.8.1). Instrumental error of the load cell is declared by the manufacturer as ±0.5%, and the same error can be assumed for strength estimation.

Additionally, it is useful to emphasise that mortar deformation capacities are seldom reported, hence, enhancing the importance of data reported herein that is necessary for non-linear micromechanical modelling [Zucchini and Lourenco, 2007]. Instrumental error of the displacement transducer is ±1.0%, and the same error can be assumed for deformation estimation.

Finally, modulus of elasticity of masonry mortar, reported in Table 7, presents a scatter greater than that of strength. Sample 17.1 has a modulus of elasticity nearly constant during the two tests. Observed values are very low compared to the seven in [Liberatore et al., 2014] all larger than 1 GPa. The worst combination of instrumental error in load cell and displacement transducer leads to a Young's modulus measurement uncertainty of ±0.6%.

Table 7 – Modulus of elasticity

Sample	Failure	S_2 (MPa)	S_1 (MPa)	ε_2 (-)	E (MPa)
17.1	No	0.85	0.01	0.0038	232
	Yes	0.85	0.01	0.0033	258
17.2	Yes	0.85	0.04	0.0014	615

4. Conclusions

During 2016 and 2017 a dramatic sequence of seismic events heavily damaged small towns in the Centre of Italy in regions as Lazio, Abruzzo, Marche and Umbria, causing a large number of victims. In this work the bedding mortars of some masonry partially or completed collapsed during earthquakes have been sampled in the surroundings of Arquata del Tronto and analyzed by different techniques.

X-Ray diffraction analysis revealed the use of lime mortars with the presence mainly of quartz and calcite and the presence of feldspars and phyllosilicates. In some cases dolomite has been identified. Some samples also evidenced the absence of the binder or its presence in traces. FTIR and Calcimetry confirmed the presence of carbonates and silicates and that of dolomite in some specimens, while other measurements revealed the presence of low concentrations of soluble salts.

Several samples presented poor mechanical characteristics and could be easily fragmented. Compression tests have been performed on two samples that showed higher cohesion and could be worked without fragmentation. The tests showed that the mortar, of presumed lime type from calcareous and dolomitic rocks, has poor mechanical behavior, with normalized compressive strength lower than 1.8 MPa, i.e. at the lower bound of the values reported in the literature, and significantly lower than the minimum strength prescribed by the code for new constructions in seismic prone areas (5 MPa). Similar results were found for the modulus of elasticity.

This work evidences, through a multidisciplinary approach, some highlights on the bedding mortars used in these historical sites. The results of the analysis reported in this paper could be useful as support for future research, supplying information for establishing priorities of intervention for

repairing and consolidation and also for reconstruction activities which would take into account construction materials of this ancient masonries. In the future a campaign of measurements could be carried out in order to design a sort of vulnerability map of masonries as aid for lawmakers, municipalities and experts.

References

- Albini, P., L. Arcoraci, M. Berardi, F. Bernardini, C. Bignami, B. Brizuela, R. Camassi, V. Castelli, C. Castellano, S. D'Amico, V. D'Amico, S. Del Mese, E. Ercolani, A. Fodarella, L. Graziani, M. Locati, I. Leschiutta, A. Maramai, V. Pessina, A. Piscini, A. Rossi, A. Rovida and M. Sbarra (2016). QUEST - Rilievo macrosismico in EMS98 per il terremoto di Amatrice del 24 agosto 2016 – Report finale, www.questingv.it.
- ASTM C 469 - 02 (2002). Standard Test Method for Static Modulus of Elasticity and Poisson's Ratio of Concrete in Compression, ASTM International, West Conshohocken, PA, 2014, www.astm.otg, DOI: 10.1520/C0469_C0469M-14.
- BS EN 772-1:2011 + A1:2015 (2015). Methods of test for masonry units. Determination of compressive strength.
- Cardinale, V., F. Persia, L. Campanella, F. Cardellini and S. Omarini (2002). Storia costruttiva del complesso monastico di San Vincenzo al Volturno attraverso la determinazione di differenze composizionali nelle malte. Risultati preliminari, Atti del 2° Congresso Nazionale AIAr, Bologna 29 gennaio-1 febbraio 2002, 505-513, ISBN 88-555-2688.
- Carrara, C. and F. Persia (2001). Indagini mineralogichepetrografiche e di diffrazione dei raggi X sulle incrostazioni calcaree e sulle malte in Gli acquedotti Claudio e Aniene Nuovo nell'area della Banca d'Italia in Via Tuscolana, Ed Istituto Poligrafico e Zecca dello Stato, 193-197.
- Chiari, G., M.L. Santarelli and G. Torraca (1992). Caratterizzazione delle malte antiche mediante l'analisi di campioni non frazionati, anno II, n. 3.
- Chiari, G., M.L. Santarelli and G. Torraca (1993). Caratterizzazione delle malte antiche mediante l'analisi di campioni non frazionati, Materiali e Strutture, 2, 111-137.
- DMIT (2018). Decreto del Ministro delle Infrastrutture e dei Trasporti 17 gennaio 2018. Aggiornamento delle "Norme tecniche per le costruzioni". Gazzetta Ufficiale della Repubblica Italiana, n. 42 del 20 febbraio 2018, Supplemento Ordinario n. 8.
- Groot, C., G. Ashall and J. Hughes (1996). Characterization of Old Mortars with Respect to their Repair, Final Report of RILEM TC 167-COM.
- Guidoboni, E. and G. Ferrari (2009). Historical variables of seismic effects: economic levels, demographic scales and building techniques, Annals of Geophysics, 43 (4), 687-705.

- Gulmini, M., G. Roselli, F. Scognamiglio and G. Vaggelli (2015). Composition and microstructure of maiolica from the museum of ceramics in Ascoli Piceno (Italy): evidences by electron microscopy and microanalysis, Applied Physics A, 120 (4), 1643-1652.
- Liberatore, D., A. Marotta and L. Sorrentino (2014). Estimation of clay-brick unreinforced masonry compressive strength based on mortar and unit mechanical parameters, 9th International Masonry Conference, Guimaraes, Portugal, 5-7 July, paper 1400, 12 pp.
- Locati, M., R. Camassi, A. Rovida, E. Ercolani, F. Bernardini, V. Castelli, C.H. Caracciolo, A. Tertulliani, A. Rossi, R. Azzaro, S. D'Amico, S. Conte and E. Rocchetti (2016). DBMI15, the 2015 version of the Italian Macroseismic Database, Istituto Nazionale di Geofisica e Vulcanologia, DOI: http://doi.org/10.6092/INGV.IT-DBMI15.
- Marotta, A., D. Liberatore and L. Sorrentino (2016). Estimation of unreinforced tuff masonry compressive strength based on mortar and unit mechanical parameters, Brick and Block Masonry: Trends, Innovations and Challenges - Proceedings of the 16th International Brick and Block Masonry Conference, IBMAC 2016, 1715-1722.
- Montoya, C., J. Lanas, M. Arandigoyen, I. Navarro, P.J. Garcìa Casado and J.I. Alvarez (2003). Study of ancient dolomitic mortars of the church of Santa Maria de Zamarce in Navarra (Spain): Comparison with simulated standards, Thermochimica Acta, 398(1), 107-122.
- Zucchini, A. and P.B. Lourenço (2007). Mechanics of masonry in compression: Results from a homogenisation approach, Computers and Structures, 85, 193–204.

Conclusions

The recent global "weak" transition to a "green economy", aimed to minimise the human and industrial effects on the environment (consider, for example, the disasters caused by the massive use of syntethic plastic), has underlined the importance of a better utilization of renewable sources and reuse of waste biomasses. The issue has taken on an urgency, as testified by the multiplicity of studies on these topics, in particular in the field of materials engineering.

This PhD project, on the heels of this scientific production, concerned the recycling of cellulose waste (Cellulosic Solid Residue – CSR, zero waste strategy) obtained from different sources, which guarantee a large and reasonably constant availability, to be specific cotton waste from worn out textiles and cladodes of *Opuntia ficus indica* (OFI, also referred to as Nopal) plants. The experimental procedures carried out (with the idea of operating as much as possible in conditions of circular economy) aimed: i) to optimize the low-cost extraction of valuable substances, Cellulose Nanocrystals (NCC) in the first case, Nopal (mucilage and fibers) in the second one; ii) to introduce NCC and Nopal into different modern materials [Paper and Thermoplastic Starch (TPS) Films], in order to obtain their performance improvement; iii) to evaluate the possibilities and drawbacks of these practices in order to suggest solutions for future use. Broadly speaking, the general objective of the entire work was to identify suitable applications for the specific waste materials mentioned above, of scarce or null economical value, suggesting the optimal processes for their treatment and final reuse, the whole in collaboration with important economic and cultural actors of Marche and Lazio regions (Italy) [among all: the University of Camerino, the companies NEST S.r.l. and Cartiere Miliani Fabriano S.p.A., the Italian Research Agency ENEA (engaged for years in experimentations and projects regardind Nopal), the National Research Council of Italy CNR, "Sapienza" University of Rome].

If on the one hand there is a large bibliography about the extraction processes of NCC and Nopal, and their application in several sectors (among all, for NCC: Börjesson and Westman, 2015; Moon et al., 2011; Klemm et al., 2011; Dufresne, 2013; Brinchi et al., 2013; for Nopal: Persia et al., 2016; Sepùlveda et al., 2007; Saenz et al., 2004; Del Valle et al., 2005; Gheribi et al., 2018), on the other the project-choices of setting up low-cost production methods and utilizing these materials in the field of papermaking (NCC and Nopal) and biocomposites (Nopal) were quite innovative. On this last point, in particular, the introduction of NCC in modern Paper was justified by the promising mechanical results (tensile strenght and bending number) of a previous study (Coccia et al., 2014)

achieved introducing cellulose nanocrystals as reinforcing filler in a Paper sheet, while the use of Nopal in two so different areas of technology (Paper and TPS) was aimed to investigate new high potential applications of this material.

The research activies regardind NCC can be so summarized:

I. Extraction of Cellulose Nanocrystals from different sources [microcrystalline cellulose (Bondeson et al., 2006), bacterial cellulose (Roman and Winter, 2004) and cotton bush (Saraiva Morais et al., 2013)] and morphological characterization via SEM of the obtained material, in order to validate the correctness of the process.
II. Extraction of NCC from cotton textile waste (70% long fibers, 30% cotton linter) resulting from discarded materials obtained from the development of pure cellulose paper products at a dedicated technical school (Istituto di Istruzione Superiore – I.I.S. "Merloni Miliani") in Fabriano (Italy). The process was performed through the action of sulfuric acid followed by solution neutralization with two different alkalis, namely ammonia and sodium bicarbonate, which yielded microcellulose (MCC), then centrifuged to NCC. (1st Article)
III. Scientific characterization [optical/polarized light microscopy and Dynamic Light Scattering (DLS) analysis] of the obtained NCC solutions, in order to compare the action of the two alkalis as for fiber repeatability and morphology. (1st Article)
IV. NCC introduction into modern Paper materials [blue dyeing of the fibers, application of each NCC solution (NH_3 and $NaHCO_3$ neutralization) on a paper strip (surface treatment) previously impregnated with poly(vinylalcohol) (PVA), preconditioning chamber], subsequently characterized from a mechanical point of view [double fold test, (Baker, 2001)] in order to evaluate their performance improvement. (Appendix to NCC)

For what it concerns Nopal application in modern Paper materials (Appendix to Nopal and 2nd Article), the project regarded:

I. Extraction of mucilage from residues of *Opuntia Ficus Indica* (OFI) plants, namely from cladodes (Sepùlveda et al., 2007). Three methods were adopted: i) bare maceration for 24 hours in the dark, with parenchymal material (g) – distilled water (ml) proportion of 1:1 (MA1); ii) bare maceration for 72 hours in the dark, with parenchymal material (g) – distilled water (ml) proportion of 1:9 (MA9); iii) mechanical blending (ME).
II. Zeta potencial analysis: addition of OFI mucilage (MA1, MA9 and ME) to the pulp without additives, in order to verify the possible zeta potential variation. For each Nopal solution there

was an increase in absolute value: this result was considered of interest to substitute OFI mucilage for Carboxymethil Cellulose (CMC).

III. Introduction of Nopal solution (MA1, MA9 and ME) into the pulp containing Kymene wet-strength additives. Exploiting natural tendency of Nopal to replace CMC, it was added until a zeta potencial default value was reached. The following steps were paper sheet forming and its mechanical characterization (double fold test).

IV. Surface treatment: two different types of paper supports, one previously impregnated with poly(vinylalcohol) (PVA) and one untreated, were immersed in OFI mucilage (MA1, MA9 and ME) heating to 60 °C, and then dried in an oven at 105 °C for 1 minute; a mechanical (double fold test) and morphological (optical microscopy) characterization of the sheets was performed, in order to evaluate the effects of Nopal introduction.

As regards the application of Nopal (mucilage and fibers from OFI) as filler of Thermoplastic Starch (TPS) Films (2nd and 3rd Articles), the experimental procedures carried out involved:

I. Self-production of several starch-based composites (Mohammadi Nafchi et al., 2013; Rodriguez-Gonzalez et al., 2004), originating from three different commonly available starch types (potato, corn and rice) and with a variable content in glycerol, in order to select the most appropriate formulation and procedure. The choice fell upon a TPS based on potato starch, with a high content in glycerol (ca. 30%).

II. Extraction of mucilage from Opuntia cladodes [Sepùlveda et al., 2007]. Three methods were adopted: i) bare maceration (MA); ii) mechanical blending (ME); iii) mechanical blending following maceration (MPM).

III. Introduction of OFI mucilage (MA, ME and MPM) into TPS matrix, obtaining three different TPS-Nopal mucilage Films.

IV. Comparison between TPS Films as such and after the introduction of Nopal mucilage, in order to evaluate their performance improvement. The measurements carried out involved, apart from basic morphological characterization, such as film thickness measurement, other sounder methods of analysis, which included in particular: i) optical microscopy and scanning electron microscopy (SEM) of the films as received, to evaluate their morphology and after tensile tests, to study the fracture surfaces; ii) tensile tests using dog-bone specimens with a gauge length equal to 40 mm; iii) differential scanning calorimetry (DSC) to evaluate the evolution of the films' behavior with temperature; temperatures for the different transition moments were determined using the first derivative of the heat capacity calculated from DSC.

V. Pre-treatment of OFI fibers coming from garden waste: cleaning, cutting, sonication, drying and mashing in ball mill. The final sizes of the fibers obtained were not higher than 1 mm in length, and with very variable aspect ratios, from close to 1, therefore in powder form, to others with up to 10–20.

VI. Introduction of Nopal dry fibers into TPS matrix (Curvelo et al., 2001; Ma et al., 2005), producing three types of TPS-Nopal fibers Films: i) composite A, with an amount of fibers equal to 16 wt% of the total starch + glycerol content, obtained after a stirring of 1 h; ii) composite B, with an amount of fibers equal to 16 wt% of the total starch + glycerol content, obtained after a stirring of 5 h to increase homogeneity; iii) composite C, produced as composite A, but with an amount of fibers equal to 8 wt% of the total starch + glycerol content.

VII. Comparison between TPS Films as such and after the introduction of OFI dry fibers, in order to evaluate their performance improvement. The measurements carried out involved, apart from basic morphological characterization, such as film thickness measurement, other sounder methods of analysis, which included in particular: i) optical microscopy and scanning electron microscopy (SEM) of the films as received, to evaluate their morphology and after tensile tests, to study the fracture surfaces; using SEM, qualitative analysis of the elements present on the surface were also carried out by energy-dispersive X-ray spectrometry (EDS); ii) tensile tests using dog-bone specimens; iii) differential scanning calorimetry (DSC) to evaluate the evolution of films and composites behavior with temperature.

VIII. Plannig of a series of tests in collaboration with the company NOVAMONT S.p.A. of Novara (Italy), interested in patenting the products, in order to complete the characterization of the obtained materials from the point of view of their biodegradability.

For what it concerns the detailed results of each study, please refer to the here presented 1st, 2nd an 3rd Articles and Appendices to NCC and Nopal.

The extraction of cellulose nanocrystals (NCC) from cotton textile waste through the action of sulfuric acid followed by solution neutralization with two different alkalis, namely ammonia and sodium bicarbonate, proved effective in general terms. This yielded microcellulose (MCC) of good quality and uniformity, although in the latter case the fibers were thinner and of less regular shape than in the former one. A subsequent action of centrifugation led to obtaining NCC. Comparing the action of the two neutralizing alkalis, the materials obtained using ammonia can be considered superior. The evidence provided by optical/polarized light microscopy observation and dynamic light scattering (DLS) results suggested a higher geometrical regularity and fibrillar adhesion, together

with a lower dimensional dispersion with respect to those yielded by applying sodium bicarbonate neutralization.

Regarding NCC application in modern Paper materials, the analysis highlighted that the contribution to the mechanical resistance was negative. Nevertheless, the results obtained with the combined application of PVA+NCC, in particular that extracted using NH_3 neutralization, were quite appreciable if compared to that of raw material. This outcome was considered of interest to evaluate the possible use of NCC for the restoration of ancient Paper: the principal aim of this research would be that of reducing the quantity of synthetic PVA utilized in this field, in favor of a natural product obtainable from a plurality of different renewable sources.

As for the use of Nopal mucilage in the field of papermaking, also here the tests proved that its contribution to the mechanical resistance of modern Paper (introduction into the pulp and surface treatment of the sheet) was negative. In spite of that, the results obtained on Paper without additives were quite appreciable, as confirmed by optical microscopy analysis, which evidenced an increment of the cohesion of fibers after the introduction of OFI mucilage. This was considered of interest to investigate the application of Nopal for the restoration of ancient Paper, so as to substitute this natural product for the synthetic PVA actually utilized in this field. In addition, future studies should investigate the possible use of Nopal (opportunely modified), which guarantees a large and reasonably constant availability, as a promising substitute of the expensive CMC, achieving several benefits in terms of cost, sustainability and fully compatibility of the additives utilized in moder papermaking.

With reference to the application of OFI mucilage as filler of Thermoplastic Starch (TPS) Films, the MPM extraction method (mechanical blending after maceration) provided both the highest yielding in terms of mucilage extracted and offered an elongation considerably higher than it is the case for pure TPS. In contrast, pure mechanical extraction (ME) gave rise to the large presence of defects and air bubbles, leading to ineffective tensile loading. Limits observed are the fact that the production of film blends was not sufficient to improve neither the mechanical strength of TPS nor its variable performance. It might be suggested that the considerable presence of calcium carbonate and other calcium or magnesium salts would be suitable for the application of other types of loading, such as shear, which could be the objective of further investigation in the future.

Finally, the preliminary work on the introduction of dry Nopal fibers into TPS led to some interesting observations on the possibilities and limits of this application. More specifically, some critical points were observed in terms of possible improvement of fiber mixing so that their addition would not result in a substantial decrease of mechanical properties (reduction of tensile stress and strain). On the other side, it is suggested that inserting a considerable amount of fibers in a TPS composite of

thickness exceeding a few mm may lead to some improvement in the melting temperature with respect to bare TPS, provided that the mixing before material production is increased. Future work would need to include the further characterization of opuntia fibers also in terms of their adhesion to the matrix, once inserted in variable morphology and with a very scattered aspect ratio.

Generally speaking, even though the results of the application of NCC and Nopal were not appreciable in terms of performance improvement of the hosting materials (modern Paper and TPS), this PhD project satisfied two fundamental objectives: i) the total recycling of CSR obtained from two specific sources, namely cotton waste from worn out textiles and OFI cladodes, for which innovative final reuses were suggested; ii) the optimization of low-cost processes for the extraction of NCC and Nopal (mucilage and fibers from OFI), that are able to provide products with characteristics comparable with the commonly used industrial ones. On this last point, the foundation has been laid for an important future research project in the field of modern papermaking, aimed to investigate the possible use of Nopal as a promising substitute of the expensive CMC.

As stated above, the possibility of using NCC and Nopal for the restoration of historical Paper artifacts and ancient Mortar (Càrdenas et al., 1998; Ventolà et al., 2011; Ravi et al., 2016; Hernandez-Zaragoza et al., 2008), joined to the disasters (loss of human lives and collapses of a very high number of buildings, churches and architectural monuments) caused by the 2016-2017 Central Italy earthquake sequence in several old historic towns in the Abruzzo, Lazio, Marche and Umbria regions (Italy), justified the project-choice of devoting the last part of the research activities to these investigations. Three preliminary multidisciplinary studies were carried out, one on handmade Paper manufacts (13^{th} – 15^{th} century) from Camerino-Fabriano area (Marche, Italy) (4th Article), and two on Mortar from sites damaged during the recent seismic sequence (5th and 6th Articles). In both cases, the principal achievement was the setup of a multi-analytical procedure to perform a diagnostic analysis of these ancient materials, so as to proceed with comparative studies between extremely similar materials (before and after NCC and Nopal application) and to evaluate minimal differences or similarities among them. Moreover, the work on ancient Paper improved and confirmed knowledges on Paper production in Marche region, and for the first time presented an innovative scientific data, the amino acid composition of the glue, that could be helpful in the future to solve the longstanding dispute over the paternity of western Paper among the cities of Fabriano and Camerino.
At the moment, they are being set up two experimental procedure for: i) the introduction of Cellulose Nanocrystals and OFI mucilage into ancient Paper materials; ii) the production of Mortars in

laboratory, replicating the observed ancient compositions, and the introduction of Nopal into the obtained materials. The results of both projects will be available in future works.

Finally, regarding the application of OFI materials in the field of Computer Science, at the moment it is being set up an experimental procedure for the modification of the TPS-Nopal composites in view of their possible application in the field of 3D biomaterial printing. The results of this project will be available in future works.

Author's Note: all the commented papers are authors'final drafts for personal use, and therefore exempt from copyright. The contribution of the PhD student Fabrizio Scognamiglio to each presented article is reported.

References

- Baker, N. 2001). Double Fold: Libraries and the Assault on Paper. Random House. ISBN: 0-375-50444-3.
- Bondeson, D., A. Mathew, K. Oksman (2006). Optimization of the isolation of Nanocrystals from microcrystalline cellulose by acid hydrolysis. Cellulose, 13: 171-180.
- Börjesson, M., G. Westman (2015). Crystalline Nanocellulose – Preparation, Modification and Properties. In Cellulose – Fundamental Aspects and Current Trends, M. Poletto and H. Luiz Ornaghi, editors, Chapter 7, 159-191.
- Brinchi, L., F. Cotana, E. Fortunati, J.M. Kenny (2013). Production of nanocrystalline cellulose from lignocellulosic biomass: Technology and applications. Carbohydrate Polymers, 94: 154-169.
- Càrdenas, A., W.M. Arguelles, F.M. Goycoolea (1998). On the possible role of Opuntia ficus-indica mucilage in lime mortar performance in the protection of historical buildings. J. Prof. Ass. for Cact. Develop., 3: 64-71.
- Coccia, V., F. Cotana, G. Cavalaglio, M. Gelosia, A. Petrozzi (2014). Cellulose Nanocrystals Obtained from *Cynara Cardunculus* and Their Application in the Paper Industry. Sustainability, 6: 5252-5264.
- Curvelo, A.A.S., A.J.F. De Carvalho, J.A.M. Agnelli (2001). Thermoplastic starch-cellulosic fibers composites: preliminary results. Carbohydrate Polymers, 45: 183-188.
- Del Valle, V., P. Hernandez-Muñoz, A. Guarda, M.J. Galotto (2005). Development of a cactus-mucilage edible coating (*Opuntia Ficus Indica*) and its application to extend strawberry (*Fragaria Ananassa*) shelf-life. Food Chemistry, 91 (4): 751-756.
- Dufresne, A. (2013). Nanocellulose: a new ageless bionanomaterial. Materials Today, 16 (6): 220-227.
- Gheribi, R., L. Puchot, P. Verge, N. Jaoued-Grayaa, M. Mezni, Y. Habibi, K. Khwaldia (2018). Development of plasticized edible films from *Opuntia Ficus Indica* mucilage: A comparative study of various polyol plasticizers. Carbohydrate Polymers, 190: 204-211.
- Hernandez-Zaragoza, J.B., A. Coronado-Marquez, T. Lopez-Lara, J. Horta-Rangel (2008). Mortar improvement using Nopal additive. Journal of the Professional Association for Cactus Development, 10: 120-125.

- Klemm, D., F. Kramer, S. Moritz, T. Lindström, M. Ankerfors, D. Gray et al. (2011). Nanocelluloses: A New Family of Nature-Based Materials. Angew Chem. Int. Ed., 50: 5438-5466.
- Ma, X., J. Yu, J.F. Kennedy (2005). Studies on the properties of natural fibers-reinforced thermoplastic starch composites. Carbohydrate Polymers, 62: 19-24.
- Mohammadi Nafchi, A., M. Moradpour, M. Saeidi, A.K. Alias (2013). Thermoplastic starches: Properties, challenges, and prospects. Starch/Starke, 65: 61-72.
- Moon, R.J., A. Martini, J. Nairn, J. Simonsen, J. Youngblood (2011). Cellulose nanomaterials review: Structure, properties and nanocomposites. Chem. Soc. Rev., 40: 3941-3994.
- Pachego-Torgal, F., S. Jalali (2011). Cementitious building materials reinforced with vegetable fibres: A review. Construction and Building Materials, 25(2): 575-581.
- Persia, F., C. Alisi, L. Bacchetta, E. Bojorquez, C. Colantonio, M. Falconieri, M. Insurralde, A. Meza-Orozco, A.R. Sprocati, A. Tatì (2016). Nopal as organic additive for bio-compatible and eco-sustainable lime mortars. VII Conference "Diagnosis, Conservation and Valorization of Cultural Heritage", 15-16 December 2016, 245-251.
- Ravi, R., T. Selvaraj, S.K. Sekar (2016). Characterization of Hydraulic Lime Mortar containing *Opuntia Ficus Indica* as a Bio-Admixture for Restoration Applications. International Journal of Architectural Heritage, 10 (6): 714-725.
- Rodriguez-Gonzalez, F.J., B.A. Ramsay, B.D. Favis (2004). Rheological and thermal properties of thermoplastic starch with high glycerol content. Carbohydrate Polymers, 58: 139-147.
- Roman, M. and W.T. Winter (2004). Effect of Sulfate Groups from Sulfuric Acid Hydrolysis on the Thermal Degradation Behavior of Bacterial Cellulose. Biomacromolecules, 5: 1671-1677.
- Saenz, C., E. Sepùlveda, B. Matsuhiro (2004). Opuntia spp. Mucilage's: A Functional Component with Industrial Perspectives. Journal of Arid Environments, 57 (3): 275-290.
- Saraiva Morais, J.P., R. Morsyleide de Freitas, M. Moreira de Souza Filho, L. Dias Nascimento, D. Magalhães do Nascimento, A. Ribeiro Cassales (2013). Extraction and characterization of nanocellulose structures from raw cotton linter. Carbohydrate Polymers, 91(1): 229-35.
- Sepùlveda, C., C. Sàenz, E. Aliaga, C. Aceituno (2007). Extraction and characterization of mucilage in Opuntia spp. Journal of Arid Environments, 68, 534-545.
- Ventolà, L., M. Vendrell, P. Giraldez, L. Merino (2011). Traditional organic additives improve lime mortars: New old materials for restoration and buinding natural stone fabrics. Construction and Building Materials, 25 (8): 3313-3318.

Acknowledgements

Thanks to:

- Fondazione CARIFAC (Fondazione Cassa di Risparmio di Fabriano e Cupramontana), for its financial support, without which the activities and the achievements of this PhD project would not have been possible.
- Prof. Claudio Pettinari, Rector Magnificus of the University of Camerino, for strongly believing in this PhD project and in my capabilities.
- Marche Region, for accepting and funding this PhD project through the EUREKA program.
- Prof. Carlo Santulli, my Supervisor, for his constant support and assistance, and for all the efforts to publish the results of this PhD research.
- Eng. Daniele Mirabile Gattia, my Co-supervisor and Researcher at Italian Research Agency ENEA, for his valuable contribution to the activities of this Phd project.
- Prof. Graziella Roselli, my Co-supervisor, for her tireless efforts to the promotion of this multidisciplinary research.
- The company NEST S.r.l. of Fabriano, in particular Mr. Domenico Ciappelloni and Mr. Giancarlo Evangelisti.
- Prof. Juan Manuel Madariaga, from the University of the Basque Country, and Prof. Cecilia Bartùli, from "Sapienza" University of Rome, as for external referees of this PhD thesis.
- All several scientific research institutes and groups with which I had the opportunity to collaborate, so as to work together with experts from different fields (cultural heritage, chemistry, physics, engineering, biology and architecture) and to develop a multiple knowledge approach to my research topic.

- All my friends.
- My Old and New Family. I love you.
- Myself, cause I keep thinking that "Happiness is beyond that obstacle".